Functions of GDNF/Ret signaling in models of autosomal recessive Parkinson's disease

Dissertation

Der Fakultät für Biologie der
Ludwig–Maximilians–Universität München

Pontus Klein

Functions of GDNF/Ret signaling in models of autosomal recessive Parkinson's disease

Dissertation zur Erlangung des Doktorgrades
der Naturwissenschaften an der Fakultät für Biologie der
Ludwig–Maximilians–Universität München

Angefertigt am Max-Planck-Institut für Neurobiologie,
Abteilung Molekulare Neurobiologie

Vorgelegt von
Pontus Klein
München 2011

Ehrenwörtliche Versicherung:

Ich versichere hiermit ehrenwortlich, dass ich die Dissertation mit dem Titel "Functions of GDNF/Ret signaling in models of autosomal recessive Parkinson's" selbstandig und ohne unerlaubte Hilfe angefertigt habe. Ich habe mich dabei keiner anderen als der von mir ausdrucklich bezeichneten Hilfen und Quellen bedient.

Erklärung:

Hiermit erklare ich, dass ich mich nicht anderweitig einer Doktorprufung ohne Erfolg unterzogen habe. Die Dissertation wurde in ihrer jetzigen oder ahnlichen Form bei keiner anderen Hochschule eingereicht und hat noch keinen sonstigen Prufungszwecken gedient.

München, den 21 Februar 2012
Pontus Klein

Contents

3.   Discussion   76

4. Materials and Methods   91

5. References   104

Acknowledgments   121

Curriculum Vitae   123

Abbreviations

4E-BP	Eukaryotic translation initiation factor 4E-binding protein
6-OHDA	6-hydroxy-dopamine
AD	autosomal dominant
AR	autsomal recessive
ARTN	artemin
Ask1	apoptosis signaling kinase-1
ATP	adenosine triphosphate
Bcl-XL	b-cell lymphoma extra large
BDNF	brain-derived neurotrophic factor
Braf	rapidly accelerated fibrosarcoma-B
BSA	bovine serum albumine
CaMK1α	calmodulin-dependent protein kinase 1 alpha
CCCP	carbonyl cyanide m-chlorophenylhydrazone
CDK1	cyclin-dependent kinase 1
cDNA	complementary DNA
CDNF	cerebral dopamine neurotrophic factor
CHIP	HSC-70 interacting protein
CREB	Cre-binding protein
CTRL	control
DA	dopamine
DAB	diaminobenzidine
DAT	dopamine transporter
DBS	deep brain stimulation
DL-IFM	dorsal longitudinal indirect flight muscles
Dlk1	delta-like 1 homolog
DMEM	Dulbecco's modified Eagle's medium
DMSO	dimethyl sulphoxide
DNA	deoxyribonucleic acid
Dok	docking protein
Dret	Drosophila ret
Drp1	dynamin related protein 1
ECL	enhanced chemiluminescence
EDTA	ethylenediamine-tetra acetic acid
EGFR	endothelial growth factor receptor
ENS	enteric nervous system
EPS15	endocytosis mediator EGFR substrate 15
ER	endoplasmic reticulum
Erk	extracellular signal-regulated kinase
FAK	focal adhesion kinase
FCS	fetal calf serum
Fis1	mitochondrial fission 1
FMTC	familial MTC
FPD	familial PD
Frs2	Fibroblast growth factor receptor substrate 2
Gab1	Grb-associated-binding protein 1
GABA	gamma-aminobutyric acid
GAPDH	Glyceraldehyde 3-phosphate dehydrogenase
GBA	glucocerebrosidase
GDNF	glia cell line-derived neurotrophic factor
GFL	GDNF family of ligands
GFP	green fluorescent protein
GFRα	GDNF family receptor alpha
GIRK2	the G-protein-activated inward rectifier potassium channel
GMR	glass multiple reporter
GPI	glycosylphosphatidylinositol
Gppe	globus pallidus pars externa
GPpi	globus pallidus pars interna
Grb	growth factor-bound protein
GWAS	genome-wide association studies
HIPK1	homeodomain-interacting protein kinase 1
HPLC	high-performance liquid chromatography
HRP	horse radish peroxidase
HSCR	Hirschprung's disease
HSP-70	heat shock protein 70
IBR	in-between RING domain
IGF1	Insulin-like growth factor-1
IKK	inhibitor of kappa-B kinase
IRS	insulin receptor substrate
ISH	*in situ* hybridization
JNK	c-jun N-terminal kinase
Keap1	kelch-like ECH-associated protein
L-DOPA	L-3,4-dihydroxyphenylalanine

LRRK2	leucine-rich repeat kinase 2	PLCγ	phospholipase C-gamma
LTD	long-term depression	PPL1	posterior lateral protocerebral cluster
MANF	mesencephalic astrocyte-derived neurotrophic factor	PSPN	persephin
MAPL	mitochondrial-anchored protein ligase	PTEN	phosphatase and tensin homolog
MAPT	microtubule-associated protein tau	PVDF	Polyvinylidene fluoride
MEF	mouse embryonic fibroblast	Ret	rearranged during transfection
mef2	*myocyte enhancer factor 2*	RING	really interesting new gene
MEK	Dual specificity mitogen-activated protein kinase kinase 1	RNA	ribonucleic acid
		RNAi	RNA interference
MEKK1	MEK kinase 1	RT	room temperature
MEN2	multiple endocrine neoplasia type 2	RT-PCR	reverse transcriptase PCR
		S6K	S6-kinase
Mfn	mitofusin	SDS	soidium dodecyl sulphate
Mnk	map-kinase interacting substrate	SDS-PAGE	SDS polyacrylamide gel electrophoresis
MOMP	mitochondrial outer membrane permeabilization	SEM	standard error of the mean
MPIN	Max Planck Institute of Neurobiology	SH2	Src homology
		Shc	Src homology domain-containing
MPP+	1-methyl-4-phenylpyridinium	Shp2	Src homology domain-containing phosphatase 2
MPTP	1-methyl-4-phenyl-1,2,3,6-tetrahydropyridine	siRNA	small interfering RNA
mRNA	messenger RNA	SN	substantia nigra
MTC	medullary thyroid carcinoma	SNCA	*α-synuclein*
MTS	mitochondrial target sequence	SNpc	sustantia nigra pars compacta
NCAM	neural cell adhesion molecule	SNpr	substantia nigra pars reticulata
NeuN	neuronal nuclei	SOS	son of sevenless
NFκB	nuclear factor kappa-b	STAT3	signal transducer and activator of transcription 3
NGF	nerve growth factor	STN	subthalamic nucleus
Nrf1/2	nuclear respiratory factor 1/2	SUMO	Small ubiquitin-like modifier
NRTN	neurturin	TAE	Tris-acetate EDTA
Opa1	optic atrophy 1	TBS	Tris buffered saline
PAEL-R	Parkin-associated endothelin-like receptor	TE	Tris-EDTA
PARIS	Parkin interacting substrate	TEM	transmission electron microscopy
PARL	presenilins-associated rhomboid-like protein	TGF-ß	transforming growth factor beta
PBS	phosphate buffered saline	TH	tyrosine hydroxylase
PCR	polymerase chain reaction	TOM	translocase of outer mitochondrial membrane
PD	Parkinson's disease	TOR	target of rapamycin
PFA	paraformaldehyde	TRAP1	tumor necrosis factor receptor-associated protein 1
PGC-1α	PPAR-gamma coactivator-1 alpha	UAS	upstream activating sequence
PI3K	phosphoinositide-3 kinase	UBL	ubiquitin-like domain
PINK1	PTEN induced putatative kinase 1	VDAC1	voltage dependent anion channel 1
PIP₃	phosphatidylinositol 3,4,5 triphosphate	VMAT	vesicular monoamine transporter
PKA	cAMP dependent kinase	VTA	ventral tegmental area

List of tables

List of figures

14

Abstract

The common neurodegenerative disorder Parkinson's disease (PD) affects millions of people world-wide. The disease is characterized by slow, progressive, and age-dependent neuronal cell death, most pronounced in a particularly vulnerable subset of dopamine-containing neurons in the substantia nigra (SN), which are involved in locomotor control. While the etiology is still largely unknown, during the last decade a number of genetic mutations that cause inheritable forms of the disease have been mapped. Surprisingly, knockout mouse models of three genes causing autosomal recessive PD (ARPD) - *Parkin, PINK1* and *DJ-1;* show no overtly degenerative phenotypes.

Another group of proteins that has been connected to the survival of dopamine neurons is the neurotrophic factors and their receptors. Glial cell line-derived neurotrophic factor (GDNF) signals via the co-receptor GDNF family receptor α1 (GFRα1) and the receptor tyrosine kinase rearranged during transfection (Ret). GDNF treatment in animal models of PD has proven to protect against cell death, moreover, GDNF and Ret are physiologically required for survival of dopamine neurons, since conditional ablation of GDNF or Ret causes neurodegeneration. However, how GDNF/Ret signaling promotes survival of dopamine neurons remains unknown. In this project, I studied the functions of Ret signaling in different models of ARPD, with the hypothesis that Ret co-operates with ARPD-associated genes in maintaining critical cellular functions.

I participated in a study that, using mouse genetics, found that combined ablation of *Ret* and the ARPD-associated gene *DJ-1* causes increased loss of SN neurons compared to *Ret* and *DJ-1* single mutants in a synergistic manner, indicating that DJ-1 is required for survival of neurons that are impaired in receiving trophic support. In cell culture, I investigated cellular pathways that could biochemically link Ret signaling to DJ-1 function. It was previously reported that DJ-1 positively regulates Akt and Erk phosphorylation. However, by depleting or overexpressing DJ-

1 in HeLa, SH-SY5Y, COS7, and A549 cells, or by comparing wildtype and DJ-1 knockout fibroblasts, I found no evidence supporting either of the two previously reported findings.

I also hypothesized that Ret signaling can compensate for the loss of two other ARPD-associated genes, *Parkin* and *PINK1,* which function in controlling mitochondrial integrity. Depleting Parkin and PINK1 from mammalian cells is known to cause mitochondrial fragmentation, and here I found that this can be reversed with GDNF treatment.

Furthermore, I investigated whether this function of Ret is conserved in the fruit fly *Drosophila melanogaster*. Mutants for *park* and *Pink1* have enlarged and dysfunctional mitochondria in several tissues, together with degenerated indirect flight muscles (IFMs), including abnormal myofibrils. Overexpression of a constitutively active version of the *Drosophila* homolog of Ret (Dret[MEN2A]) did not rescue the mitochondrial deficiencies of *park* and *Pink1* mutants in dopamine neurons or IFMs. However, Dret[MEN2A/B] overexpression also caused abnormal myofibrils, and interestingly, I found that Dret[MEN2B] functioned in partial epistasis with *Pink1,* and restored myofibrillar abnormalities in *Pink1* mutants.

Finally, I asked whether combined ablation of *Ret* and *Parkin* or *Ret* and *PINK1* in dopamine neurons of mice causes increased neurodegeneration upon aging, compared to *Ret* single mutants. Unexpectedly, all combinations of mutants, as well as *Ret* single mutants, were devoid of degeneration up to 24 months of age, indicating that other additional factors may be required to sensitize *Ret* mutants for them to develop a neurodegenerative phenotype.

1. Introduction

1.1. Background to Parkinson's disease

1.1.1. Clinical manifestation and neuropathology

Parkinson's disease (PD), first described by the British physician James Parkinson in 1817 (Parkinson 1817), is the second most common neurodegenerative disorder, affecting an estimated 1-2 % of the population older than 65 years. For people older than 85 years, the prevalence increases to 5 %, and as the average life span of the population in the developed world steadily increases, it is predicted to become an even greater problem for society in the future (Van Den Eeden *et al.* 2003; de Lau & Breteler 2006). The cardinal clinical feature of PD is the so-called parkinsonism syndrome, which is defined by resting tremor, bradykinesia (slowness of movement), postural instability and rigidity. In addition to the motoric symptoms, patients commonly present with cognitive and psychiatric problems such as anxiety or depression, and even symptoms related to peripheral autonomic nerves such as constipation (Stanley Fahn 2003). Pathologically, the disease is characterized by neurodegeneration, most pronounced in the dopamine (DA) neurons of the substantia nigra *pars compacta* (SNpc), which form the nigrostriatal pathway, together with depletion of dopamine in the striatum, which also is the cause of parkinsonism. Another hallmark of the disease is the presence of cytoplasmic proteinaceous inclusions in remaining SNpc neurons, so-called Lewy bodies, as well as dystrophic neurites, known as Lewy neurites (Lewy 1912). A thorough neuropathological post-mortem analysis by Braak and colleagues found Lewy pathology in vast areas of the brain, and by analyzing PD patients of different progression they proposed a staging system of the pathology, with the earliest pathology found in the dorsal motor nucleus of the vagal nerve and Raphe nuclei of the lower brain stem. From there, it appeared to progress rostrally to the SN and ventral tegmental area (VTA) in the ventral midbrain, and later continued to the amygdala, hippocampus and neocortex (H. Braak *et al.* n.d.). The large Lewy body aggregates contain several different proteins; however, the main components are α-synuclein and ubiquitin. The mechanism of aggregate formation is an intensively studied topic, but it remains unclear whether the aggregates are pathological themselves or merely an inert byproduct. In particular, α-

synuclein oligomeric species have attracted particular interest as they appear to be toxic (Venda *et al.* 2010).

1.1.2. Current and developing treatment options

Major leaps towards understanding the pathology of PD and the development of therapy were taken in the late 1950's and 1960's with research by Swedish neuroscientist Arvid Carlsson, as he discovered that dopamine is in fact a neurotransmitter and not just a precursor in the noradrenaline synthesis. When he treated mice with the drug reserpine, a vesicular monoamine transporter (VMAT) inhibitor, they showed reduced dopamine levels and developed parkinsonism symptoms. This finding led him to administer the dopamine precursor L-dopa to reserpine-treated mice, and with that he was able to alleviate the symptoms (Carlsson *et al.* 1957). Still today, more than 50 years after this discovery, L-dopa-based pharmaceuticals are the primary therapy for PD patients. During the last decade, a new therapy of deep brain stimulation (DBS) has proven effective in later stage-patients, which aims at directly modulating the basal ganglia circuitry by electrical currents. Both dopamine-replacement therapy and DBS can ultimately only alleviate symptoms (and in that, only the motoric symptoms), but cannot halt disease progression.

Cell replacement therapy has for the past thirty years been under development and some early open-label transplantation studies using fetal midbrain cells have had successful outcomes (Lindvall *et al.* 1990; Freed *et al.* 1992). However, later, double-blinded trials showed no statistical improvement compared to sham surgery (Freed *et al.* 2001; Olanow *et al.* 2003). The possibility of cell replacement has boosted the field of stem cell research, with a view to developing sources of cells for transplantation. However, even with recent tremendous advances the road to functionally and safely restoring the nigrostriatal tract in PD patients will be long (Arenas 2010; Wakeman *et al.* n.d.). Another developing approach aims at neuroprotection using neurotrophic factors. The US National Institutes of Health is currently conducting a phase II clinical trial for the use of glial cell line-derived neurotrophic factor (GDNF) administered by gene therapy and the US biotechnology company Ceregene has recently started phase II trials of the GDNF homolog neurturin. The biological basis for neurotrophic factor-based therapies is discussed further in section 1.3.
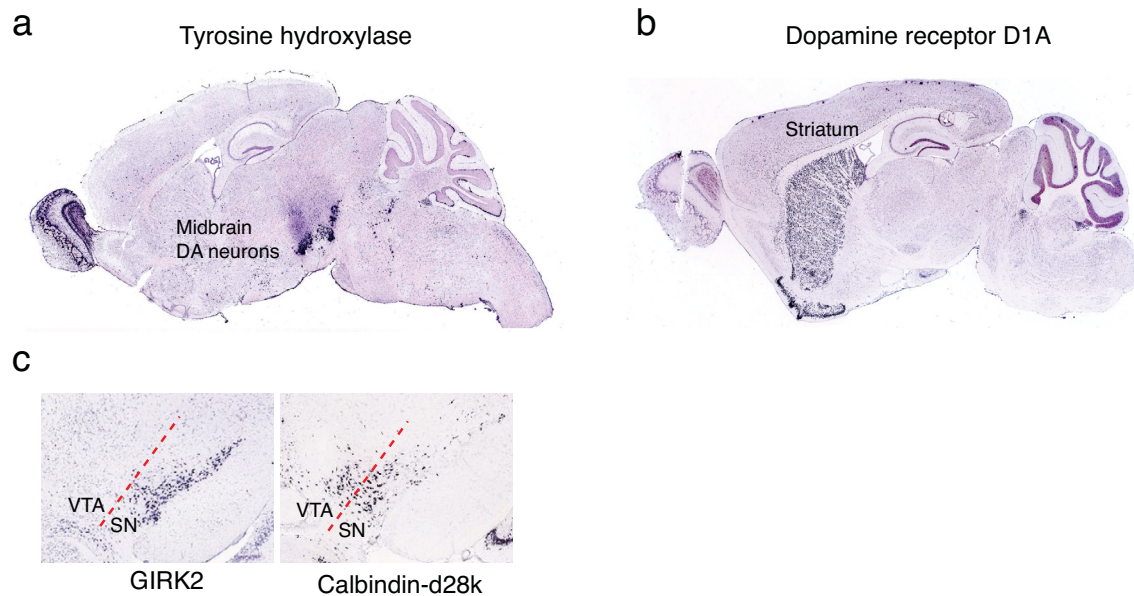
Figure 1-1 Dopaminergic cells of the mouse brain. *In situ*-hybridizations of (a,b) sagittal-sectioned mouse brains, for (a) tyrosine hydroxylase, indicating DA neuron cell bodies, (b) dopamine receptor D1A, indicating DA neuron synapses, and of (c) coronal sectioned mouse ventral midbrains for GIRK2 or calbindin-d28k with the ventral tegmental area (VTA) and substantia nigra (SN) depicted. All images were taken from the Allen Brain Atlas (www.brain-map.org).

1.1.3.   Nigrostriatal dopamine neurons – function and selective vulnerability

The human and mouse brains contain eleven groups of dopamine cell bodies, the majority of which are located in the midbrain, basal ganglia and olfactory bulb, as illustrated by an *in situ* hybridization (ISH) for the dopamine neuron marker tyrosine hydroxylase (Allen Brain Atlas, figure 1-1a). Dopamine receptors, indicating post synapses for dopamine neurons, are found mainly in the striatum, neocortex and olfactory bulb, as illustrated by D1A receptor ISH (Allen Brain Atlas, figure 1-1b). The ventral midbrain can be separated into VTA, involved in reward circuitry, and the SN, involved in motor control. The SN can in turn be divided in the *pars compacta* (*pc*), the neurons of the nigrostriatal pathway, and the *pars reticulata* (*pr*), projecting to the thalamus. The *compacta* neurons are also not a fully homogenous cell population. The expression of two marker proteins, the G-protein-activated inward rectifier potassium channel (GIRK2) and the calcium binding protein calbindin, mark two subsets of ventral midbrain neurons. The two populations do partly, but not fully, correspond to the anatomical division of SNpc and VTA, and show little overlap (Allen Brain Atlas, figure 1-1c). GIRK2+ neurons make up approximately 75 % of the SNpc and project to the putamen in the dorsal striatum, where they control locomotion, while the remaining 25 % calbindin+ neurons project to limbic and

neocortical areas (Björklund & Dunnett 2007). The striatum, SN, basal ganglia and thalamus together form a circuitry that fine-tunes locomotion (figure 1-2a). The SNpc neurons synapse in the striatum with both the excitatory D1 type of dopamine receptors, a part of the 'direct pathway' which increases movement, and also with the inhibitory D2 type of receptors, which function in the 'indirect pathway' that decreases movement (Rodriguez-Oroz *et al.* 2009). In Parkinson's disease, both the D1 and D2 projections are lost, causing a subsequent increase in the indirect pathway signaling, and a decrease in the direct pathway signaling (figure 1-2b). In a recent study, researchers were able to directly activate the D1 or D2 receptor expressing striatal neurons individually, using optogenetics (Kravitz *et al.* 2010). When D1 expressing neurons were activated, mice became hyperactive, and when activating the D2 expressing neurons, mice instantly showed typical parkinsonism-type movements, proving the validity of this model.

The axonal projections of SNpc neurons are believed to be affected first in the degenerative process as the striatum is depleted of dopamine (Bernheimer *et al.* 1973), and this has led to a dying-back model of degeneration (Dauer & Przedborski 2003). Interestingly the SNpc neurons are more affected in PD, showing a higher level of cell death, than the VTA neurons (Uhl *et al.* 1985). Similarly calbindin+ neurons are relatively spared in comparison to GIRK2+ neurons in animal models of PD (C. L. Liang *et al.* 1996; C. Y. Chung *et al.* 2005). What causes this difference between DA neuron cell types adjacent to each other in the ventral midbrain? One possibility is that their diverse projections make the difference, as activities or signaling in the target area may render them more or less sensitive. Another possibility lies in their physiology and gene expression, irrespective of projections. It is possible that calbindin expression is protective, or alternatively that GIRK2 expression sensitizes them, a theory that is supported by the finding that GIRK2 overexpression in PC12 cells renders them more vulnerable to toxin treatment (C. Y. Chung *et al.* 2005). An intriguing series of research from the Surmeier laboratory has focused on the regional selectivity of SNpc neuron cell death. They found that SNpc neurons, as opposed to VTA neurons express a pace making L-type calcium channel (Ca$_V$1.3), and when this channel is selectively blocked in mice, SNpc neurons were protected from toxin-induced cell death (C. S. Chan *et al.* 2007).
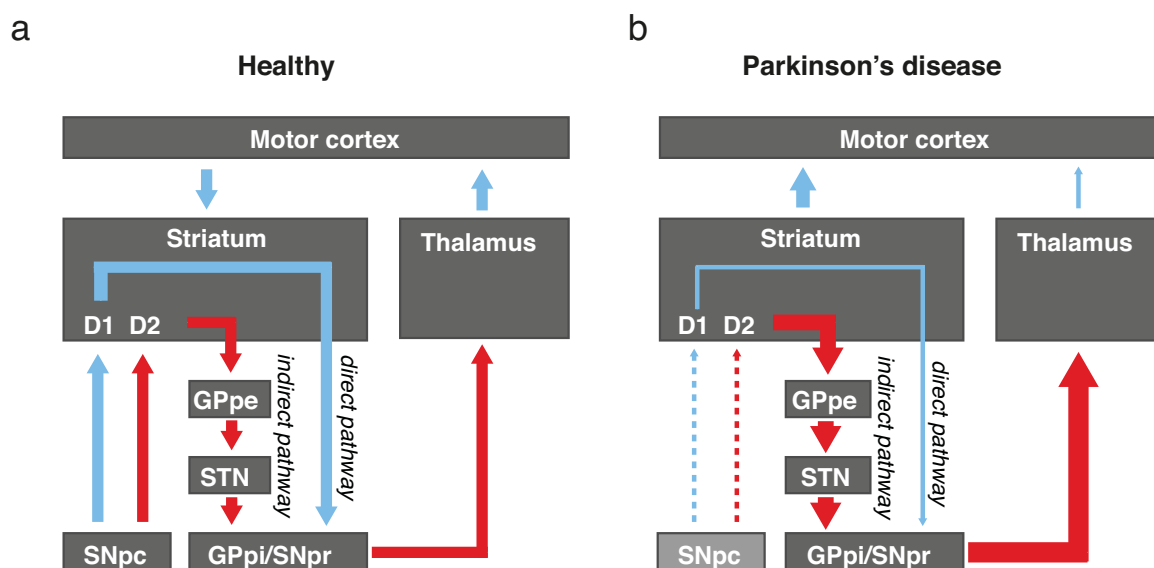
Figure 1-2 Circuitry of movement control by the basal ganglia. In a healthy brain (a), The striatum is innervated by the motor cortex, but also by the substantia nigra pars compacta (SN*pc*), which forms synapses on two types of neurons. The first type receives excitatory (blue arrows) DA input via dopamine D1 receptors, forming the direct pathway. The second type receives inhibitory (red) input via dopamine D2 receptors, forming the indirect pathway. The direct pathway further continues with inhibitory GABAergic neurons, which project to the globus pallidus *pars interna* (GP*pi*) and substantia nigra *pars reticulata* (SN*pr*), which in turn contains inhibitory GABAergic neurons projecting to the thalamus, which sends excitatory glutamatergic signals back to the motor cortex. Conversely, the indirect pathway, continues with striatal GABAergic neurons that project to the globus pallidus *pars externa* (GP*pe*), inhibiting the subthalamic nucleus (STN), which in difference to the direct pathway, sends excitatory input to the GP*pi* and SN*pr*. In Parkinson's disease (b), the SN*pc* neurons degenerate, causing a loss both D1 and D2 receptor transmission in the striatum, which leads to decreased signaling via the direct pathway, and increased signaling via the indirect pathway, in the end causing decreased excitation of the motor cortex.

1.1.4.   Etiology and genetics of PD

PD is a complex multifactorial disorder, of which aging, genetics and environmental factors all increase disease risk. The majority of cases (estimated as up to 90 %) is sporadic, also known as idiopathic, and can vary to a large extent in the expression of symptoms. The pathogenic agents behind these cases are still largely unknown. In 1983 mitochondrial toxicity was first linked to PD, when a group of opioid drug abusers all presented with parkinsonism symptoms, which could be tracked back to the accidental intake of 1-methyl-4-phenyl-1,2,3,6-tetrahydropyridine (MPTP), with the active metabolite 1-methyl-4-phenylpyridinium (MPP+), which interferes with complex I of the mitochondrial electron transport chain (Langston *et al*. 1983). Epidemiological studies suggest that environmental toxins, such as the pesticide rotenone, another mitochondrial complex I inhibitor, or the herbicide paraquat may be involved, but strong evidence is missing (T. P. Brown *et al*. 2006). Further support for a central role of

mitochondria in the etiology of PD came from the 'MitoPark' mouse model, a dopaminergic conditional knockout of the mitochondrial transcription factor *tfam* gene, which develops a parkinsonian phenotype including progressive SNpc neuron degeneration, impaired motor function and intraneuronal inclusions (Ekstrand *et al.* 2007).

It was long believed that PD was a non-genetic disorder, but successively autosomal-inherited Mendelian forms have been discovered, and during the later part of the 1990's and early 2000's, major breakthroughs in genetics lead to the identification of several distinct causative loci, the *PARK* genes. To date, up to 16 loci have been confirmed to cause PD or parkinsonism-like disorders some dominant, others recessive, and the list continues to grow as new loci are frequently reported (table 1). The line between sporadic and genetic PD is becoming increasingly blurred, as loci only acting as risk factors for sporadic PD are discovered, such as the genes for microtubule-associated protein tau (MAPT) or glucocerebrosidase (GBA), which also causes Gaucher's disease (Zabetian *et al.* 2007; Sidransky *et al.* 2009). Interestingly, genes of the Mendelian *PARK* loci, with complete disease penetrance of certain mutations, have recently turned up in genome-wide association studies (GWAS) as low-penetrant increased-susceptibility-loci for sporadic PD with polymorphisms in different positions, further blurring the distinction between genetic and sporadic PD (Simón-Sánchez *et al.* 2009; Satake *et al.* 2009). In addition, there are several conditions such as spinocerebellar ataxia, Wilson's disease, and frontotemporal dementia that can present with parkinsonism. Another complicating factor of studying genetic PD, is the fact that different *PARK* loci cause syndromes with considerable differences in their neuropathology, clinical symptoms, and age of onset. For example, the autosomal-recessive PD (ARPD) forms, *PARK2*, *PARK6*, and *PARK7* discussed in detail later in this thesis, differ significantly from sporadic and autosomal-dominant forms with very early ages of onset, and symptomologies restricted to parkinsonism. The mutations of these three genes all appear to result in loss of function, and therefore studying the function of such genes can hopefully teach us something about the mechanisms behind dopamine neuron cell death. Even though these recessive forms differ from sporadic PD, the two likely share mechanistic features. Linking the disease-causing pathways of recessive *PARK* genes and toxin models such as MPTP, which all seem to be connected to mitochondrial pathology, with the protein misfolding and aggregation pathway observed in *α-synuclein (SNCA)* and *leucine-rich repeat kinase 2 (LRRK2)* PD, as well as

in sporadic disease, remains an unsolved issue for PD research, and may be fundamental in our understanding of the pathogenic process.

Table 1-1 Genes associated with monogentic inherited PD

PARK-locus	Location	Gene	Inheritance	Protein function
PARK1/4	4q21-q23	*SNCA* (point mutation/triplication)	AD	Synaptic vesicle transport
PARK2	6q25.2-q27	parkin	AR	E3 Ubiquitin ligase
PARK3	2p13	unclear	AD	
PARK5	4p14	UCHL1	AD	Ubiquitin hydrolase
PARK6	1p35-p36	PINK1	AR	Mitochondrial kinase
PARK7	1p36.33 - p36.12	DJ-1	AR	Oxidative stress sensor
PARK8	12p11.23-q13.11	LRRK2	AD	Multidomain-kinase
PARK9	1p36	ATP13A2	AR	Cation-transporting ATPase
PARK10	1p32	unclear	unclear	
PARK11	2q36-q37	GIGYF2	AD	GRB10 interactor
PARK12	Xq21-q25	unclear	X-linked	
PARK13	2p12	HTRA2	AD	Mitochondrial serine peptidase
PARK14	18q11	PLA2G6	AR	Phospholipase
PARK15	22q12-q13	FBXO7	AR	F-box, ubiquitination component
PARK16	1q32	unclear	unclear	

1.2.   Functions of ARPD-associated proteins

1.2.1.   DJ-1 functions as a redox sensor, and as a regulator of transcription, translation and signal transduction pathways

The first reports on DJ-1 were concerned with oncogenic activity, as DJ-1 had been found to be upregulated in cancers and to have transforming activity in cell culture (Nagakubo *et al*. 1997; Le Naour *et al*. 2001). PD-linked mutations in the *DJ-1* gene *(PARK7)* were initially identified in two independent families (Bonifati *et al*. 2003), but are an extremely rare cause of PD as was demonstrated by a recent study (Anvret *et al*. 2011). The DJ-1 protein has puzzled researchers for several years, due to apparent difficulties in elucidating its true physiological function and role in PD-pathogenesis. Even though an astonishing number of molecular functions have been reported, most of the studies are based solely on cell culture data and it remains elusive which functions are physiologically relevant *in vivo*. It would be impossible to describe every function

that has been reported, however a selection of them are described and illustrated below (figure 1-3).

The 189 amino acid small protein (figure 1-4), found natively as a dimer, shares some homology with the ThiJ/PfpI family of bacterial molecular chaperones, and indeed chaperone activity for DJ-1 has been reported (Shendelman et al. 2004; Deeg et al. 2010; Bandyopadhyay & Cookson 2004). The most conclusive finding about DJ-1 function is that it responds to, and protects against, oxidative stress-induced cell death (Taira *et al.* 2004; Canet-Avilés *et al.* 2004; Martinat *et al.* 2004; Meulener *et al.* 2006; Görner *et al.* 2007). DJ-1 has a highly conserved cysteine residue (human DJ-1 C106) that reacts with reactive oxygen species to form a sulfonic acid group upon oxidative stress (Canet-Avilés *et al.* 2004; Kinumi *et al.* 2004; Ooe *et al.* 2006; Andres-Mateos *et al.* 2007; Hulleman *et al.* 2007). Details of the response to oxidation of this cysteine residue remains to be clarified, but interestingly it was shown to be critical for DJ-1-mediated protection against MPP+ (Canet-Avilés *et al.* 2004). The same study also found that DJ-1 translocated to mitochondria during oxidative stress, and recently, it was shown that oxidized DJ-1 interacts with b-cell lymphoma extra large (Bcl-X$_L$) (Ren *et al.* 2011). In addition to functioning as a chaperone and reacting to oxidative stress, many other functions have been reported: DJ-1 was found to bind to p53 and either repress (J. Fan, Ren, Jia, *et al.* 2008; J. Fan, Ren, Fei, *et al.* 2008; Bretaud *et al.* 2007) or enhance (Shinbo *et al.* 2005) its transcriptional activity. Furthermore, DJ-1 was reported to bind and regulate the androgen receptor (Tillman *et al.* 2007; K Takahashi *et al.* 2001), to have protease activity (Koide-Yoshida *et al.* 2007), act as a transcription factor for tyrosine hydroxylase (TH) (J. Xu *et al.* 2005), and regulate transcription of antioxidant response factors by stabilizing the kelch-like ECH-associated protein (Keap1)/nuclear respiratory factor 2 (Nrf2) transcription activation complex (Clements *et al.* 2006). However, this finding could not be reproduced in another study (L. Gan *et al.* 2010). Moreover, DJ-1 was found to act as a peroxiredoxin-like peroxidase (Andres-Mateos *et al.* 2007), regulate translation by directly binding GC-rich mRNA (van der Brug *et al.* 2008; Blackinton *et al.* 2009), interact with the protein kinases MEK kinase 1 (MEKK1) and homeodomain-interacting protein kinase 1 (HIPK1) (Mo *et al.* 2008; Sekito *et al.* 2006), and regulate apoptosis signaling kinase-1 (Ask1) by sequestering its activator death-associated protein 6 (DAXX) (Junn *et al.* 2005). Interestingly DJ-1 was reported to promote Akt signaling, one of the major pro-survival signaling pathways activated by receptor tyrosine kinases, by negatively regulating
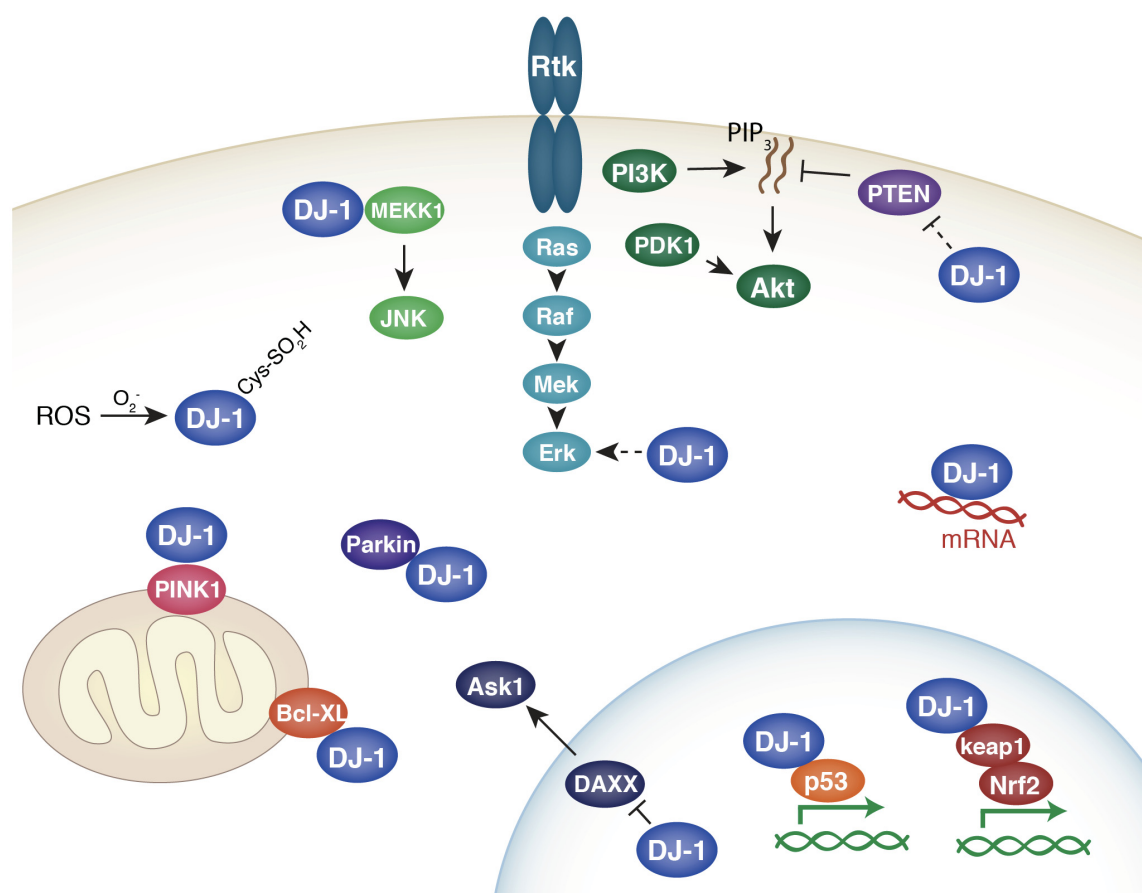
Figure 1-3 Reported biochemical functions of DJ-1. DJ-1 was reported to respond to oxidative stress, and regulate a number of signal transduction pathways including PI3K-Akt, MEKK1-JNK, Ras-Erk, and DAXX-Ask1. In addition, DJ-1 was reported to regulate transcription by binding to p53 and Keap1/Nrf2. DJ-1 has been shown to localize to mitochondria and interact with Bcl-Xl. DJ-1 was also found to interact biochemically with the other ARPD associated proteins PINK1 and Parkin.

phosphatase and tensin homolog (PTEN) (Y. Yang *et al.* 2005; R. H. Kim, Peters, *et al.* 2005). Recently, DJ-1 was also reported to increase extracellular signal-regulated kinase 1/2 (Erk1/2) phosphorylation (L. Gu *et al.* 2009). Yet another role for DJ-1 was reported when it was found that it can control mitochondrial dynamics (Kamp *et al.* 2010; K. J. Thomas *et al.* 2011). DJ-1 was also found to bind to two of the other ARPD-associated proteins, Parkin (D. J. Moore *et al.* 2005) and PTEN induced putataive kinase 1 (PINK1) (Tang *et al.* 2006).

At least five independent DJ-1 knockout mouse lines have been generated, but in contrast to *PARK7* PD patients, DJ-1 knockout mice do not display any loss of SNpc DA neurons or loss of striatal DA fibers (R. H. Kim, P. D. Smith, *et al.* 2005; Goldberg *et al.* 2005; Linan Chen *et al.* 2005; Chandran *et al.* 2008; Yamaguchi & J. Shen 2007). The mice did show subtle behavioral alterations, for example reduced activity, and one study also found impairments in striatal
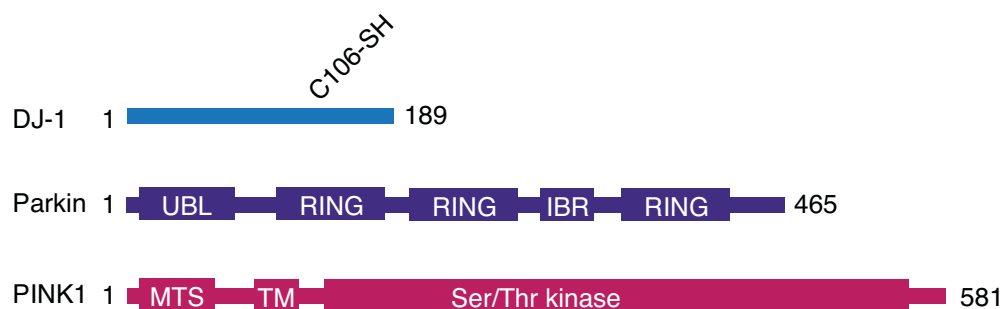
Figure 1-4 Domain structures of DJ-1, Parkin, and PINK1. The DJ-1 protein (189 amino acids) lacks known functional motifs, but harbors a cysteine residue (C106), that is oxidized by reactive oxygen species. Parkin (465 amino acids) contains a ubiquitin-like domain (UBL), three RING domains and one in-between-RING domain. PINK1 (581 amino acids) contains a mitochondrial target sequence (MTS), a transmembrane domain, and a Ser/Thr kinase domain.

dopamine D2 receptor function, with absence of long-term depression (LTD), and reduced synaptic dopamine release (Goldberg *et al.* 2005). Guzman *et al* found that DJ-1 mutant mice show increased sensitivity to pacemaking calcium transients, due to decreased mitochondrial uncoupling, and that DJ-1 upregulates uncoupling protein 4/5 (Guzman *et al.* 2010), proposing a model that explains why SNpc neurons are selectively vulnerable to DJ-1 mutations.

How can a small protein with limited functional domains perform all of these greatly varied functions? One possibility is that many of the observed effects of regulating various pathways are secondary to one major function, such as controlling a transcriptional master regulator, which again also was reported, for example with p53 and Nrf2, but many of the functions above could still not be explained by such a mechanism. Further studies are required to clarify which of the biochemical effects found *in vitro* are physiologically relevant *in vivo*. Such a clarification could shed important light on the etiology of *PARK7* PD.

1.2.2. The E3 ubiquitin ligase Parkin

The most common causes of ARPD are mutations in the *PARK2* locus, which harbors the *parkin* gene first mapped in 1998 (Kitada *et al.* 1998). *Parkin* mutations are estimated to account for 50 % of all ARPD cases (Lücking *et al.* 2000) and are also frequently found in sporadic cases (Periquet *et al.* 2003). The highly conserved and ubiquitously expressed Parkin protein belongs to the family of E3 Ubiquitin ligases, and contains three Really interesting new gene (RING) domains, with an in-between RING domain, and a N-terminal ubiquitin-like domain (figure 1-

4). As such, Parkin can form complexes with several E2 ligases and can mediate both K48 and K63 polyubiquitination (Doss-Pepe *et al.* 2005).

1.2.3.   Non-mitochondrial targets of Parkin

The literature on Parkin is far less divergent than in the case of DJ-1, since its E3 ligase function is clear, but still many different targets have been reported (figure 1-5). Recently a mitochondrial function for Parkin in cooperation with PINK1 has emerged and is described in sections 1.2.5-6. However, apart from a function in mitochondria, several other interesting findings have been made: Imai *et al* reported in two studies that Parkin ubiquitinates unfolded Parkin-associated endothelin-like receptor (PAEL-R) in a complex with C terminus of HSC70 interacting protein (CHIP) and heat shock protein 70 (HSP-70), which otherwise may cause endoplasmic reticulum (ER) stress-induced cell death, placing Parkin in the unfolded protein response (UPR) system (Y. Imai *et al.* 2001; Y. Imai *et al.* 2002). Corti *et al* reported that Parkin ubiquitinates the aminoacyl transferase p38 (Corti *et al.* 2003). Interestingly, Parkin has also been shown to target a specific glycosylated form of α -synuclein (α -sp22), which is accumulated in Parkin-deficient brains, providing a functional link between α -synuclein aggregation and *parkin*-linked PD (Shimura *et al.* 2001). Later, it was also found that Parkin could bind LRRK2 (W. W. Smith *et al.* 2005), DJ-1 (D. J. Moore *et al.* 2005) and recently PINK1 (Matsuda *et al.* 2010; Vives-Bauza *et al.* 2010; Narendra *et al.* 2010). Furthermore, it was shown that Parkin upregulates endothelial growth factor receptor (EGFR) signaling by ubiquitinating the endocytosis mediator EGFR substrate 15 (EPS15), causing reduced EGFR endocytosis (Fallon *et al.* 2006). This finding provides yet another link between the function Parkinson-associated proteins and receptor tyrosine kinases. Parkin was also reported to mediate neuroprotective effects through nuclear factor kappa-b (NFκ-B) signaling (Henn *et al.* 2007).

Parkin knockout mice have been generated by several groups, but as in the case of DJ-1 and also PINK1, Parkin knockout mouse have until recently failed to show a loss of dopamine neurons. The mice instead display phenotypes related to synaptic transmission and mitochondrial function (Goldberg *et al.* 2003; Palacino *et al.* 2004; Itier *et al.* 2003; Perez & Palmiter 2005). In 2011, an intriguing study identified a novel target of Parkin, named Parkin interacting substrate (PARIS) (Shin *et al.* 2011). Parkin was found to control PARIS levels by targeting it for proteasomal degradation. The authors showed that PARIS represses transcription of PPAR-gamma
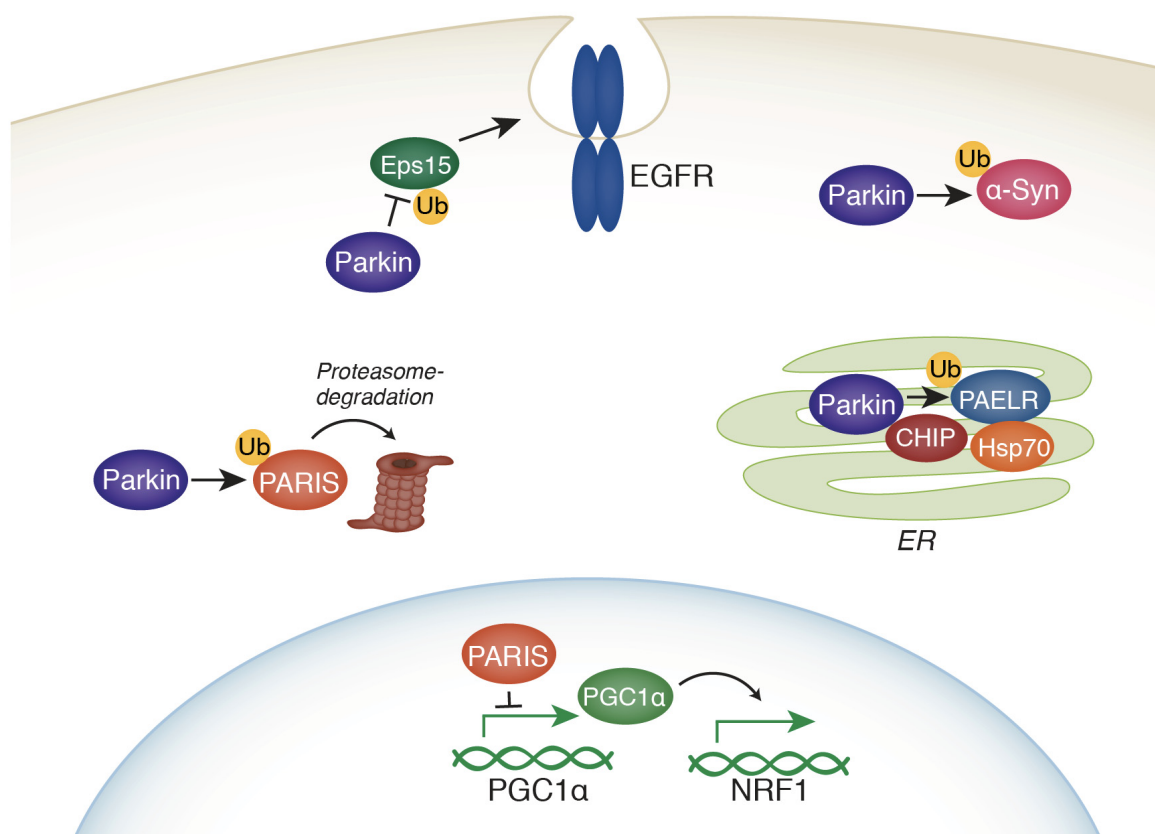
Figure 1-5 Non-mitochondrial targets of Parkin-mediated ubiquitination. Parkin was shown to decrease EGFR endocytosis by inhibiting Eps15, ubiquitinate sp22 alpha-synuclein, reduce ER stress by targeting PAEL-R in a complex with CHIP and HSP70, and to label PARIS for degradation, thereby preventing it from inhibiting PGC1-alpha/Nrf1 transcription, which activate stress response pathways.

coactivator-1 alpha (PGC-1α), which in turn regulates expression of another master transcription factor, nuclear respiratory factor-1 (NRF-1) – important for mitochondrial function and biogenesis. By injecting Cre recombinase-expressing lentiviral vector in the brains of Parkin^{lx} mice, Parkin was deleted first in adult mice, and through this knockout strategy, mice lacking Parkin showed a striking 40 % loss of dopamine neurons after 6 months. Intriguingly, the phenotype was fully rescued with the overexpression of PARIS. Protein levels of PARIS were also found to be elevated in brains of PD patients carrying Parkin mutations, as well as in sporadic cases. Further studies are required to characterize the Parkin-PARIS pathway in detail and investigate the relevance for PD.

1.2.4.   The mitochondrial kinase PINK1

In 2004, Valente *et al* mapped the *PARK6* locus to the *PINK1* gene, and also found somatic *PINK1* mutations in sporadic disease (Valente, Abou-Sleiman, *et al*. 2004; Valente, Salvi, *et al*.
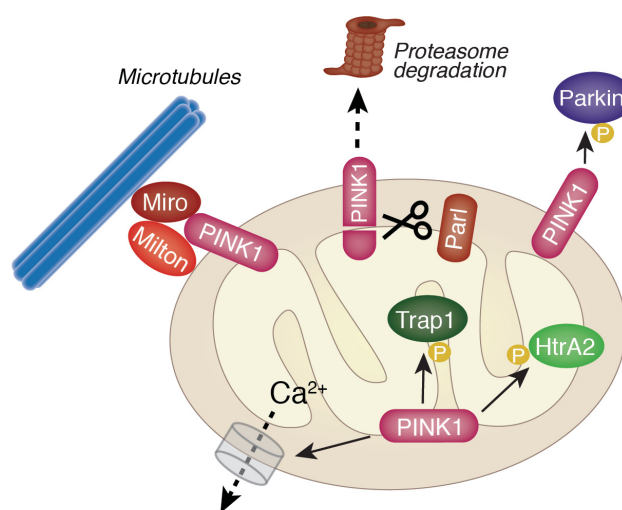
Figure 1-6 Biochemical functions of PINK1. The PINK1 protein exists in a full length 63 kDa form and a processed 52 kDa form. Proteolysis of PINK1 is mediated by the protease PARL, after which the cleaved 52 kD form is degraded by the proteasome. Furthermore, PINK1 was implicated to promote mitochondrial transport on microtubules in a complex with Miro and Milton. PINK1 was also found to regulate calcium efflux, and to phosphorylate Trap1, HtraA2 and Parkin.

2004). *PINK1* mutations are more common in ARPD than *DJ-1* mutations, but are still rare (Bonifati *et al.* 2005). Whether heterozygous *PINK1* mutations increase the risk of developing sporadic disease has been proposed but is controversial (C. Klein *et al.* 2007; Bonifati *et al.* 2005). *PINK1* encodes a serine/threonine kinase with an N-terminal mitochondrial targeting sequence and a transmembrane domain (figure 1-4). The PINK1 protein is localized both in the cytosol and in mitochondria, where it was found in several different mitochondrial compartments, however the details of the localization is a complex and controversial issue (Beilina *et al.* 2005; C. Zhou *et al.* 2008; Y. Yang *et al.* 2005; Narendra *et al.* 2010). To understand the various functions of PINK1 (figure 1-6), it is of importance that the protein exists in two isoforms, a full length form of approximately 63 kDa and a cleaved form of approximately 52 kDa (Beilina *et al.* 2005). Recently, it was reported by several groups that the proteolytic processing of PINK1 is mediated by the protease presenilins-associated rhomboid-like protein (PARL), located at the inner mitochondrial membrane (Jin *et al.* 2010; Deas *et al.* 2011; G. Shi *et al.* 2011; Meissner *et al.* 2011). This is also supported by the genetic interaction between *Pink1* and the *Drosophila* homolog of PARL, *rhomboid-7* (Whitworth *et al.* n.d.). When disrupting the mitochondrial membrane potential, using valinomycin or carbonyl cyanide m-chlorophenylhydrazone (CCCP), the proteolysis is abolished, stabilizing the full length form, which suggests that mitochondrial membrane potential is a key regulator of PINK1 function

(Silvestri *et al.* 2005; Narendra *et al.* 2010; Matsuda *et al.* 2010). The cleaved form is rapidly degraded by the proteasome, which was demonstrated by blocking proteasome activity, leading to accumulation of the full length form (Takatori *et al.* 2008; Gandhi *et al.* 2009). A model of PINK1 activity proposes that in healthy mitochondria, PINK1 is cleaved by PARL at the inner membrane, after which the 52 kDa fragment is transported to the proteasome and degraded. When mitochondria lose their membrane potential due to impairments, PINK1 can no longer be imported through the potential-dependent translocase of outer mitochondrial membrane (TOM) complex, hence it cannot be accessed by PARL and instead, it integrates in the outer membrane (Jin *et al.* 2010). This claim that the 52 kDa form is primarily localized at the inner membrane, while the full length resides at the outer membrane, was demonstrated in an experiment where cells were treated with a proteasomal inhibitor, together with proteinase K, which rapidly degraded the 63 kDa form, while the 52 kDa form was protected. This model, on the other hand, does not fit well with a report showing cytosolic activity, which used a mitochondrial targeting sequence-mutant, but still protected against MPTP toxicity (M Emdadul Haque *et al.* 2008). At least three different substrates of PINK1 kinase activity have been reported. One study showed that the mitochondrial chaperone tumor necrosis factor receptor-associated protein 1 (TRAP1) was phosphorylated directly by PINK1, protecting it from cell death by suppressing cytochrome-c release (Pridgeon *et al.* 2007). Another study found that PINK1 phosphorylates HtrA2/Omi, a candidate *PARK*-gene, in response to p38MAPK signaling (Plun-Favreau *et al.* 2007). A *Drosophila* study confirmed a genetic interaction between the PINK1 and HtrA2 *in vivo* (Tain, Chowdhury, *et al.* 2009). Several reports have shown that PINK1 binds Parkin and two controversial reports also showed that Parkin phosphorylation is dependent on PINK1 (Y. Kim *et al.* 2008; Sha *et al.* 2010), however others found no evidence of phosphorylation (Narendra *et al.* 2010; Vives-Bauza *et al.* 2010). The significance of the PINK1-Parkin interaction is discussed in detail below. Another function of PINK1 is in regulation of mitochondrial calcium buffering, as was shown in several studies where mitochondria in PINK1 deficient cells have elevated calcium levels in neuronal cell lines, cultured neurons, and recently in SNpc neurons of PINK1 deficient mice (Marongiu *et al.* 2009; Gandhi *et al.* 2009; Akundi *et al.* 2011). Using fluorescent probes specific for cytosolic and mitochondrial calcium, Gandhi *et al* demonstrated that PINK1 activity is specifically required for calcium efflux through the Na^+/Ca^{2+} exchanger (Gandhi *et al.* 2009). In a proteomics study, PINK1 was also implicated in the control of mitochondrial transport along microtubules, since the molecular complex of PINK1 and the

two kinesin-binding proteins Miro and Milton was found (Weihofen *et al.* 2009). PINK1 knockout mice, like Parkin and DJ-1 do not show any neurodegenerative phenotypes, even DJ-1/Parkin/PINK1 triple mutants have normal numbers of DA neurons (Kitada *et al.* 2009). Instead, PINK1 knockout mice resemble the embryonic Parkin knockouts, with minor mitochondrial deficiencies and decreased dopamine release (Kitada *et al.* 2007; Gautier *et al.* 2008; Gispert *et al.* 2009). In the future, it will be interesting to learn whether adult deletion of PINK1 and DJ-1 causes neurodegeneration, as seems to be the case for Parkin.

1.2.5. Parkin and PINK1 regulate mitochondrial dynamics

The first evidence for a function of Parkin in regulating mitochondria came in 2003 from *Drosophila*, when Greene *et al* analyzed a null mutant line for the *Drosophila* ortholog *park,* and found several phenotypes including severe muscle degeneration, which caused locomotive deficiencies and impaired sperm function causing sterility (J. C. Greene *et al.* 2003). Later, an additional small loss of dopamine neurons was reported (Whitworth *et al.* 2005). All of these tissues displayed dramatically enlarged, blob-like mitochondria with broken cristae. A year later, mitochondrial dysfunction was also reported in Parkin mutant mice (Palacino *et al.* 2004). In 2006, three groundbreaking studies were published simultaneously, which had analyzed *Pink1* mutant or RNAi depleted flies (J. Park *et al.* 2006; Clark *et al.* 2006; Y. Yang *et al.* 2006). Intriguingly, *Pink1* deficient flies phenocopied *park* mutants, and when Parkin was overexpressed in *Pink1* mutants, the phenotypes were fully rescued, but interestingly PINK1 overexpression did not rescue the *Pink1* mutant phenotypes. These two observations suggest that Parkin and PINK1 act in a common pathway regulating mitochondria, critical for the integrity of the phenotypic tissues, with PINK1 upstream of Parkin. A year later it was shown in HeLa cells that PINK1 knockdown causes mitochondrial fragmentation, which could be rescued by Parkin overexpression (Exner *et al.* 2007).

In many cell types, mitochondria appear as long tubules, interconnected in a dynamic network together with small round structures (D. C. Chan 2006; Westermann 2010). The morphology of the network is highly regulated by fusion and fission events, controlled by specific proteins. In mammals, mitofusins 1/2 (Mfn1/2) mediate outer membrane fusion, and optic atrophy 1 (Opa1) mediates inner membrane fusion, while the cytosolic dynamin related protein 1 (Drp1) together with mitochondrial fission 1 (Fis1) mediate fission. For many reasons, fusion and fission

are critical for maintaining a healthy pool of mitochondria, but fission also appears to be connected with apoptosis (Der-Fen Suen *et al.* 2008). In *park* and *Pink1* mutant *Drosophila,* the mitochondria appeared blob-like, indicating that the balance is shifted towards fusion, and indeed, decreasing fusion or increasing fission rescues the phenotypes (Poole *et al.* 2008; Deng *et al.* 2008; J. Park *et al.* 2009). In contrast, in mammalian cells where Parkin or PINK1 were acutely depleted, or in fibroblasts from *PINK1*-PD patients, the mitochondria appeared fragmented, indicating increased fission (Exner *et al.* 2007; Dagda *et al.* 2009; Lutz *et al.* 2009). Indeed, it was later shown that depleting Drp1 or overexpressing Opa1 could rescue mitochondrial phenotypes from Parkin or PINK1 depletion in SH-SY5Y cells, and conversely PINK1 or Parkin overexpression could rescue fragmentation from Drp1 overexpression (Lutz *et al.* 2009). The differences between the results from *Drosophila* and cultured mammalian cells are unlikely to be due to a complete switch of function of Parkin and PINK1 between the species. A more likely explanation is that Parkin and PINK1 control mitochondrial dynamics via an indirect mechanism, where Parkin or PINK1 deficiencies cause a basic mitochondrial dysfunction that is handled differently in the two systems.

1.2.6. A PINK1-Parkin pathway initiates mitophagy

Further insight into how Parkin and PINK1 might function in mitochondria came when it was shown that the normally cytosolic Parkin is recruited to mitochondria with decreased membrane potential by binding to PINK1, and promotes their degradation through mitophagy, the autophagy of mitochondria (Matsuda *et al.* 2010; Narendra *et al.* 2010; Vives-Bauza *et al.* 2010) (figure 1-7). One study reported that Parkin controls this process by ubiquitinating the voltage dependent anion channel 1 (VDAC1) (Geisler *et al.* 2010), whereas three other studies showed that Parkin ubiquitinates Mfn1/2 and proposed that this initiates mitophagy (Gegg *et al.* 2010; Ziviani *et al.* 2010; Poole *et al.* 2010). However, Tanaka *et al* showed that even though Parkin ubiquitinates Mfn1/2, Parkin-dependent mitophagy also occurred in Mfn1$^{-/-}$/Mfn2$^{-/-}$ mouse embryonic fibroblasts (MEFs). The function of mitophagy is believed to be clearing the cell of damaged mitochondria (Youle & Narendra 2011). How does the PINK1-Parkin mitophagy pathway fit with the studies showing a regulatory effect on fusion or fission? The question remains unanswered, but it is possible to speculate on different scenarios. For example, damaged mitochondria might undergo increased fission, as in the well known fragmentation upon oxidative stress or prior to cytochrome-c release (Der-Fen Suen *et al.* 2008). When blocking the
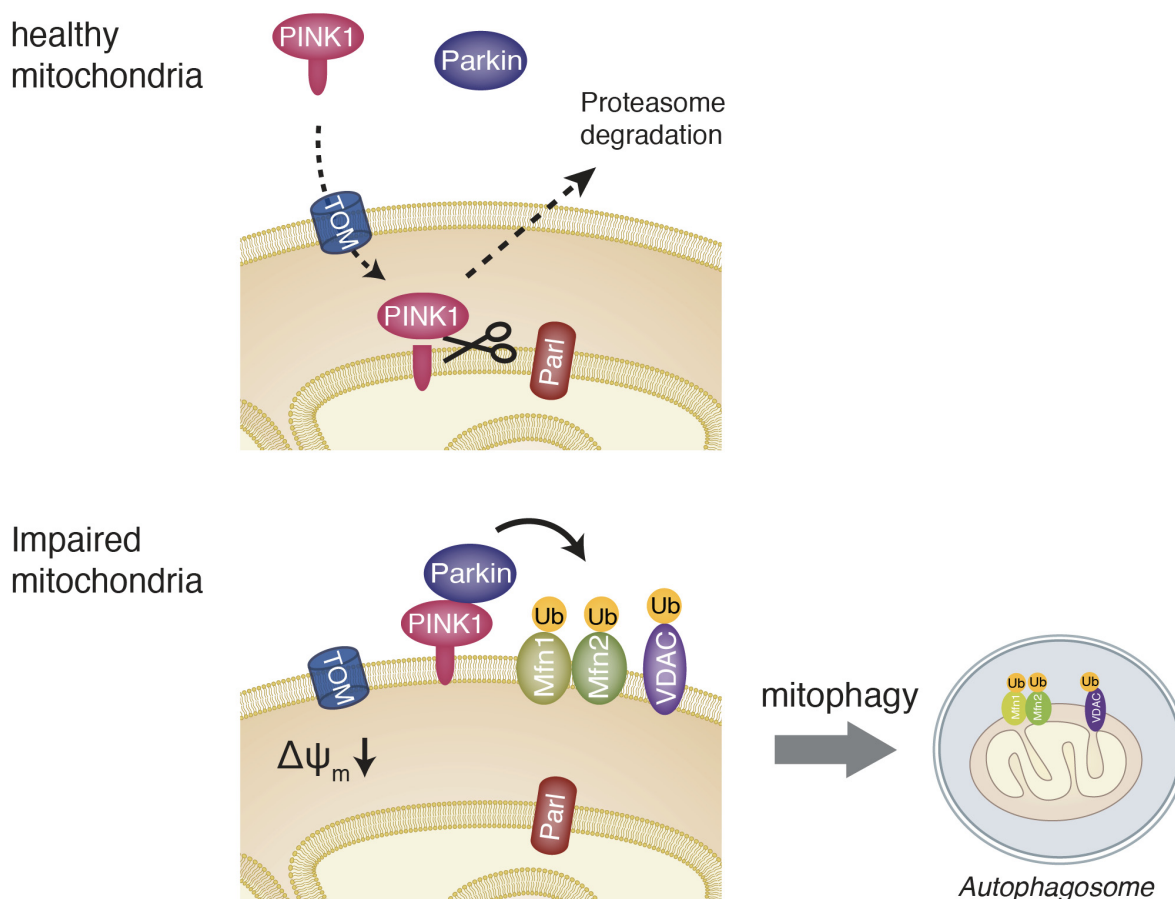
Figure 1-7 Model of the PINK1-Parkin pathway of mitochondrial quality control and initiation of mitophagy. In healthy mitochondria, PINK1 is maintained at low levels, as it is cleaved at the inner membrane by PARL, causing proteasomal degradation. When mitochondria are impaired and lose membrane potential, PINK1 is no longer imported to the inner mitochondrial membrane, instead it integrates in the outer membrane. There, PINK1, recruits Parkin, which ubiquitinates mitochondrial proteins such as Mfn1/2 and VDAC, and this initiates a mitophagic pathway leading to degradation of impaired mitochondria.

autophagic pathway by removing PINK1 or Parkin function, the mitochondrial fragments would accumulate, giving a fragmented morphology in the cell, without directly regulating fusion or fission. On the other hand, Parkin-mediated ubiquitination of mitofusins may simply target them for degradation, causing a shift in the balance towards fusion, as argued by Tanaka *et al* (A. Tanaka *et al*. 2010). The mitophagic pathway provides a cell biological and biochemical explanation for the genetic link between PINK1 and Parkin in *Drosophila*, and disruption of this pathway may be a step towards PD pathology. The model is somewhat inconsistent concerning the requirement of PINK1 in recruiting Parkin to the mitochondria, considering the fact that Parkin overexpression rescues the phenotypes of *Pink1* mutant *Drosophila*, without Pink1 being present for the recruitment. Most of the studies concerning the mitophagy pathway discussed above were performed in HeLa or similar cell lines, and interestingly a study using cultured
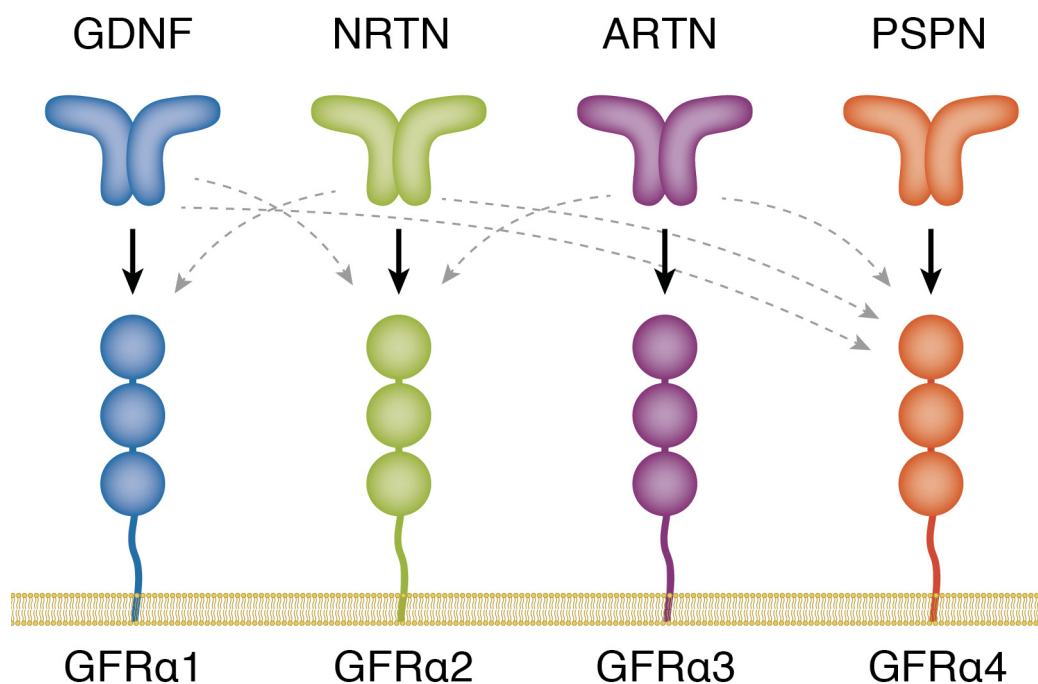
Figure 1-8 GDNF family of ligands bind to GDNF family receptor alpha's. GDNF binds primarily to GFRα1, and with low affinity to GFRα2 and GFRα4. Neurturin (NRTN), binds primarily to GFRα2, and with low affinity to GFRα1 and GFRα3, while Artemin (ARTN) binds primarily to GFRα3, and with low affinity to GFRα2 and GFRα4. Persephin (PSPN) on the other hand, binds selectivily to GFRα4

neurons failed to see Parkin translocation to depolarized mitochondria, due to their different bioenergetic properties (Van Laar *et al.* 2011). Also, it cannot be ruled out that loss of other functions of PINK1 and Parkin cause independent mitochondrial impairments – for PINK1 in regulating TRAP1, HtrA2 and calcium efflux, and for Parkin in regulating mitochondrial transport or the recently indentified PARIS transcription factor. The fact that PINK1 knockdown in HeLa cells, which due to oncogenic mutations in the cell line lack a functional Parkin gene (Denison *et al.* 2003), still causes robust mitochondrial fragmentation (Exner *et al.* 2007), also suggests that independent functions of PINK1 and Parkin control mitochondrial integrity. Further studies are required to clarify the link between mitophagy and mitochondrial dynamics, to explain the differences between the studies of *Drosophila* and mammalian cell lines, and to show the significance for Parkinson's disease.

1.3. GDNF/Ret signaling and its function in dopamine neurons

1.3.1. Overview of neurotrophic factors and their receptors
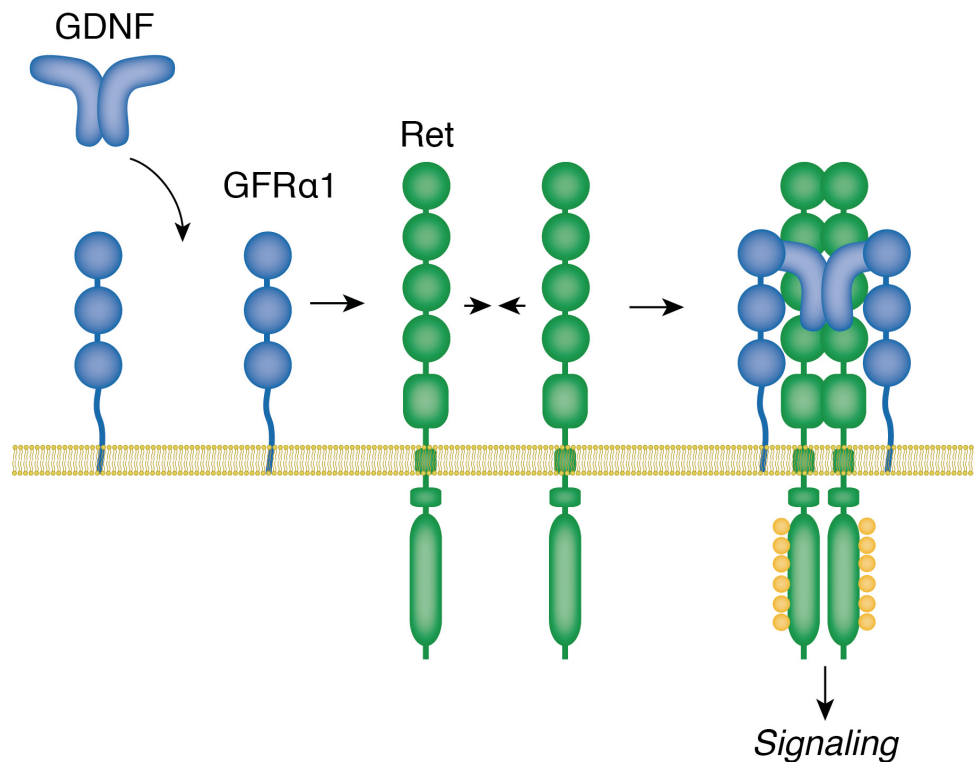
Figure 1-9 Model of GDNF signaling via GFRα1 and Ret. The secreted GDNF protein forms a native homodimer, which binds to a dimer of GPI linked GFRα1 on the cell surface. Upon GDNF binding, GFRα1 can bind to a dimer of the transmembrane receptor tyrosine kinase Ret, which causes trans-autophosphorylation of the intracellular kinase domains and subsequent activation of intracellular signaling cascades. Whether Ret is predimerized at an inactive state prior to GDNF/GFRα1 binding, or whether it dimerizes upon binding is unclear.

Neurotrophic factors are secreted proteins that can promote the survival, development and plasticity of neurons. The original neurotrophic theory postulates that during development of the nervous system, neurons are formed in excess but are dependent on neurotrophic factors for their survival. These factors are secreted by the target tissues and taken up by the terminals of the growing axons. Neurons that extend their axons to the correct target will survive, while neurons that do not find the sources of target-derived neurotrophic factors are eliminated. Such a system allows a target tissue to regulate its innervation by eliminating both excess of innervation and misprojecting fibers. The neurotrophic factors can be grouped into four families, the first being the neurotrophins, comprised of nerve growth factor (NGF) and the structurally related brain-derived neurotrophic factor (BDNF), neurotrophin 3 and neurotrophin 4/5. A second family is the GDNF family of ligands (GFLs), distantly related to the TGF-ß superfamily, which in addition to GDNF contains its three paralogs artemin (ARTN), neurturin (NRTN), and persephin (PSPN). The third family of neurotrophic factors is the neuropoietic cytokines, and

the fourth family is formed by the recently discovered cerebral dopamine neurotrophic factor (CDNF) and mesencephalic astrocyte-derived neurotrophic factor (MANF). Currently, many other functions of neurotrophic factors have been discovered, outside the scope of the original neurotrophic theory, such as regulation of migration, neurite branching, synaptogenesis, and synaptic plasticity (A. M. Davies 1996).

1.3.2. The GDNF family of ligands signal via GFRαs, -Ret, and NCAM

Each of the GFLs binds to a GDNF family receptor alpha 1-4 (GFRα-14) (figure 1-8) in a homodimeric state. GDNF itself binds primarily to GFRα1, although some promiscuity exists (Airaksinen & Saarma 2002). The GFRαs cannot transduce signaling to the cell by themselves as they lack an intracellular domain, instead they bind to the plasma membrane with a glycosylphosphatidylinositol (GPI) anchor and function as co-receptors. Two receptors for the GFRα/GFL complexes have been found: The first identified was rearranged during transfection (Ret), belonging to the receptor tyrosine kinase family of receptors (Durbec *et al.* 1996; Trupp *et al.* 1996). Later, it was found that the neural cell adhesion molecule (NCAM) can serve as a receptor for GDNF/GFRα1 (Paratcha *et al.* 2003). GDNF signaling via NCAM activates focal adhesion kinase (FAK) and Fyn kinase, which function in neuronal migration. GDNF signaling via NCAM was also found to act as a chemoattractant for cells in the rostral migratory stream (Paratcha & Ledda 2008). According to the established model of Ret signaling, Ret does not bind to GFRα alone, but rather to the GFL/GFRα complex, after which Ret undergoes dimerization and trans-autophosphorylation of the intracellular tyrosine kinase domains (figure 1-9) (Schlee *et al.* 2006). However, it has also been proposed that Ret undergoes predimerization prior to GFL/GFRα binding, but does not turn catalytically active until the GFL binds (Knowles *et al.* 2006).

1.3.3. Ret is evolutionary conserved in vertebrates and *Drosophila*

Ret is evolutionary conserved in all vertebrates examined from human to zebrafish (Airaksinen *et al.* 2006). Also, *Drosophila* has a clear *Ret* homolog, *Dret*, and in addition another possibly related gene, the recently cloned *stitcher* (S. Wang *et al.* 2009). Orthologs of the four GFRα's have been identified in all examined vertebrates, but not all four of the GFLs appear to be conserved, suggesting a certain redundancy in the system. *Drosophila* has a homolog of the GFRαs called GFR-like, but to date no *Drosophila* homologs of the GFLs have been described. Interestingly, Dret was overexpressed in cell culture and could activate many of the same
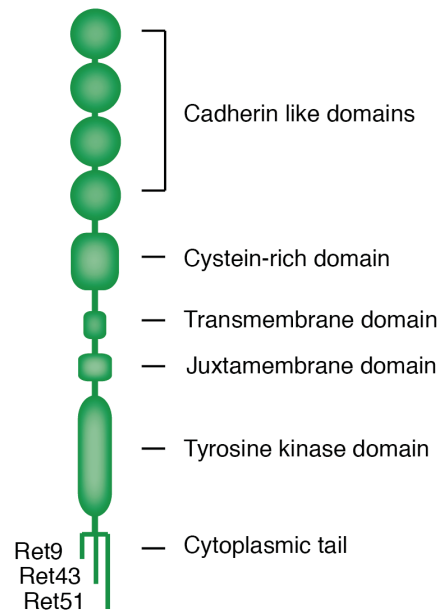
Figure 1-10 Domain structure of mammalian Ret. The Ret protein contains an extracellular domain with four cadherin-like domains and a cystein-rich domain. A transmembrane domain spans the plasma membrane, and the intracellular domain, in turn, contains a juxtamembrane domain, a tyrosine kinase domain, and a cytoplasmic tail. Ret is found in three splice isoforms with different lengths of the cytoplasmic tail, Ret9, Ret43, and Ret51.

pathways as mammalian Ret (Abrescia *et al.* 2005) and expression analysis studies have shown that Dret is expressed in many analogous tissues to human Ret, such as in neuroendocrine cells, peripheral neurons, and the ventral nerve cord during development, suggesting a conserved function (Sugaya *et al.* 1994; Hahn & Bishop 2001; Fung *et al.* 2008).

1.3.4.   Ret domain structure and tyrosine kinase signaling

The human Ret transcript is spliced into three isoforms, expressing proteins with different lengths of the carboxy-terminal cytoplasmic tail: Ret9, Ret43 and Ret51, representing the number of amino acids in the tail domain. However Ret43 is not as evolutionarily conserved as the others, and also not as well studied (figure 1-10). The extracellular domain of Ret contains four cadherin-like domains, and a cysteine-rich domain. The intracellular domain contains a juxtamembrane domain, and a tyrosine kinase domain with 16-18 tyrosines residues, out of which six have been implicated to be involved in signaling. In addition, the long isoform Ret51 has the additional Y1096 not not present in the cytoplasmic tails of the shorter isoforms. When phosphorylated, these tyrosines can recruit a large number of adaptor proteins (figure 1-11): Y752 and Y928 bind signal transducer and activator of transcription 3 (STAT3), Y905 binds growth factor-bound protein 7/10 (Grb7/10) (Pandey *et al.* 1996), Y981 binds Src and Y1015
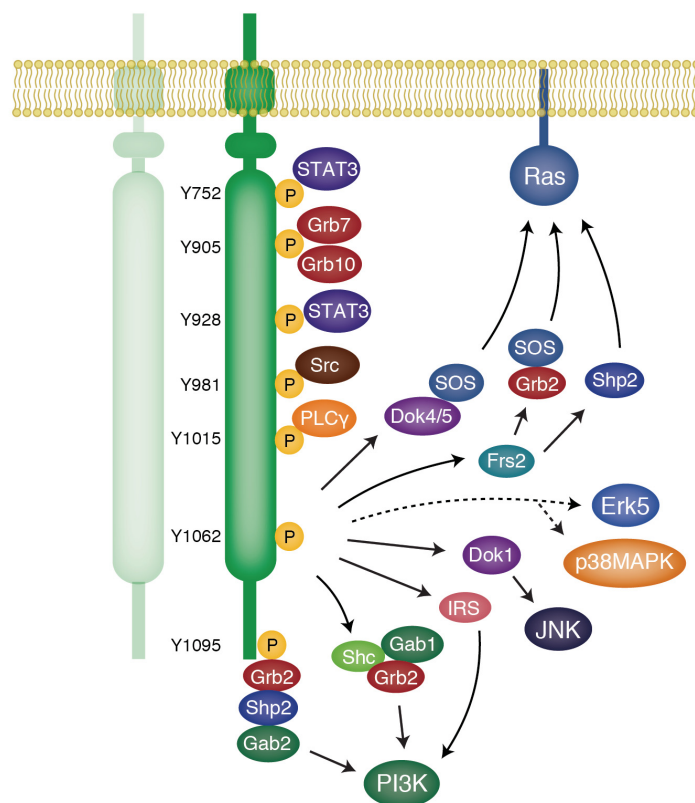
Figure 1-11 Phosphotyrosines of the kinase domain recruit adaptor proteins and initiate signal transduction. The kinase domain of mammalian Ret contains six signaling tyrosines, and in addition, the long isoform Ret[51], contains the additional Y1095. The signaling tyrosines recruit a number of adaptor protein complexes, which leads to the activation Ras, PI3K, JNK, p38MAPK, Erk5, PLCγ, STAT3, Src, and their downstream signaling pathways.

binds phospholipase C-gamma (PLC γ) (Schuringa *et al*. 2001; Pandey *et al*. 1996; Mario Encinas *et al*. 2004; Borrello *et al*. 1996). Of particular importance is Y1062, which acts as a binding site for a variety of adaptors and thereby, is responsible for the activation of several different signaling pathways (Hayashi *et al*. 2000). Binding of Fibroblast growth factor receptor substrate 2 (Frs2) causes activation of Ras-Erk signaling, either in a transient manner via Grb2 and son of sevenless (SOS), or alternatively by binding to Src homology domain-containing phosphatase 2 (Shp2), which leads to a more sustained activation (Hayashi *et al*. 2000; Kurokawa *et al*. 2001). In addition, docking protein (Dok) 4/5 binding to Y1062 together with SOS also activates Ras. Dok1 binding to Y1062, on the other hand, was reported to active c-jun N-terminal kinase (JNK) signaling (Hayashi *et al*. 2000). Y1062 also mediates phosphoinositide-3-kinase (PI3K) signaling via recruitment of the Src homology domain-containing (Shc)/Grb2/Grb-associated-binding protein 1 (Gab1) complex, or via insulin receptor substrate (IRS) binding (Besset *et al*. 2000; R M Melillo *et al*. 2001). In addition, Y1062 has been shown to be critical for activation of ERK5 and p38MAPK signaling through an unknown mechanism

(Drosten & Pützer 2006; Kodama *et al.* 2005). The last signaling tyrosine, Y1092 which is only present in the long Ret51 isoform, binds to Grb2, but only mediates activation of PI3K via a Gab2/Shp2 complex (Besset *et al.* 2000).

1.3.5.   Functions of Ret in development

Ret has important functions during development and is expressed in the kidney, the enteric nervous system (ENS), testis, cranial ganglia, motor neurons in the spinal cord, and midbrain. GDNF/Ret signaling appears to be particularly critical for kidney and ENS morphogenesis, as mice lacking either Ret, GFRα1 or GDNF die soon after birth due to severe kidney dysfunction and intestinal aganglionosis (Schuchardt *et al.* 1994; M. W. Moore *et al.* 1996; Pichel *et al.* 1996; Sánchez *et al.* 1996; Enomoto *et al.* 1998; Cacalano *et al.* 1998). In the developing kidney, GDNF is secreted by the nephrogenic mesenchyme, whereas Ret is expressed in the tips of the uretic buds. By secreting GDNF, the mesenchyme can induce bud-branching (Hellmich *et al.* 1996; Sainio *et al.* 1997). Another example of how GDNF/Ret signaling functions in development, is during spermatogenesis, where Sertoli cells secrete GDNF, which is received by Ret in undifferentiated spermatogonia (Meng *et al.* 2000). Mice heterozygous for GDNF have lower numbers of spermatogenic stem cells, whereas mice overexpressing GDNF show increased numbers of undifferentiated spermatogonia (Viglietto *et al.* 2000). Together these data suggest that GDNF promotes self-renewal of spermatogonia, in favour of differentiation. A third developmental function of GDNF/Ret signaling is to promote growth of motor neurons during hind limb development. At the choice point of dorsal or ventral innervation, axons in GDNF or Ret null mice were shown to choose a ventral trajectory to a higher extent than in controls, as GDNF act as a chemoattractant (Kramer *et al.* 2006; Dudanova *et al.* 2010). Interestingly the two main isoforms of Ret, Ret9 and Ret51 are differentially expressed in some tissues and are believed to have somewhat different functions. In a study by Graaf *et al*, monoisoformic mice were generated, and the mice lacking the Ret9 isoform showed a similar phenotype to null mice, whereas mice lacking Ret51 only showed minor phenotypes (de Graaff *et al.* 2001). These results were, however, contradicted by another study where both Ret9 and Ret51 monoisoformic mice developed normally, suggesting that they compensate for each other (Jain, Mario Encinas, *et al.* 2006).

1.3.6.   Ret signaling in disease
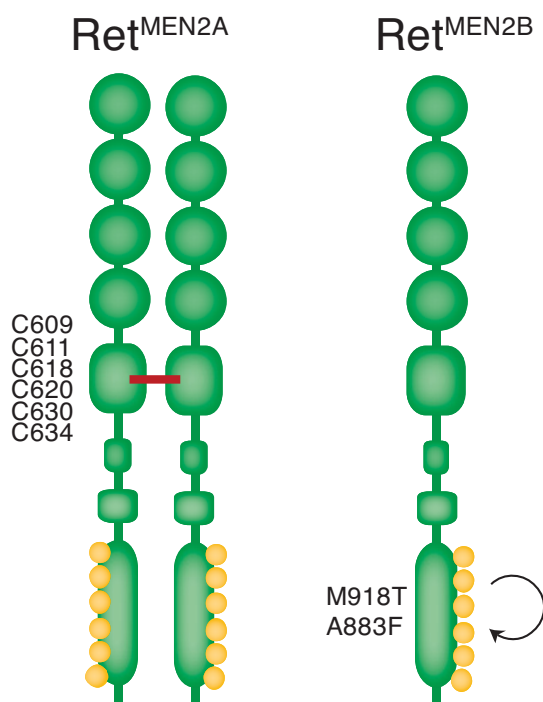
Figure 1-12 Activating mutations in Ret cause multiple endocrine neoplasia type 2. The majority of mutations causing MEN2A are located in the cysteine-rich domain, creating abnormal disulphide bridges, leading to dimerization and constitutively active signaling. Conversely, most MEN2B-causing mutations are located in the kinase domain, generating a conformational change, also leading to constitutive activity, either as a monomer or dimer.

Ret was originally identified in a transformation assay with DNA from a T-cell lymphoma, and has been implicated in several diseases. Ret gain-of-function mutations are the primary cause of multiple endocrine neoplasia type 2 (MEN2), a syndrome characterized by medullary thyroid carcinoma (MTC), together with other symptoms. Depending on which other symptoms accompany the carcinoma, MEN2 can be subdivided in MEN2A, MEN2B and FMTC (familial MTC). Interestingly, patients with MEN2A typically have mutations in one of six cysteines in the cysteine-rich domain, causing dimerization through the formation of abnormal covalent disulphide bridges and subsequent autoactivation of the receptor (figure 1-12) (Massimo Santoro *et al.* 2002). MEN2B patients, on the other hand, typically have mutations in the intracellular kinase domain; around 95 % of the cases are specifically caused by the M918T mutation (figure 1-13). These mutations are thought to cause a conformational change of the kinase domain, generating autoactivation either as a monomer or a dimer (R. M. Hofstra *et al.* 1994). Patients with MEN2B mutations are also reported to have increased autophosporylation of Y1062 (D. Salvatore *et al.* 2001), leading to a shift in substrate specificity. FMTC patients do not show any additional symptoms, and may have mutations either in the cysteine-rich domain or in the kinase domain. To date, it is not clear why the different types of mutations cause different symptoms in

MEN2A and MEN2B patients. Mutations in Ret can also cause Hirschprung's disease (HSCR), characterized by a lack of the distal segments of the enteric nervous system. HSCR mutations are scattered all over the *Ret* gene, some of them in the kinase domain were studied in detail and were found to cause kinase inactive receptors (Francesca Carlomagno *et al.* 1996), suggesting that HSCR is a *Ret* loss-of-function disease.

1.3.7. GDNF/Ret signaling protects dopamine neurons from toxins and promotes resprouting

GDNF was first isolated from primary ventral midbrain cultures in 1993 for its ability to promote survival of cultured dopamine neurons (L. F. Lin *et al.* 1993). When supplying recombinant GDNF to the cultures at a low concentration of 1 ng/ml over three weeks, it tripled the survival specifically of DA neurons. After this initial discovery, it did not take long until other researchers reported that GDNF infusion protects dopamine neurons in mice from MPTP or 6-hydroxy-dopamine (6-OHDA) lesions (Tomac *et al.* 1995) and soon thereafter, the same effect was reported in primates (Gash *et al.* 1996). Two early clinical trials showed positive results with improvements of motor functions in patients that were delivered GDNF by intracranial infusion (Gill *et al.* 2003; Slevin *et al.* 2005), but a larger phase II trial unfortunately did not show the same positive results and had to be cancelled prematurely (Lang *et al.* 2006). However, there is a large ongoing clinical development of GDNF and other GFL-based therapies for PD using viral vectors and other delivery systems (Kordower *et al.* 2000). There is also an ongoing effort to develop small molecule GDNF mimetics that could allow more efficient delivery (Bespalov & Saarma 2007).

1.3.8. Physiological function of GDNF/Ret in survival of dopamine neurons

The studies described above have collectively shown that supplying exogenous GDNF to various systems can protect against dopamine cell death, and promote resprouting of axonal fibers after lesions. However, after 18 years of GDNF-signaling research, our understanding of its physiological function in dopamine neurons is still very limited. GDNF is expressed in several areas of the adult mammalian brain, with the highest levels are found in the striatum, cerebellum, olfactory bulb and hippocampus. The origin of striatal GDNF is debated, but it has been suggested that it is secreted by GABAergic and cholinergic interneurons (Bizon *et al.* 1999). Ret and GFRα1 are expressed on the terminals of dopaminergic striatal axons, but also in cell bodies in the midbrain. Mice overexpressing a constitutively active version of Ret, analogous to human Ret^{MEN2B} mutations, showed an increased number of DA neurons in the SNpc (Mijatovic *et al.*

2007). Surprisingly however, knockout mouse models of GDNF, GFRα1or Ret, even though they die soon after birth, develop with a normal complement of DA neurons, suggesting that GDNF-Ret signaling does not play an important role in DA neuron development (M. W. Moore *et al.* 1996; Enomoto *et al.* 1998; Schuchardt *et al.* 1994). In a recent study, mice with a floxed *Ret al*lele, recombined at early embryonic stages using either a dopamine neuron specific *Cre* line (*DAT*) or a pan-neuronal *Cre* line (*nestin*), were followed until 24 months of age. At 9 months, a small decrease in the density of striatal DA fibers was seen, and at 12 months there was a significant loss of TH+ neurons in the SNpc. At 24 months, the decrease of TH+ striatal fibers had reached 60 %, and the loss of TH+ SNpc neurons had reached 38% (Kramer *et al.* 2007). These results were however not supported by another study where no neurodegeneration was observed up to 12 months, although it is possible that by pooling mice between 6 and 12 months, a milder phenotype may have been obscured (Jain, Golden, *et al.* 2006).

Another recent study investigated the physiological role of GDNF in dopamine neurons by ablating GDNF in the brains of two month old mice using a floxed *GDNF* allele and a tamoxifen-inducible Cre line. These mice underwent a dramatic degeneration - at seven months they showed a loss of 60-70 % of TH+ neurons in SNpc, and the noradrenergic neurons in the coeruleus locus were almost absent. However, the authors used an unusually high dosage of tamoxifen, and it is possible that the effects may partially be due to toxicity of this drug, since Ret signaling was shown to protect against tamoxifen toxicity (Plaza-Menacho *et al.* 2010). Still, it opens up the question of whether the significantly stronger phenotype of the *GDNF* knockout than of that of the *Ret* knockout is due to the presence of alternative GDNF receptors, or whether it is an effect of adult deletion, circumventing potential mechanisms that might compensate for an embryonic loss of function. No pro-survival function of NCAM has been reported for DA neurons, but it is worth considering NCAM as such an alternative. Further studies that delete *Ret* and *GDNF* using the same method are required to better characterize the difference of ablating the two genes.

1.3.9. Mechanism of GDNF/Ret mediated neuroprotection remains unclear

The studies deleting GDNF or Ret in mice have shown that Ret has a physiological function in promoting the survival of dopamine neurons during aging. It remains largely unclear, however, what underlying mechanism that protects against cell death in these aging cells on a

cellbiological/biochemical level, and importantly how it functions. In cultured neurons or neuronal cell lines, Ret has been shown to activate the PI3K/Akt, Ras/Erk, PLCγ, JNK, p38MAPK, and Src kinase signaling pathways (Kurokawa *et al.* 2003). The PI3K/Akt pathway in particular, has been shown several times to be highly important for neuronal survival and is activated by GDNF (Dudek *et al.* 1997; Ries *et al.* 2006; Neff *et al.* 2002), however, the role of the Akt pathway in the specific context of Ret signaling during aging has not been investigated. Even less certain is which critical cellular functions such a pathway helps to maintain, to be able to protect against dopamine neuron degeneration. In a study using cultured sympathetic neurons from knockin mice with different signaling mutant versions of Ret, it was found that sympathetic neuron survival is independent of Akt, but instead relies on a B-Raf/inhibitor of kappa-B kinase (IKK) pathway (M Encinas *et al.* 2008). It was also recently reported that GDNF overexpression in the striatum of rats caused an upregulation of TH and delta-like 1 homolog (Dlk1), a transcription factor involved in proliferation, in the SN but the mechanism of upregulation is unclear (Christophersen *et al.* 2007). Now that it is known that GDNF/Ret signaling has an important function for the survival of aging nigrostriatal neurons, future studies are required to elucidate the nature of this function.

1.4.   Purpose of thesis project

In this project I sought to gain new insight into the mechanisms by which GDNF/Ret signaling promotes the survival of midbrain dopamine neurons during aging. Novel information in this field would contribute to our general understanding of the functions of neurotrophic factors in adults, and in particular, it would help answer the important question of why dopamine neurons need GDNF.

During the past decade, familial forms of Parkinson's disease have been mapped and the functions of the associated proteins are rapidly being elucidated by scientists worldwide. These novel functions led us to hypothesize that Ret signaling cooperates with the ARPD-associated proteins in maintaining certain cellular functions that are specifically critical for SNpc dopamine neuron survival. Such cellular functions may include signal transduction pathways, transcriptional regulation, and mitochondrial integrity. This hypothesis would explain why *GDNF* and *Ret* mutant mice develop parkinsonism like phenotypes, it would also provide an important mechanism of action for a potential future Parkinson's disease therapeutics. In addition, exploring this theory may provide new insight into the physiological functions of ARPD-associated proteins.

To test the hypothesis, I asked the following specific questions:

i.   Is combined *Ret* and *DJ-1* activity critical for the survival of dopamine neurons in aging mice?

ii.   Do Ret and DJ-1 target a common signal transduction pathway?

iii. Can Ret signaling reverse mitochondrial impairments caused by Parkin or PINK1 depletion *in vitro*?

iv.   Can Ret signaling complement *park* or *Pink1* loss-of-function in *Drosophila*?

v.   Is combined *Ret/Parkin* and/or *Ret/PINK1* activity critical for the survival of dopamine neurons in aging mice?

2. Results

2.1. Genetic interaction between Ret and DJ-1 in maintenance of nigrostriatal dopamine neurons during aging in mice

2.1.1. Combined activity of Ret and DJ-1 required for the survival of midbrain dopamine neurons in aging mice

Dopaminergic conditional Ret knockout mice, (DAT-Cre;Ret$^{lx/lx}$), hereafter named "Ret", have previously been reported by our group to develop a progressive, mild and highly age dependent loss of dopaminergic neurons in the SNpc, together with a larger loss of dopaminergic axonal fibers in the striatum – a phenotype that in many aspects resembles Parkinson's disease. Knockout models of the mouse homolog of the ARPD-causing gene DJ-1 however, do not show neurodegenerative phenotypes, only mild synaptic defects, but importantly no loss of nigral neurons (R. H. Kim, P. D. Smith, *et al.* 2005; Goldberg *et al.* 2005; Linan Chen *et al.* 2005; Chandran *et al.* 2008; Yamaguchi & J. Shen 2007). Thus, we hypothesized that Ret signaling interacts genetically with DJ-1, and we wanted to test whether mice lacking both Ret and DJ-1 undergo increased neurodegeneration. For this purpose, Ret mice were crossed with mice carrying a DJ-1 null allele ("DJ-1") (T.-T. Pham *et al.* 2010), resulting in mice that lack Ret specifically in dopaminergic cells and DJ-1 in all cells. In addition to being active in dopaminergic cells, the DAT-Cre recombinase is also expressed in the germ line, hence when crossing DAT-Cre;Ret^{lx} to the DJ-1 allele, Ret was frequently recombined in all cells, generating lx/null heterozygous mice, which is the final genotype that was analyzed.

2.1.2. Increased loss of substantia nigra neurons in mice lacking both *Ret* and *DJ-1*

DAT-Cre;Ret$^{lx/-}$;DJ-1$^{-/-}$ (*Ret/DJ-1)* double mutant mice, together with *DJ-1* and *Ret* single mutants and mixed littermate controls were analyzed at 3, 18, and 24 months of age. Stereological quantifications of dopamine neurons of the ventral midbrain were performed in coronal brain sections immunostained for the dopamine neuron marker tyrosine hydroxylase (TH). At 3 months, the number of dopamine neurons in *Ret/DJ-1* double mutant mice remained unchanged as compared to control mice, in both the SNpc and in the VTA (data not shown). At 18 months, *DJ-1* mutant mice showed no significant loss of neurons in the SNpc, in agreement with previous reports (figure 2-1a,c). *Ret* mice showed a 24% reduction of TH+ neurons in the
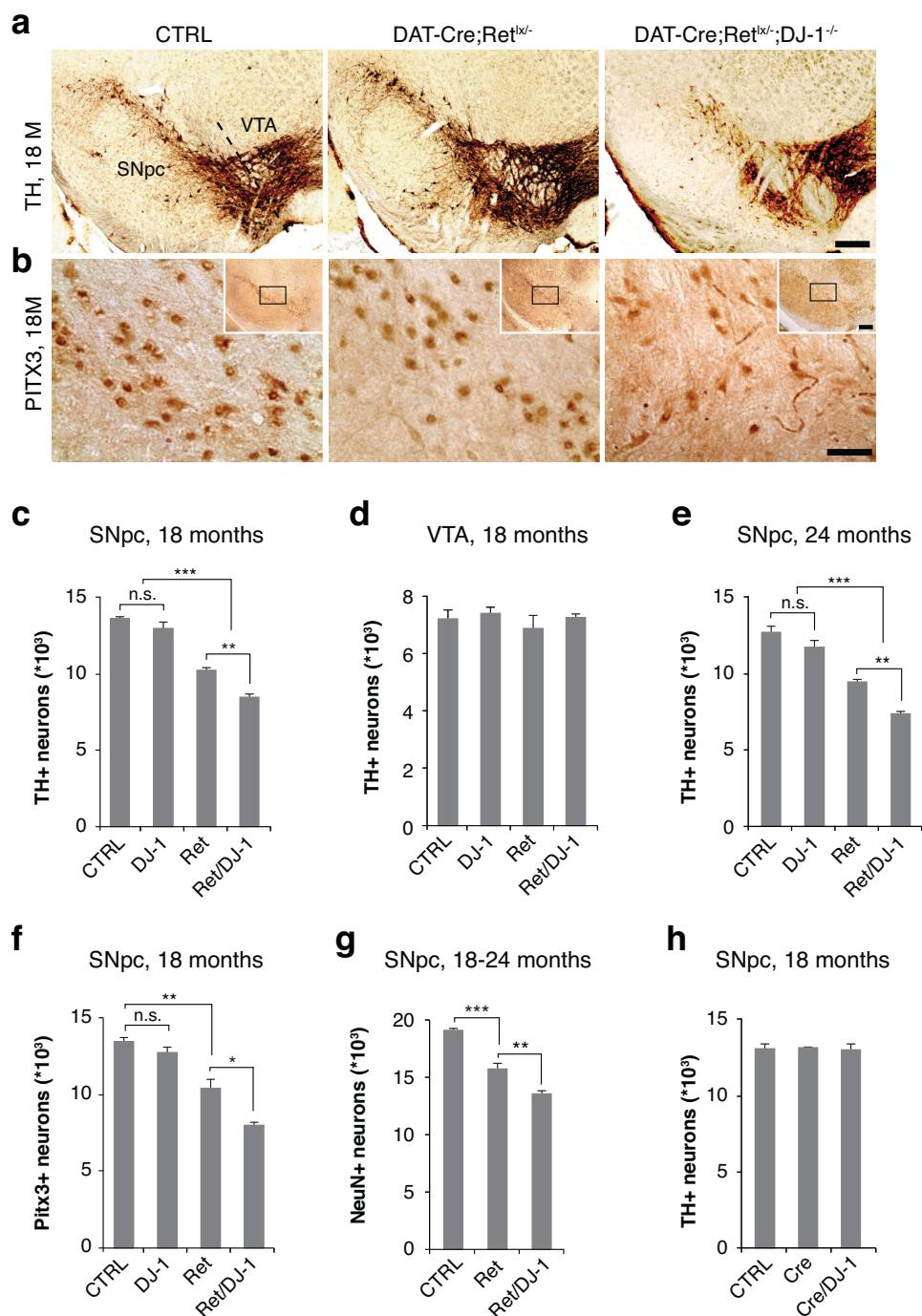
Figure 2-1 Combined activity of *Ret* and *DJ-1* is required for the survival of dopamine neurons in aged mice. (a-b) Photomicrographs of coronal brain sections from 18 month old control, *DJ-1*, *Ret*, and *Ret/DJ-1*, *DAT-Cre* and *DAT-Cre/DJ-1* mutant mice showing dopamine neurons in the substantia nigra (SNpc) and the ventral tegmental area (VTA) stained for the DA markers TH (a) and Pitx3 (b). (c-h) Stereological quantifications of DA neurons: (c) TH+ SNpc neurons at 18 months, (d) TH+ VTA neurons at 18 months, (e) TH+ SNpc neurons at 24 months, (f) Pitx3+ SNpc neurons at 18 months, (g) NeuN+ SNpc neurons at 18-24 months, (h) TH+ SNpc neurons at 18 months. n=5 mice per genotype, means ± SEM, * $p<0.05$, ** $p<0.01$, *** $p<0.001$, Student's t-test. n.s. = not significant. Scale bars: (a) 250 µm, (b) 50 µm. Complete genotypes: *mixed controls, DJ-1^-/-, DAT-Cre;Ret^lx/-, DAT-Cre;Ret^lx/-;DJ-1^-/-, DAT-Cre, DAT-Cre;DJ-1^-/-*. Mice were bred by Liviu Aron, perfusions and histological preparations were performed by L. Aron and P. Klein, immunostainings were performed by L. Aron, stereological quantifications in (c),(e),(f),(g),(h) were performed by L. Aron, (d) and (f) by P. Klein.

SNpc as compared to controls, while *Ret/DJ-1* double mutant mice showed a reduction of 37%, indicating that combined loss of *DJ-1* and *Ret* in SNpc neurons caused increased neurodegeneration. There was no reduction in the number of neurons in the VTA indicating an intrinsic difference in sensitivity to *Ret/DJ-1* loss-of-function between the two neuronal populations (figure 2-1d). In 24 month old mice, the loss of TH+ neurons in the SNpc remained similar to that of 18 month (25%), while *Ret/DJ-1* double mutants displayed a 41% reduction compared to controls - a further reduction in double mutants compared to *Ret* single mutants with increasing age. To verify that the reduced quantified number of neurons was not due to decreased expression of TH, sections were also stained for another dopaminergic marker, Pitx3 and counted, with similar results (2-1b,f). Also the pan-neuronal marker neuronal nuclei (NeuN) indicated a loss of total neurons in the SNpc area (figure 2-1g). To control for a genetic interaction between *DJ-1* and the *DAT-Cre* line, TH+ neurons in *DJ-1/DAT-Cre* mice were quantified at 18 months, but no loss of neurons was observed as compared to control or *DAT-Cre* (2-1h). Therefore, the possibility that the loss of neurons was due to an interaction between *DJ-1* and the *DAT-Cre* line could be excluded.

2.1.3.   No further loss of striatal dopaminergic fibers in double mutant mice

It has previously been shown that *Ret* mice lose a substantial amount of fibers in the striatum, reaching approximately 40% at 12 months and 63% at 24 months (Kramer *et al.* 2007) – numbers that highly exceed the loss of TH+ SNpc cell bodies at the same time points. To assess whether *Ret/DJ-1* double mutant mice lose additional fibers, coronal brain sections from 18 and 24 month old mice were immunostained for two independent dopaminergic markers, TH and DAT, (experiments performed by L. Aron). Fiber density in the dorsal striatum was quantified using an automated counting grid-based algorithm on thresholded images. The analysis showed that aged *Ret* mutant mice had lost approximately 33% of the TH+ fibers at 18 months and 52 % at 24 months, and 54% of the DAT+ fibers at 24 months compared to controls (data not shown). Interestingly, there was no significant further reduction of fibers in the *Ret/DJ-1* double mutant mice, indicating that *DJ-1* is only required for promoting the survival of the dopamine neurons, but not for maintaining their target innervation.

2.1.4.   Increased locomotion and striatal dopamine in *DAT-Cre* mice – no reduction in *Ret/DJ-1* double mutants
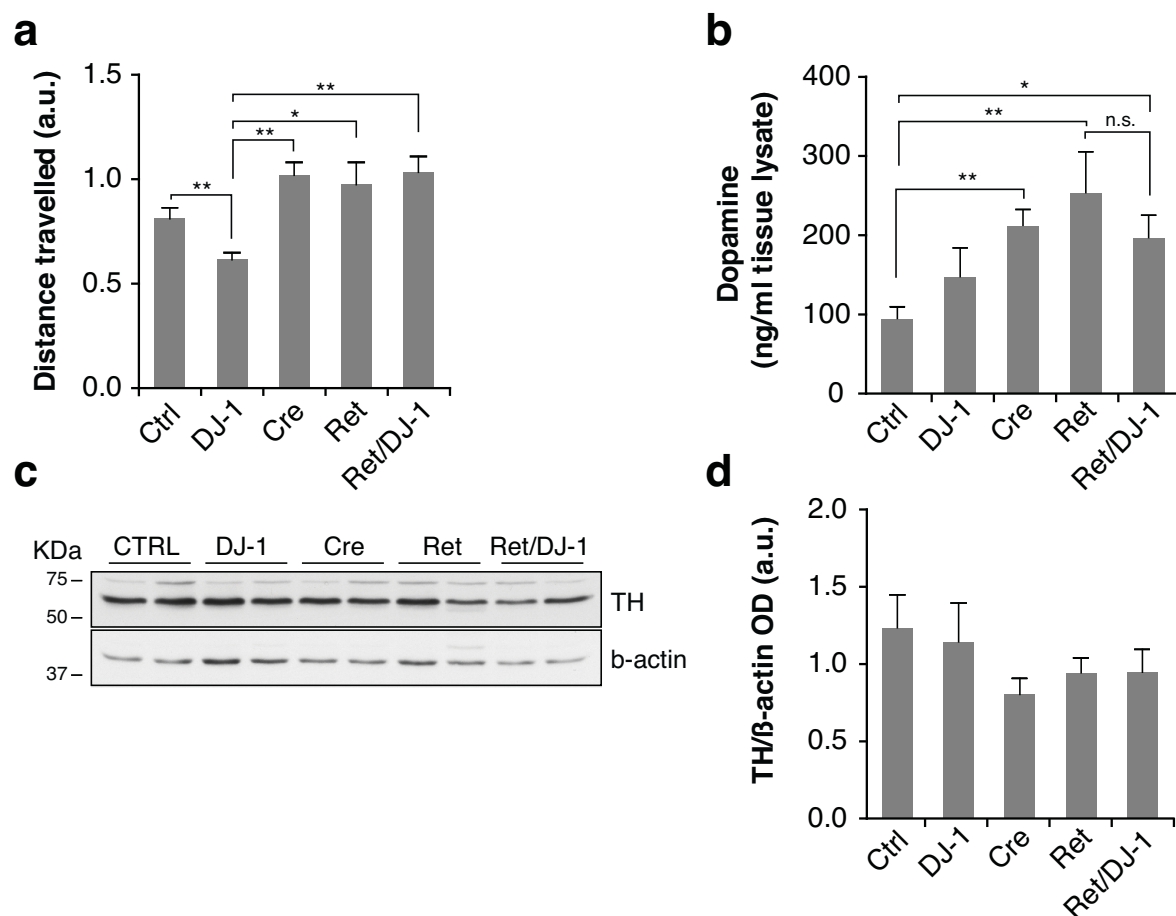
Figure 2-2 Increased behavior and striatal dopamine in *DAT-Cre* mice, no reduction in *Ret/DJ-1* mutants. (a-c) Extended analyses of 18-24 month old control, *DJ-1, Ret*, and *Ret/DJ-1, DAT-Cre* mice. (a) Behavioral assessment of 18-24 month old mice in an open-field arena where horizontal movement was automatically tracked during 20 min, n=7-16 mice per genotype, (b) HPLC measurement of total striatal dopamine content of 18 month old mice, n=5-7 mice per genotype, (c) representative western blot of striatal lysate from 24 month old mice, anti-TH and beta-actin antibodies as indicated (d). Optical density measurement of 3 western blots from (c) n=5-8 mice per genotype, means ± SEM, * $p<0.05$, ** $p<0.01$, one-way ANOVA with Bonferroni's post-hoc test. Complete genotypes: *mixed controls, DJ-1$^{-/-}$, DAT-Cre;Ret$^{lx/-}$, DAT-Cre;Ret$^{lx/-}$;DJ-1$^{-/-}$, DAT-Cre.* Behavior experiment (a) was performed by L. Aron and P. Klein. HPLC samples were prepared by P. Klein, HPLC was performed by Birgitte Nuscher (LMU, Munich).

Behavioral symptoms in PD as well as in mouse models typically appear when more than 60-70 % of the SNpc neurons are lost. On the other hand, behavioral alterations in PD models may appear without an accompanying loss of neurons being due solely to impaired synaptic function. In order to examine whether the *Ret/DJ-1* double mutant mice show any differences in overall locomotion, 18-24 month old mice were subjected to behavioral assessments, where movements were tracked during 20 minutes in an open field arena (figure 2-2a). The results indicated that *DJ-1* mutant mice had reduced locomotion as compared to controls, in agreement with previous reports (Goldberg *et al.* 2005; Chandran *et al.* 2008; Yamaguchi & J. Shen 2007). Mice carrying the *DAT-Cre* allele showed increased activity, also reported previously, and likely explained by
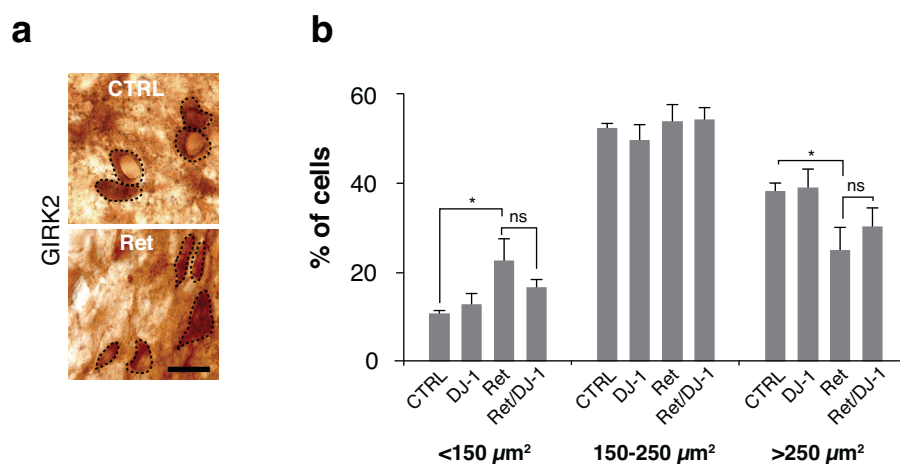
Figure 2-3 Smaller cell bodies of SNpc dopamine neurons in *Ret* mice – no increase in *Ret/DJ-1* double mutants. (a) Photomicrograph of coronal brain sections from control or *Ret* mice, immunostained for the DA marker GIRK2, with cell bodies outlined, scale bar=50 µm (b) Percentage of GIRK2+ SNpc cell bodies with areas <150 µm², 150-250 µm, or >250 µm² from control, *DJ-1*, *Ret* or *Ret/DJ-1* mutant mice. n=149-274 cells per animal, 5-7 animals per genotype, means ± SEM, * p<0.05, one-way ANOVA, Bonferroni's post-hoc test. Complete genotypes: *mixed controls, DJ-1⁻ᐟ⁻, DAT-Cre;Retˡˣᐟ⁻, DAT-Cre;Retˡˣᐟ⁻;DJ-1⁻ᐟ⁻.*

the reduced expression of the dopamine transporter, which decreases dopamine reuptake in the striatum. The *Ret* mice, as well as *Ret/DJ-1* double mutant mice showed the same increase in locomotion as compared to controls, but no difference when compared to *DAT-Cre* alone. The results indicate that the amount of neurodegeneration is not significant enough to cause behavioral impairments, but it is still possible that effects are masked to some extent by the hyperactivity caused by the *DAT-Cre* allele. Measurements of total striatal dopamine content from mice of the same age were performed using high-performance liquid chromatography (HPLC) (figure 2-2b). The results showed significantly elevated dopamine levels in *DAT-Cre*, *Ret*, and *Ret/DJ-1* mice as compared to controls. Interestingly, there was no difference between *DAT-Cre* and *Ret* and *Ret/DJ-1* mice, which suggests that dopamine levels may be upregulated in the *Ret* and *Ret/DJ-1* mutant mice, considering that the density of striatal fibers at the same time point was significantly decreased compared to controls. In order to test whether TH levels, the rate-limiting enzyme in the dopamine synthesis pathway, were altered TH protein levels were measured by western blot analysis (figure 2-2c,d). However due to a limited availability of 18 month old mice, brains from 24 month old mice were used instead. Results did not indicate an upregulation of TH, although it cannot be excluded that the levels were again downregulated at the later 24 month stage.

a

b
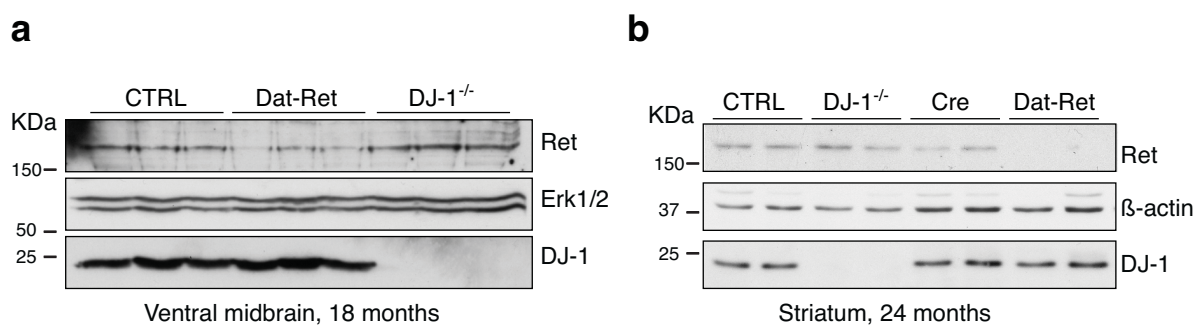
Figure 2-4 No alterations of DJ-1 or Ret protein. Western blots of (a) ventral midbrain lysate from 18 month old control, *Ret* and *DJ-1* mutant mice (n=3 mice per group), antibodies: Ret, DJ-1 and Erk1/2 as loading control. (b) Striatal lysates from 24 month old control, DJ-1, Dat-Cre, and Ret mutant mice, n=2 mice per group, antibodies: Ret, beta-actin, DJ-1. Complete genotypes: *mixed controls, DJ-1$^{-/-}$, DAT-Cre;Ret$^{lx/-}$, DAT-Cre;Ret$^{lx/-}$;DJ-1$^{-/-}$*.

2.1.5. Reduced cell soma size in *Ret* mutant mice, but no significant difference in *Ret/DJ-1* double mutants

Aged *Ret* single mutant mice display a loss of approximately 50 % of the dopaminergic axons in the striatum, but only 25 % of the dopaminergic cell bodies in the SNpc. *Ret/DJ-1* double mutants displayed a larger loss of cell bodies, but no increased loss of striatal fibers. One hypothesis that could explain these findings is that in the *Ret* mice, there is a population of neurons that have lost their target innervation, while their cell bodies remain alive but are functionally impaired. Removing *DJ-1* from these mice might specifically be detrimental for such a population of already sensitized neurons, which is why they would be lost in the double mutants without causing an additional loss of fibers. Impaired neurons that have lost their target innervation may be atrophic and have a reduced cell soma size. If these were to a greater extent lost in *Ret/DJ-1* double mutants, we would predict that the average cell size of the entire population would increase compared to *Ret* single mutants. To test this hypothesis, I quantified cell somas sizes from 24 month old mice in randomly selected SNpc neurons, immunostained for the DA marker GIRK2, which selectively labels the neurons that target the dorsal striatum, and were more specifically lost than the entire TH+ population (Aron *et al.* 2010). These results showed that the GIRK2+ SNpc neurons in the *Ret* single mutant mice indeed were smaller than in the control mice (figure 2-3a,b). In *Ret/DJ-1* double mutant mice, there was a tendency towards larger cell size larger compared to *Ret* single mutants, however due to high variation the difference was not significant (figure 2-3b).

2.1.6. No alterations of DJ-1 or Ret protein levels

Since *DJ-1* and *Ret* interacted genetically, it was possible that DJ-1 protein levels would be upregulated in *Ret* mutant mice, or conversely that Ret protein levels would be upregulated in *DJ-1* mutant mice. To test this possibility, I collected tissue lysates from the ventral midbrain or striatum of 18 or 24 month old mice, respectively, and analyzed by western blot for DJ-1 and Ret. (figure 2-4 a,b). The results indicated no major differences in DJ-1 protein levels in *Ret* mutant mice, or in Ret protein levels in *DJ-1* mutant mice, but confirmed that Ret protein levels were highly decreased by efficient gene recombination in *Ret* mice and that the DJ-1 protein was absent in *DJ-1* null mice as expected.

2.2. Analysis of biochemical pathways that could link DJ-1 with Ret signaling in mammalian cell culture

2.2.1. No evidence of DJ-1 regulating the PTEN-Akt signaling pathway

The canonical PI3K/Akt pathway is well established to be important for general cell survival (Parcellier *et al.* 2008), and is also thought to be important for survival of dopaminergic neurons in particular (Ries *et al.* 2006). It has been reported that *DJ-1* interacts genetically with *Akt* in *Drosophila* (Y. Yang *et al.* 2005; R. H. Kim, Peters, *et al.* 2005), and upregulates Akt phosphorylation in mammalian cell culture by negatively regulating PTEN, a PIP_3 phosphatase, thereby preventing Akt activation (R. H. Kim, Peters, *et al.* 2005). Since Ret is a known activator of PI3K, these reports raised the possibility that combined Ret and DJ-1 activity could lead to increased Akt activation. We therefore hypothesized that increased Ret signaling could compensate for loss of DJ-1 function by increasing Akt activation. To test this hypothesis, the first step was to establish that DJ-1, in agreement with previous studies, indeed regulates Akt phosphorylation. To this end, DJ-1 was depleted in HeLa cells using small interfering RNAI (siRNA) and subjected to western blot analysis for phospho-Akt. Contrary to our expectations, no decrease in phospho-Akt was observed (figure 2-5a). To confirm the results, I performed the same experiment in SH-SY5Y (neuroblastoma) and A549 (lung carcinoma) cells, of which the latter were used in the Kim *et al* study, to exclude that a different result was due to the different cell type used. However no decrease in phospho-Akt was observed when DJ-1 was knocked down (figure 2-5a). Increasing DJ-1 levels using transient overexpression in HeLa cells also did not alter the Akt phosphorylation (figure 2-5a). Furthermore, primary MEFs were isolated from wildtype and DJ-1 knockout embryos, starved for 6 hours, and stimulated with Insulin-like growth factor-1 (IGF-1) for 1, 15 or 120 minutes to test the possibility that DJ-1 regulates

a

c

b

d

e

f
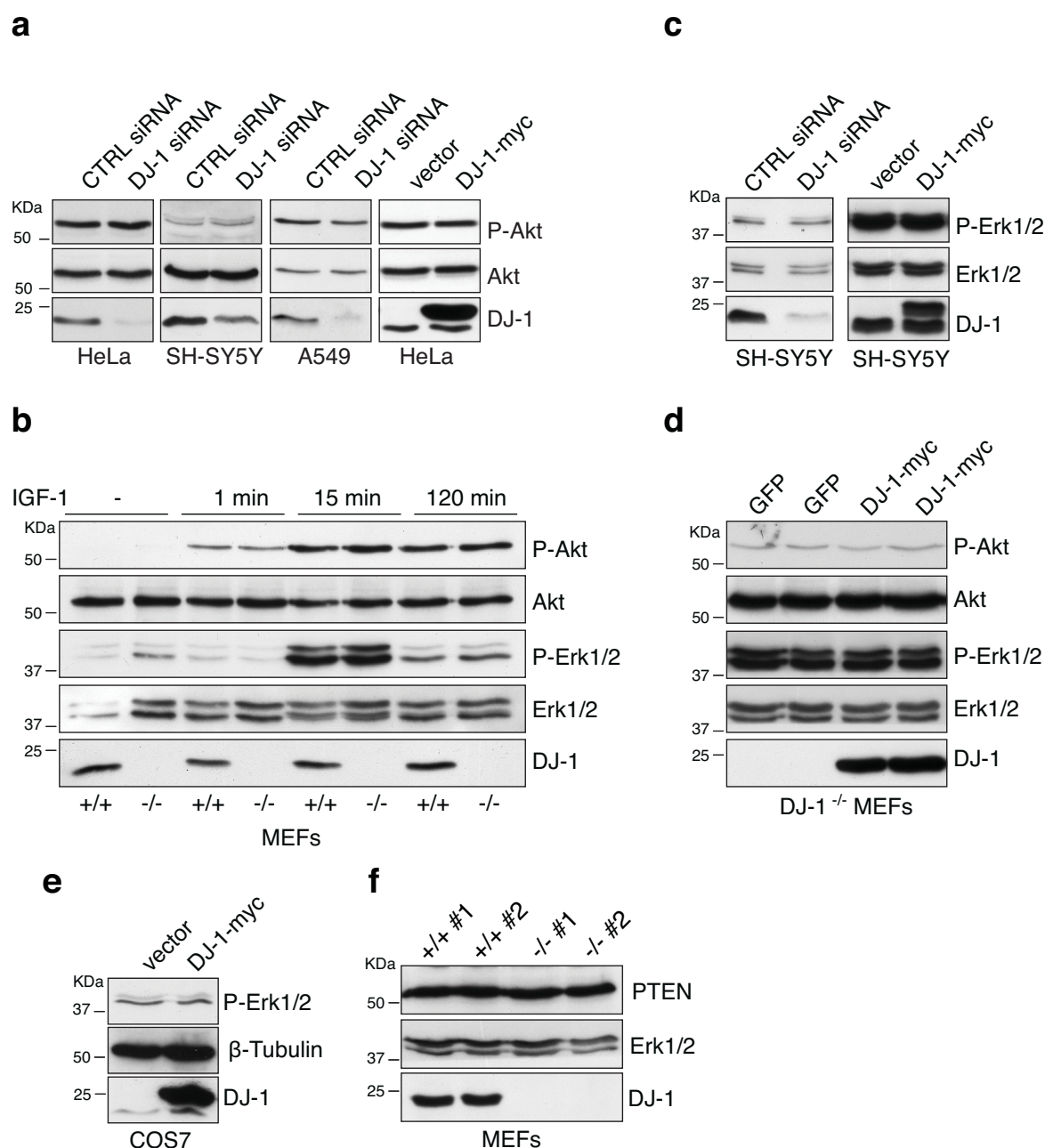
Figure 2-5 No regulation of Erk or Akt activation by DJ-1 in mammalian cell culture. Western blots of lysates from (a) Ctrl or DJ-1 siRNA transfected HeLa, SH-SY5Y and A549 cells, empty vector or DJ-1-myc plasmid transfected HeLa cells, (b) mouse embryonic fibroblasts (MEFs) from wildtype (+/+) or DJ-1 knockout (-/-) mice, treated with insulin-like growth factor-1 for 1, 15 or 120 minutes, (c) Ctrl siRNA, DJ-1 siRNA, empty vector or DJ-1-myc plasmid transfected SH-SY5Y cells, (d) DJ-1 knockout MEFs transfected with GFP or DJ-1-myc plasmids, (e) COS7 cells transfected with empty vector or DJ-1 myc plasmids, (f) Two clones (#1,2) of wild type or DJ-1 knockout MEFs. Antibodies: phospho-Akt, Akt, DJ-1 phospho-Erk1/2, Erk1/2, beta-tubulin, PTEN, as indicated.

phospho-Akt in only a particular time-frame. However, no differences between wildtype and DJ-1 knockout cells were observed (figure 2-5b). In order to exclude that native differences between the two cells lines would obscure the results, I overexpressed DJ-1 or GFP in DJ-1 knockout

cells, however no increase in phospho-Akt was observed with DJ-1 overexpression (figure 2-5d). If DJ-1 was a negative regulator of PTEN, we would expect PTEN levels to be increased in DJ-1 knockout MEFs when compared to wildtype MEFs, however I did not observe any differences (figure 2-5f). In conclusion, I found no evidence supporting a function of DJ-1 in regulating PTEN or Akt activation.

2.2.2.   No evidence of DJ-1 regulating the Ras/Erk signaling pathway

In *Drosophila*, our group has previously discovered genetic interactions between components of the Ras/Erk pathway and *DJ-1* in eye and wing development (Aron *et al*. 2010). The two *Drosophila* homologs of *DJ-1, DJ-1A/B* interact genetically with a *Drosophila Ras* gain-of-function allele and with a *Drosophila Erk* (*rolled*) loss-of-function allele. However, from these experiments, it was not possible to deduce at which level of the Ras-Erk pathway, or how, *DJ-1* interacted. To test whether DJ-1 acted upstream of Erk in mammalian cells, DJ-1 was overexpressed or depleted from SH-SY5Y cells, but no differences in phospho-Erk were observed (figure 2-5c). In addition, western blots using MEFs described above (figure 2-5b,d) were re-probed for phospho-Erk, but also there no differences were seen (figure 2-5b,d). Later, it was reported that DJ-1 overexpression in COS cells increased Erk1/2 phosphorylation (L. Gu *et al*. 2009), contrary to my observations in HeLa, SH-SY5Y and MEF cells. To test whether I could reproduce these results, I overexpressed DJ-1 in COS7 cells, but did not observe the strong increase in phospho-Erk1/2 that was reported (figure 2-5e).

2.2.3.   No evidence of serum or GDNF increasing DJ-1 expression after starvation

It has previously been reported that DJ-1 expression in cell lines can be strongly induced by serum treatment after starvation, and furthermore, that DJ-1 can have a transforming activity, which synergizes with Ras overexpression. Nagakubo *et al* suggest that the induction of DJ-1 is mediated by the Ras-pathway (Nagakubo *et al*. 1997). To test whether DJ-1 expression can be induced by Ret, I used SH-SY5Y cells, which express high endogenous levels of Ret. The cells were subjected to serum starvation for 48 or 96 hours, after which they were treated with either with 10 % serum or GDNF/GFRα1 (50 ng/ml) for 12 hours. I did not observe any difference in DJ-1 protein levels, neither with starvation, nor with GDNF/GFRα1 treatment (figure 2-6a).

2.2.4.   Absence of Ret-mediated regulation of DJ-1 subcellular localization

a

starved 48h   starved 96h

b   **3 hours treatment**   **c**   **24 hours treatment**

nucleus(P1) | mitochondria (P2) | cytosol (S3)   nucleus(P1) | mitochondria (P2) | cytosol (S3)
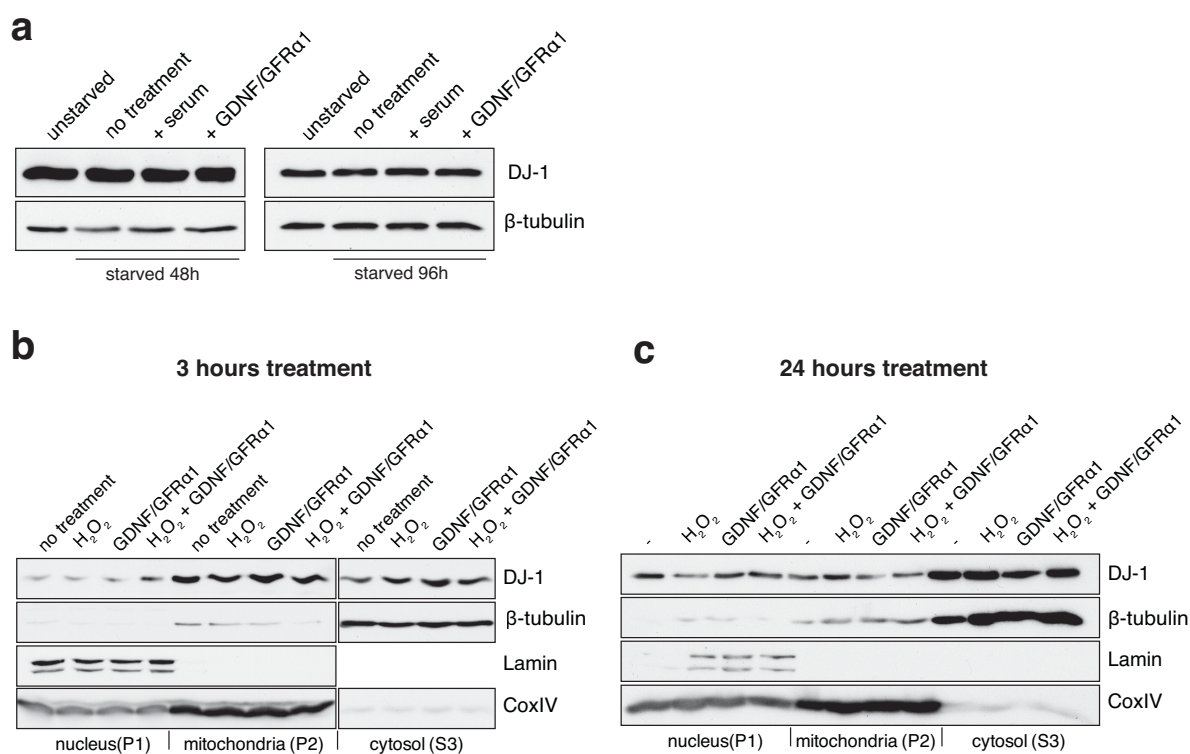
Figure 2-6 No regulation of DJ-1 levels or subcellular localization. Western blots of lysates from SH-SY5Y cells, (a) unstarved or starved for 48 or 96 hours, prior to 12 hours treatment with 10% fetal calf serum or GDNF/GFRα1 (50 ng/ml), (b,c) treated with 50 μm H_2O_2, GDNF/GFRα1 (50 ng/ml) or a both combined for (b) 3 hours or (c) 24 hours, after which cells were lysed and subjected to a crude subcellular fractionation by centrifugation. Antibodies: DJ-1, beta-tubulin (cytosolic loading control), Lamin (nuclear loading control), CoxIV (mitochondrial loading control) as indicated.

An interesting aspect of the DJ-1 protein is that it can be localized to several different subcellular compartments where it can possibly exert different functions. Two groups have previously reported that DJ-1 translocates to mitochondria upon treatment with oxidative stress-generating agents such as hydrogen peroxide or paraquat (Canet-Avilés *et al.* 2004; Junn *et al.* 2009). However, the results of these two studies differ in several points: Canet-Avilés *et al* observed an enrichment of mitochondrial DJ-1 after 24 hours of paraquat, while Junn *et al* found that DJ-1, after 3 hours of hydrogen peroxide treatment, translocated to mitochondria, however, after 24 hours it had moved to the nucleus. Another study also investigated DJ-1 translocation but no enrichment in mitochondria after paraquat treatment was seen (L. Zhang *et al.* 2005). To test whether 1) hydrogen peroxide causes DJ-1 translocation to mitochondria and/or nucleus and 2) Ret signaling regulates DJ-1 translocation, I serum-starved SH-SY5Y cells for 24 hours after which I treated them with hydrogen peroxide, GDNF/GFRα1 or both for 3 or 24 hours. I separated crude fractions by centrifugation and analyzed by western blot using CoxIV and Lamin

as
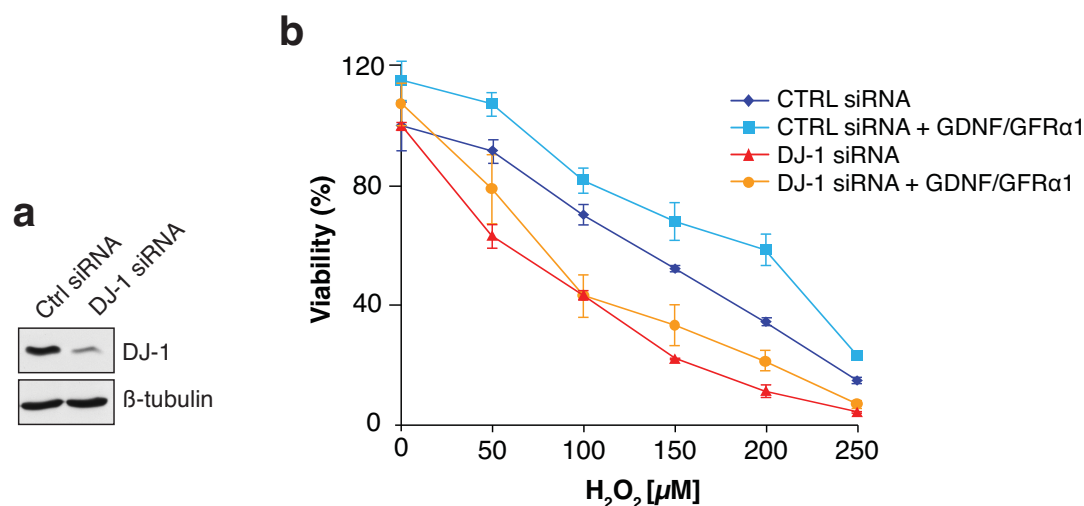
Figure 2-7 No rescue of DJ-1 knockdown induced sensitivity to oxidative stress by GDNF treatment. (a) Western blot of Ctrl or DJ-1 siRNA transfected SH-SY5Y cells, antibodies: DJ-1 and beta-tubulin, (b) cell viability (percent of Ctrl siRNA at 0 μm H_2O_2) measured by an ATP-based luminescence assay of Ctrl or DJ-1 siRNA transfected cells treated with H_2O_2 solution at 0-250 μm for 12 hours with or without the presence of GDNF/GFRα1 (50 ng/ml), means from triplicate samples ± SD

fractionation controls for the mitochondrial and nuclear fractions, respectively (figure 2-6b,c). I could not observe any enrichment of DJ-1 in mitochondria with any of the treatments at either time point. The nuclear fraction appeared to be very small and no clear differences were seen with the hydrogen peroxide and GDNF treatments.

2.2.5.   DJ-1 depletion causes increased sensitivity to oxidative stress – no evidence of specific rescue by Ret signaling

Cells lacking DJ-1 have been shown to have increased sensitivity to oxidative stress in a number of studies (Taira *et al*. 2004; Martinat *et al*. 2004; Görner *et al*. 2007). Since GDNF/Ret signaling has reported pro-survival effects in several cell types, it is possible that GDNF could rescue the increased cell death caused by DJ-1 depletion. To test this hypothesis, I depleted DJ-1 using by siRNA in SH-SY5Y cells, and monitored the knockdown efficiency by western blot analysis (figure 2-7a). I treated the cells with hydrogen peroxide in a range of concentrations, combined with GDNF and GFRα1 (50 ng/ml) or PBS (figure 2-8b). Experiments were performed in medium with reduced serum (2 %) since serum contains growth factors that could fulfill the same function as GDNF. After 12 hours of treatment, I measured viability using an ATP/luminescence-based assay. The results indicated that DJ-1 depleted cells showed increased cell death in agreement with previous studies. Samples treated with GDNF showed increased

numbers of cells at most hydrogen peroxide concentrations including the starting point of 0 μM, indicating that GDNF either stimulates proliferation, which was previously shown in SH-SY5Y cells (Hirata & Kiuchi 2003), or that it prevents the basal level of cell death caused by the serum-starvation. However, the increased number of cells with GDNF for any given hydrogen peroxide concentration was the same for DJ-1 siRNA and control siRNA treated cells, suggesting that there was no specific rescue of the additional cell death caused by DJ-1 depletion.

2.3. Ret signaling regulates mitochondrial dynamics in PINK1 or Parkin knockdown cells

2.3.1. GDNF/Ret reverses mitochondrial fragmentation

Acute knockdown of Parkin or PINK1 by RNAi in mammalian cell lines causes fragmentation of the mitochondrial network (Exner *et al.* 2007; Dagda *et al.* 2009; Lutz *et al.* 2009). It seems that the balance between fusion and fission is shifted towards increased fission; however the detailed mechanisms remain elusive. To test whether Ret signaling can regulate the mitochondrial dynamics balance after Parkin knockdown, I used SH-SY5Y cells, which express high endogenous levels of both Parkin and Ret. I depleted Parkin using siRNA, after which I treated the cells with GDNF/GFRα1 for three days. Cells were cultured on glass coverslips for imaging, and in parallel on culture dishes for western blot analysis, to monitor the efficiency of Parkin depletion (figure 2-8a) and the activation of Akt and Erk signaling (figure 2-8b). Mitochondria were fluorescently labeled for imaging using the mitochondria-specific dye Mitotracker, and with the different treatments blinded, I scored the cells in one of two categories: "tubular" or "fragmented" mitochondrial morphology (figure 2-8c, d). Parkin siRNA treated cells were not significantly more fragmented than control siRNA cells (figure 2-8d), in contrast to previous studies (Lutz *et al.* 2009). However, this was probably due to the fact that the control siRNA-treated cells had a high level of baseline fragmentation, and the siRNA transfection was not very efficient. In Parkin siRNA cells, treated with GDNF/GFRα1, the population of cells with fragmented mitochondria was significantly lower than in Parkin siRNA alone, indicating that GDNF/GFRα1 promotes mitochondrial fusion or inhibits fission. To test whether the same was true for mitochondrial fragmentation caused by loss of PINK1, I used HeLa cells, which have large mitochondrial networks (2-8e). They are also more efficiently transfected than SH-SY5Y cells, improving the quality of analysis. I transfected HeLa cells with PINK1 or control siRNA, and monitored the RNAi efficiency using RT-PCR, since the PINK1 protein is maintained at
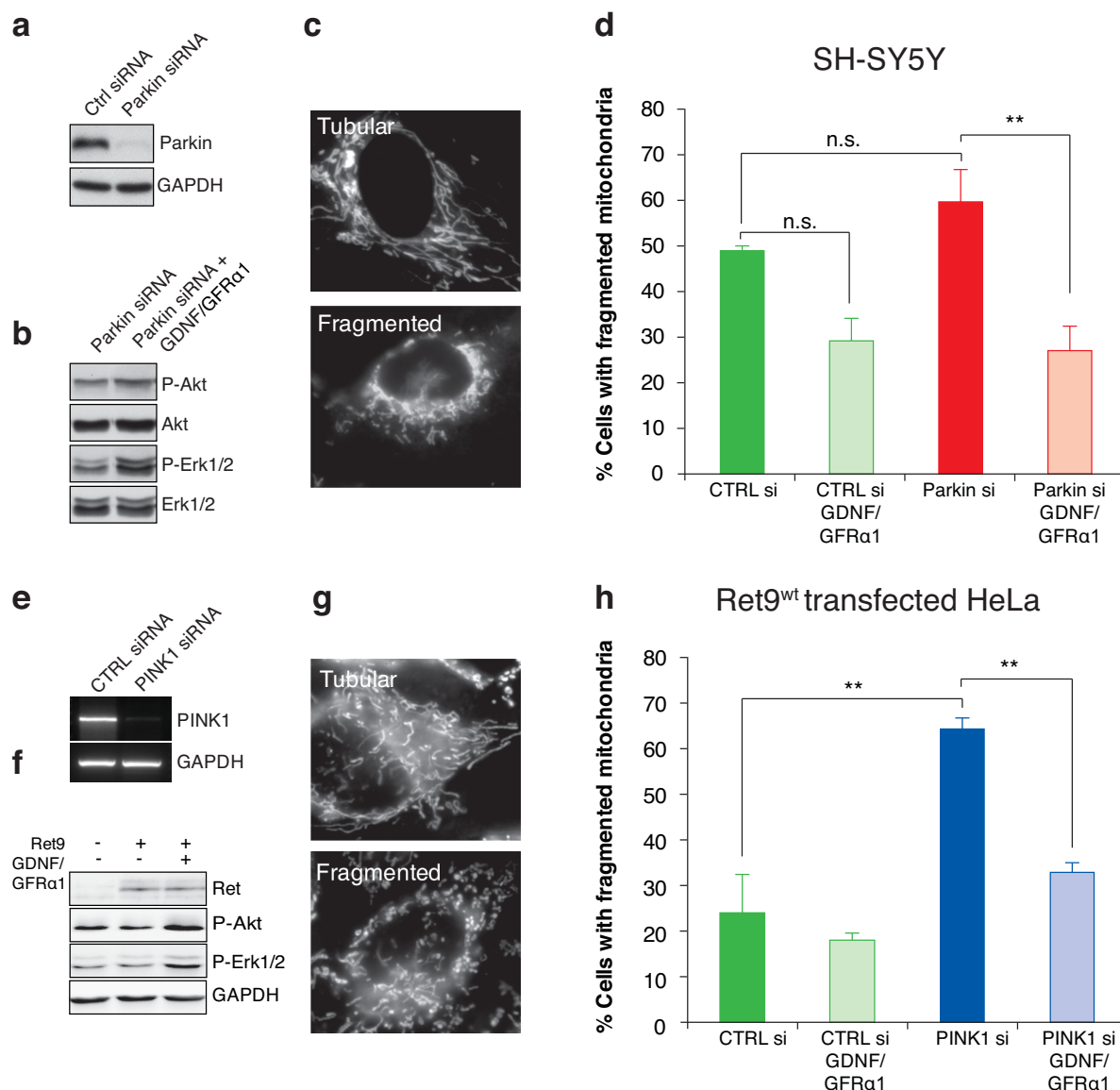
Figure 2-8 GDNF/Ret signaling reverses mitochondrial fragmentation from Parkin or PINK1 knockdown. (a,b) Western blots of lysates from SH-SY5Y cells (a) transfected with Ctrl or Parkin siRNA, antibodies: Parkin, GAPDH, (b) transfected with parkin siRNA and treated with GDNF/GFRα1 (100 ng/ml), antibodies: phospho-Akt, Akt, phospho-Erk1/2, Erk1/2, (c) photomicrographs of SH-SY5Y cells labeled with Mitotracker green FM depicting mitochondria of typical tubular or fragmented morphology, (d) percentage of SH-SY5Y cells with fragmented mitochondria, transfected with Ctrl or Parkin siRNA and treated with GDNF/GFRα1 (100 ng/ml) for 24 hours prior to analysis, (e) 30 cycles RT-PCR of lysate from HeLa cells, transfected with Ctrl or PINK1 siRNA, PCR primers for PINK1 or GAPDH, (f) western blot of lysates from HeLa cells, transfected with Ret9^{WT} and treated with GDNF/GFRα1 (50 ng/ml) for 18 hours, (g) photomicrographs of HeLa cells labeled with Mitotracker green FM depicting mitochondria of typical tubular or fragmented morphology, (h) percentage of HeLa cells with fragmented mitochondria, transfected with Ctrl or PINK1 siRNA, a Ret9^{WT} plasmid, and treated with GDNF/GFRα1 (50 ng/ml) for 18 hours prior to analysis. Averages per (a): 4 (b): 3 independent experiments, means ± SEM, ** $p < 0.01$, one-way ANOVA, Bonferroni's post hoc test, n.s.= not significant.

low levels under normal conditions, and the commercially available PINK1 antibodies are of low quality (figure 2-8f). HeLa cells do not express endogenous Ret, therefore I transiently

transfected a human Ret9 plasmid, and stimulated cells with GDNF/GFRα1. I performed western blot analysis to verify Ret overexpression and activity of downstream signaling components after stimulation (figure 2-8g). Using the same method as described above, I found that after PINK1 siRNA treatment, there was a significantly higher percentage of cells with fragmented mitochondria (67%) as compared to control siRNA cells (25 %). The GDNF/GFRα1 treated PINK1 siRNA cells showed a strong and significant reduction of fragmentation, where only 34 % had fragmented mitochondria, indicating that Ret signaling can reverse PINK1 knockdown induced mitochondrial fragmentation.

2.3.2. Analysis of Ret activated signaling pathways involved in the rescue of PINK1 knockdown induced mitochondrial fragmentation

To investigate which of the signaling pathways mediate this rescue, I used signaling mutant versions of Ret9 developed previously (Lundgren *et al.* 2006; Stenqvist *et al.* 2008). The Ret[Shc+] construct contains two amino acid substitutions, W1056A and E1058D that change the affinity of the Shc adaptor protein to Y1062, one of the main signaling tyrosines of Ret. This causes an increased activation of the PI3K/Akt pathway compared to Ret[WT]. Conversely, another version, Ret[Dok+] (G1063P) has increased affinity to the Dok4/5 adaptors, and interestingly outcompetes the binding of Shc and Frs2, causing increased activation of the Ras/Erk pathway with decreased activation of PI3K/Akt (Stenqvist *et al.* 2008). Using these constructs in the same experimental setup as described above for PINK1 siRNA, both Ret[Shc+] and Ret[Dok+] were able to reverse the mitochondrial fragmentation from PINK1 knockdown (figure 2-9a), suggesting that the effect may not require strong Akt activation. The signaling properties of the three different versions of Ret9 were examined using western blot analysis for Erk1/2 and Akt phosphorylation. Unfortunately, these results showed significant remaining Akt activation with the Ret9[Dok+] mutant, in contrast to the original publication (figure 2-9b). It still remains possible that the time course of or level of activity is shifted in the Ret9[Dok+], but the western blot analysis suggests that the results of these experiments should be interpreted with caution.

To further study the pathways downstream of Ret, I used kinase inhibitors for the PI3K/Akt and Ras/Erk pathways. The compound U0126 selectively blocks Mek1/2 activity, whereas LY294002 selectively blocks PI3K activity. To find appropriate concentrations of the compounds, I incubated HeLa cells for 12 hours with the two compounds in a series of doses (2-9d,e). High doses of these compounds caused a high degree of cell death, thus I reduced the incubation time
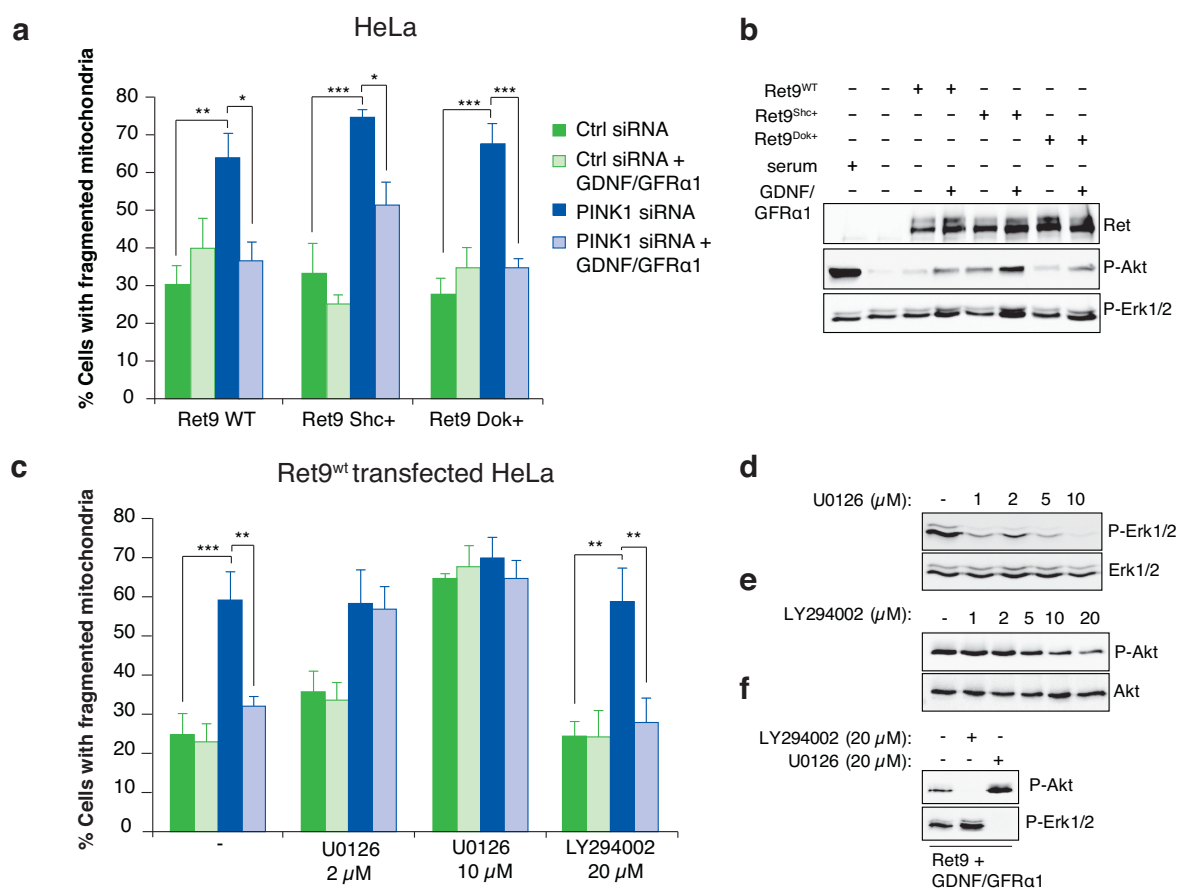
Figure 2-9 GDNF/Ret mediated reversal of mitochondrial fragmentation independent of PI3K. (a,c) Percentage of HeLa cells with fragmented mitochondria, transfected with Ctrl or PINK1 siRNA, and (a) transfected with Ret9^{WT}, Ret9^{Shc+} or Ret9^{DOK+} plasmids, and treated with GDNF/GFRα1 (50 ng/ml) for 18 hours prior to analysis, (c) treated with U0126 (2 or 10 µm) or LY294002 (20 µm) and GDNF/GFRα1 (50 ng/ml) for 3 hours prior to analysis. (b,d,e,f) western blots of lysates from HeLa cells (b) transfected with Ret9^{WT}, Ret9^{Shc+} or Ret9^{Dok+}, serum starved and treated with 10% serum or GDNF/GFRα1 (50 ng/ml) for 30 minutes, (d) treated with 0,1,2,5,10 µM of U0126 for 12 hours, (e) treated with 0,1,2,5,10,20 µM of LY294002 for 12 hours, (f) Ret9^{WT} transfected and treated with GDNF/GFRα1 (50 ng/ml) in combination with 20 µM LY294002 or 20 µM U0126. Antibodies: Ret, phospho-Akt, Akt, phospho-Erk1/2, Erk1/2, GAPDH as indicated. Bar graphs depict averages per (a): 4 (b): 3 independent experiments, means ± SEM, ** p<0,01, one-way ANOVA, Bonferroni's post hoc test, n.s.=not significant.

to 3 hours, after which the cells were subjected to western blot analysis (figure 2-9c) for phospho-Erk1/2 and phospho-Akt. I also tested for nonspecific kinase inhibition of PI3K by U0126 and of Mek by LY294002, but no such nonspecificity was seen (2-9f). The kinase inhibitor experiment was performed generally as described above using Ret^{WT}, with the difference that GDNF/GFRα1 and kinase inhibitors were added only three hours prior to analysis, to avoid too high levels of toxicity. Using 20 uM of LY294002, a concentration that reduced p-Akt by approximately 70%, did not modulate the GDNF rescue. Interestingly, 2 µM of U0126 on the other hand, abrogated the rescue effect of GDNF treatment. Increasing the concentration to 10
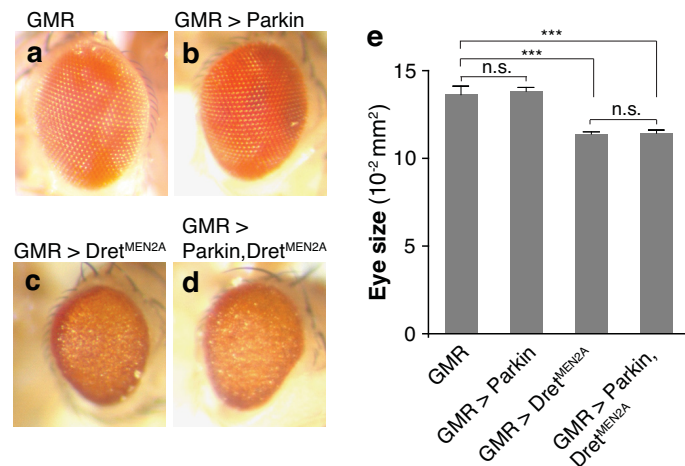
Figure 2-10 No genetic interaction between UAS-parkin and UAS-Dret^{MEN2A} in *Drosophila* eye development. (a-d) Photomicrographs of compound eyes of flies with indicated genotypes, (e) quantification of eye size, n=10-23 flies per genotype, means ± SEM, *** p<0.001, one-way ANOVA, Bonferroni's post hoc test, n.s.= not significant. Complete genotypes: *(a) Cyo/+;GMR-GAL4/+, (b) UAS-parkin/Cyo;GMR-GAL4/+ (c) UAS-Dret^{MEN2A}/+;GMR-GAL4/+, (d) UAS-Dret^{MEN2A}/UAS-parkin;GMR-GAL4/+.*

µM caused mitochondrial fragmentation, also in control siRNA treated cells. These results suggest that the rescue by GDNF/Ret signaling may be independent of Akt and that the Ras/Erk pathway may be required for rescue, but further studies are required to confirm this conclusion.

2.4. Genetic analysis of Dret, Parkin and Pink1 functions in *Drosophila melanogaster*

2.4.1. Genetic epistasis analysis of Dret^{MEN2A} and Parkin in the eye system

The *Drosophila* compound eye consists of around 800 ommatidia, and each one contains 8 photoreceptor neurons. The development of the compound eye is a highly regulated process, requiring precise cell divisions and programmed cell death. These events are regulated by several canonical signaling pathways and receptor tyrosine kinases, for example the Sevenless receptor. Alterations in these signaling pathways can cause phenotypes of incorrect number or size of photoreceptor neurons, which are seen as a rough eye with altered size, which can be easily analyzed. For these reasons, the *Drosophila* eye system has frequently been used in genetic epistasis studies. Overexpression of constitutively active versions of *Drosophila* Ret, Dret$^{MEN2A/B}$, using the eye specific GMR promoter causes a rough eye phenotype, where the photoreceptors are enlarged, creating an irregular, rough morphology, while the total size of the compound eye is reduced (Read *et al.* 2005). Our group has previously shown that Dret$^{MEN2A/B}$ interacts genetically with *DJ-1A/B*. Expressing Dret$^{MEN2A/B}$ in *DJ-1A/B* null mutant flies rescues the Dret$^{MEN2A/B}$
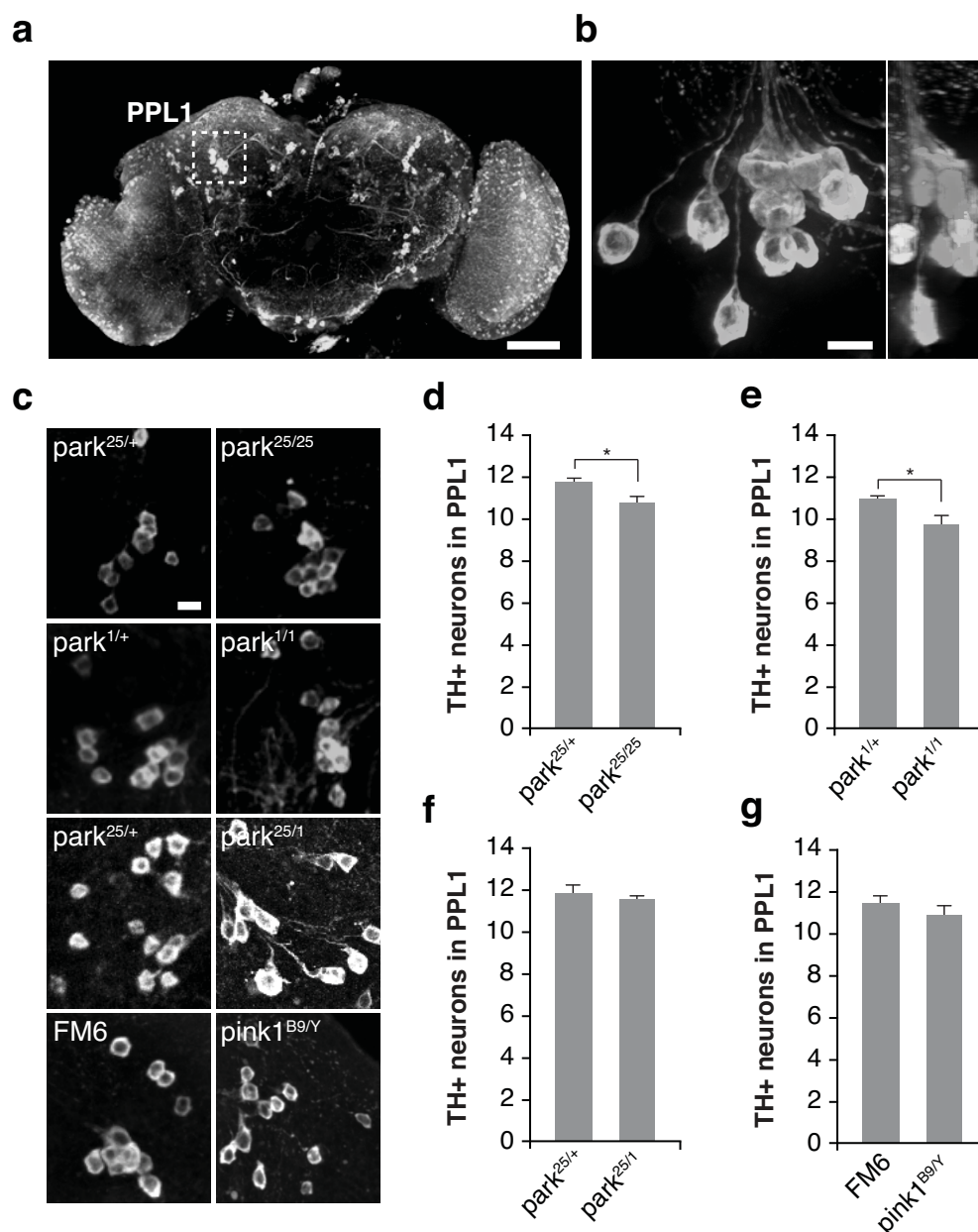
Figure 2-11 Minor or no loss of neurons in *park* or *Pink1* mutant flies. (a-c) Photomicrographs whole-mount *Drosophila* brains, immunostained for TH, maximum projections of confocal Z-sections. (a) Maximum projection of 100 μm thick segment of the posterior brain, with the posterior protocerebral lateral (PPL1) cluster indicated, (b) high magnification of PPL1 cluster of DA neurons with 90 degree rotation (right) (c) PPL1 DA neurons from 20-25 day old flies of indicated genotypes, (d-g) numbers of TH+ neurons in the PPL1 cluster, n=6-10 flies per genotype, means of left and right hemispheres per animal, means per genotype ± SEM, * p<0.05, student's t-test. Scale bars: (a) 50 μm, (b) 10 μm. Complete genotypes: (d) *park^{25}24B-GAL4/TM3, park^{25}::24B-GAL4/park^{25}::24B-GAL4, (e)*

phenotype, while combined overexpression of Dret$^{MEN2A/B}$ and DJ-1A causes an enhanced phenotype with an eye even smaller than with Dret$^{MEN2A/B}$ alone (Aron *et al.* 2010).

To test whether the *Drosophila* homolog of Parkin, (*park* refers to the endogenous *Drosophila* gene and Parkin to the overexpression-construct), interacts genetically with Dret^{MEN2A}, analogous

to DJ-1, I used the *GMR-GAL4* driver line to overexpress UAS-Parkin and UAS-Dret[MEN2A/B]. I acquired photomicrographs of eyes (figure 2-10a) and measured the eye sizes (figure 2-10b). *GMR-GAL4*;UAS-Parkin (*GMR* > Parkin) showed no alteration in gross morphology compared to *GMR* controls. *GMR* > Dret[MEN2A] showed a rough gross morphology and reduced eye size as previously reported. Flies with combined parkin and Dret[MEN2A] overexpression showed the same rough eye as Dret[MEN2A] expressing flies, and also no difference to these in terms of eye size. These results indicate that parkin is not a strong modulator of Dret[MEN2A] signaling during eye development.

2.4.2.   Small or no loss of dopamine neuron numbers in *park* and *Pink1* mutants.

The *Drosophila* brain contains approximately 200 dopaminergic neurons in 15 defined clusters. It has been reported by independent groups that *park* and *Pink1* mutant flies lose a small number of these neurons during aging. This is most pronounced in the posterior lateral protocerebral cluster (PPL1), which in wild type flies contains 12 neurons (figure 2-11a,b). However, reports are somewhat disparate regarding the extent of neuronal loss. Some studies have found an average loss of four neurons in 30 day old *park* null mutant flies (Whitworth *et al.* 2005; Tain, Mortiboys, *et al.* 2009), while other studies did not see any DA neuron loss (J. C. Greene *et al.* 2003; Pesah *et al.* 2004). For *Pink1* mutants, the first study reported a loss of two neurons after aging (J. Park *et al.* 2006), but some recent studies found only a loss of one neuron (S. Liu & Bingwei Lu 2010; Y. Imai *et al.* 2010). The discrepancies may be due to different histological techniques, or differences in the genetic background of the flies. In mammals it has been shown several times that GDNF treatment can protect dopamine neurons from cell death in various toxin models of PD. Therefore, we hypothesized that the active *Dret* (Dret[MEN2A]) can rescue the loss of neurons in *park* and *Pink1* mutants. To investigate this, I first assessed whether the neuronal loss could be reproduced under our experimental conditions. To this end, I tested two different *park* null mutant lines (*park25 and park1*) and a *Pink1* mutant line (*Pink1B9*) and aged these to 20-25 days. After aging, brains were analyzed using whole-mount immunostaining for
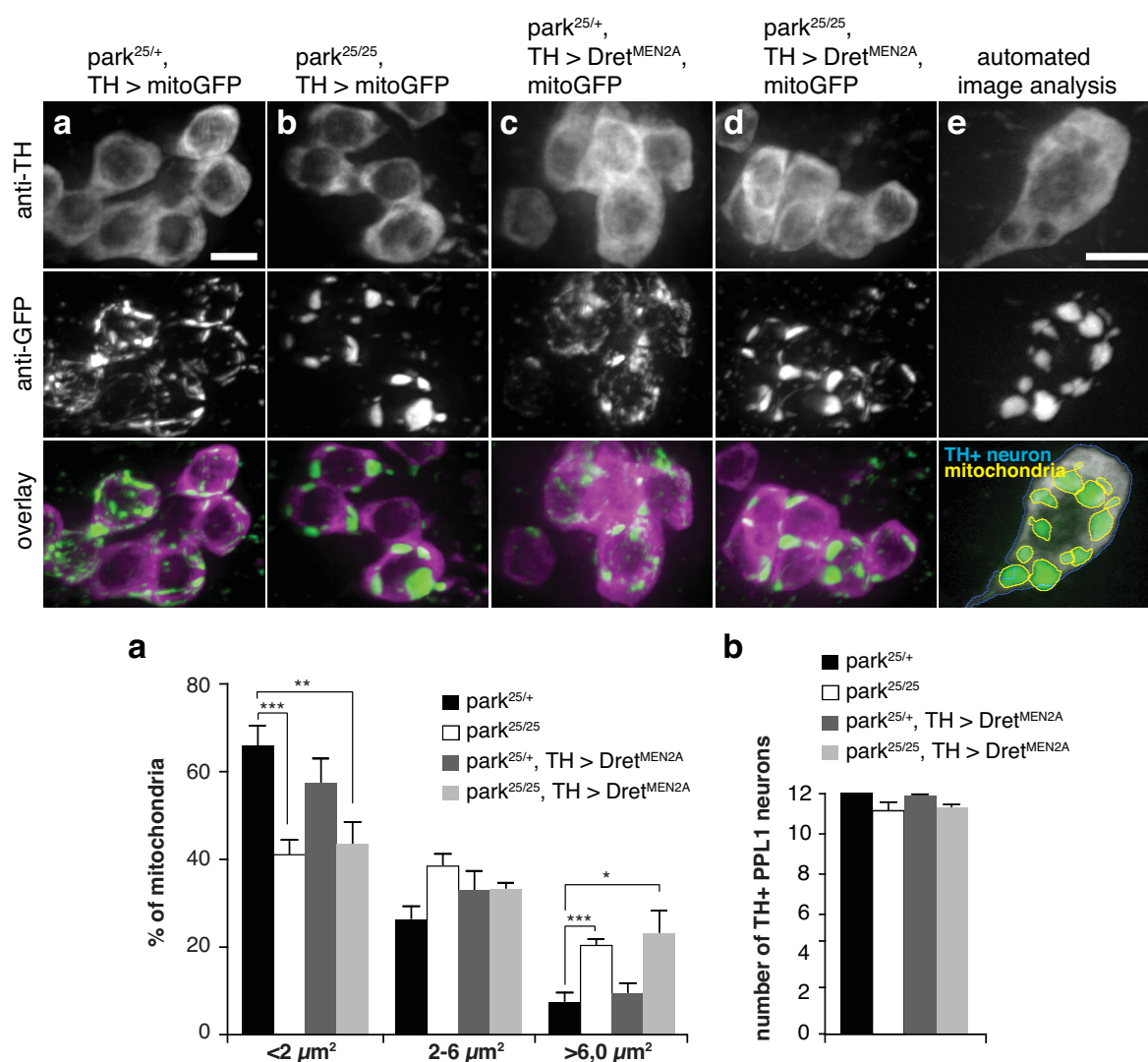
Figure 2-12 Enlarged mitochondria in DA neurons of *park* mutant flies – no rescue by Dret^MEN2A. (a-d) Photomicrographs of whole-mount *Drosophila* brains from 10-15 day old flies of indicated genotypes, immunostained for TH (upper panels) and GFP (middle panels), overlay of the two channels (lower panels), images are maximum projections of confocal Z-sections. (e) Photomicrograph of a single TH+ neuron immunostained for TH (upper panel) and GFP (middle panel) and an overlay with outlines of the neuron in blue and the mitochondria in yellow as they were detected by the automated image analysis algorithms (bottom panel), (f) quantification of mitochondria size, indicating percentage of mitochondria in the size categories <2 μm^2, 2-6 μm^2 and >6 μm^2, (g) number of TH+ neurons in the PPL1 cluster, all values are means per animal ± SEM, * $p<0.05$, **$p<0.01$, ***$p<0.001$, student's t-test. Scale bars (a,e): 10 μm. Complete genotypes: (a) *UAS-mitoGFP/+;park^{25}TH-GAL4/TM6*, (b) *UAS-mitoGFP/+;park^{25}TH-GAL4/park^{25}*, (c) *UAS-mitoGFP/UAS-Dret^{MEN2A};park^{25}TH-GAL4/TM6*, (d) *UAS-mitoGFP/UAS-Dret^{MEN2A};park^{25}::TH-GAL4/park^{25}*.

tyrosine hydroxylase, after which confocal z-sections were acquired, allowing efficient imaging of the complete PPL1 cluster (figure 2-11c). TH+ neurons were counted in a blinded manner. The *park^{25}* mutant line displayed an average loss of 0.9 neurons compared to controls (figure 2-11d) and the other allele, *park^{1}*, showed an average loss of 1.1 neurons (figure 2-11e). To control for modifiers in the genetic background of the alleles, I also crossed the two lines together to analyze

the transheterozygous condition *park^25/1^*. These flies did not display a significant loss of neurons, which could indicate that the slightly stronger phenotypes in the *park^25^* and *park^1^* homozygous flies may be due to background modifiers (figure 2-11f), but it should be stressed that the difference is minuscule. The *Pink1* mutant line (*Pink1^B9^*) also did not display a significant loss of neurons (figure 2-11g). In conclusion, in our experimental conditions, *park* and *Pink1* mutant flies lose one or no neurons in the PPL1 cluster after aging to 20-25 days, and therefore we decided not investigate the original hypothesis further.

2.4.3. Enlarged dopamine neuron mitochondria in *park* mutant flies – no rescue by Dret^MEN2A^

Park and *Pink1* mutant flies show mitochondrial alterations in several tissues, including spermatids, flight muscles and also in the dopamine neurons. While the mitochondria have highly different morphologies in these three tissues, they are all strikingly enlarged in the mutants, and ultrastructural analyses have revealed that they have significantly reduced density of cristae, which also appear broken. To test whether Ret signaling can rescue the mitochondrial morphological alterations of the PPL1 dopamine neurons, I overexpressed UAS-Dret^MEN2A^ in the *park^25^* mutant background using the *TH-GAL4* driver. I also used an allele for mitochondrial targeted GFP, UAS-mitoGFP to genetically label the mitochondria. In control flies (*park^25/+^*, *TH* > mitoGFP), the majority of the mitochondria had a tubular morphology (figure 2-12a) and this was not altered by Dret^MEN2A^ overexpression (figure 2-12b). In *park* mutant flies, the mitochondria showed a strikingly enlarged appearance (figure 2-12c), which was not altered with Dret^MEN2A^ overexpression (figure 2-12d). The sizes of the mitochondria were quantified using automated image analysis algorithms, which identified the TH+ neurons and measured the area of the mitochondria within (figure 2-12e). The results showed a significantly decreased number of mitochondria smaller than 2 µm² in *park^25/25^* as well as in *park^25/25^*, *TH* > Dret^MEN2A^, and an increased number of mitochondria larger than 6 µm², however there was no rescue in terms of mitochondrial size by Dret^MEN2A^ (figure 2-12f). The numbers of TH+ neurons in the PPL1 cluster was also counted but there were no significant differences between the genotypes (figure 2-12g).
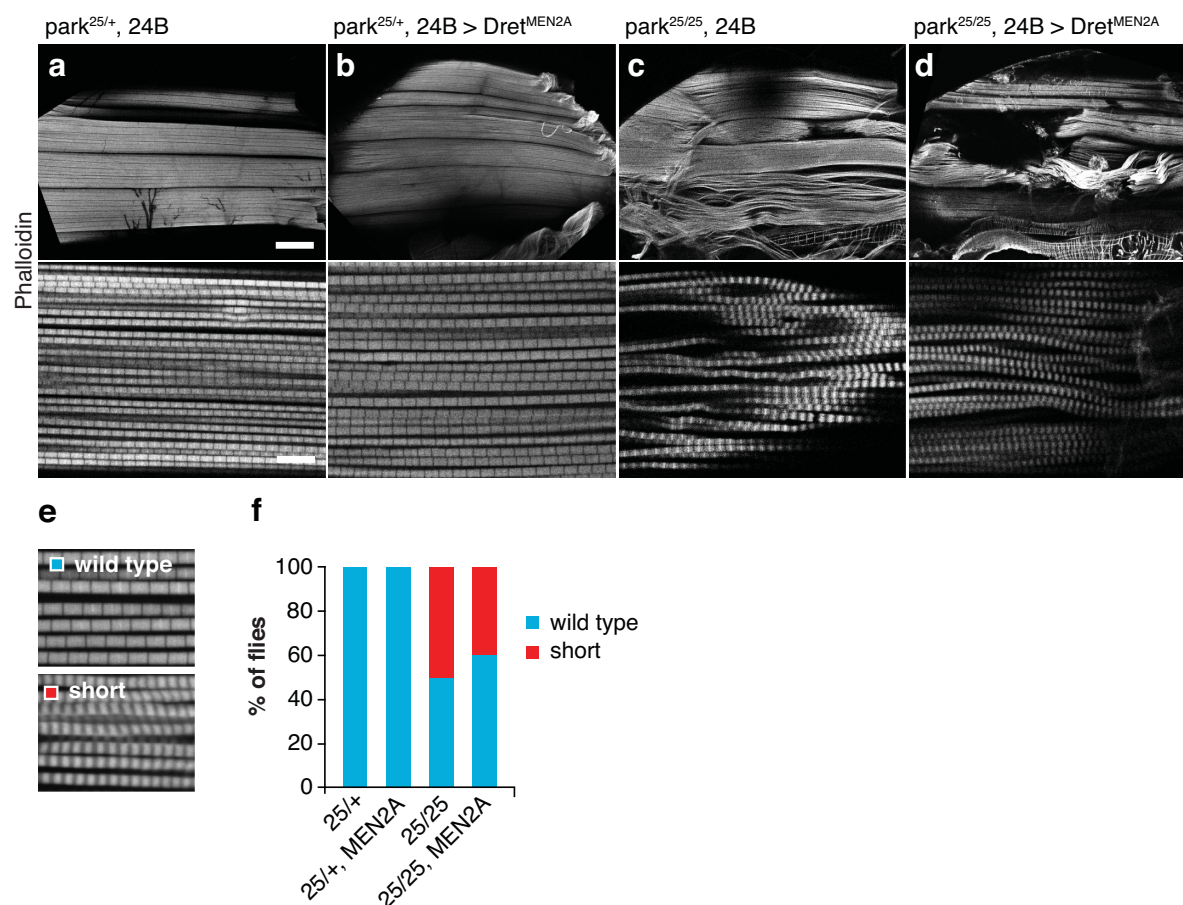
Figure 2-13 *24B-GAL4* > Dret^MEN2A does not rescue muscle degeneration in *park* mutant flies. (a-d) Photomicrographs of hemi-thoraces stained with phalloidin-alexa568 showing the six dorsal longitudinal indirect flight muscles (DL-IFM) at low magnification (upper panel) and individual myofibrils at high magnification (lower panel) of 2-5 day old flies with indicated genotypes, (e) photomicrographs of typical wild type or short sarcomeres, (f) percentage of flies with wild type (blue bars) or short (red bars) sarcomeres. n=5-9 flies per genotype, scale bars: (upper panel) 100 µm, (lower panel) 10 µm, complete genotypes: *(a) +/+;park^25::24B-GAL4/TM3, (b) UAS-Dret^MEN2A/+;park^25::24B-GAL4/TM6, (c) +/+;park^25::24B-GAL4/park^25, (d) UAS-Dret^MEN2A/+;park^25::24B-GAL4/park^25.*

2.4.4. Degeneration of indirect flight muscles in *park* and *Pink1* mutants – a system to study genetic epistasis with Dret

One of the more pronounced phenotypes of *park* and *Pink1* mutant flies is muscle degeneration, causing reduced climbing and flying ability; the latter is also manifested by an abnormal wing posture. The dorsal longitudinal indirect flight muscles are the largest muscle group in the adult fly. Made up of six large muscles on each side along the midline of the thorax, these muscles generate the main propellant force required for flying. *Park* and *Pink1* mutant flies have previously been shown to have severe alteration in these muscles: they display an irregular morphology, muscles may be truncated or absent, and a fraction of the myofibrils often display
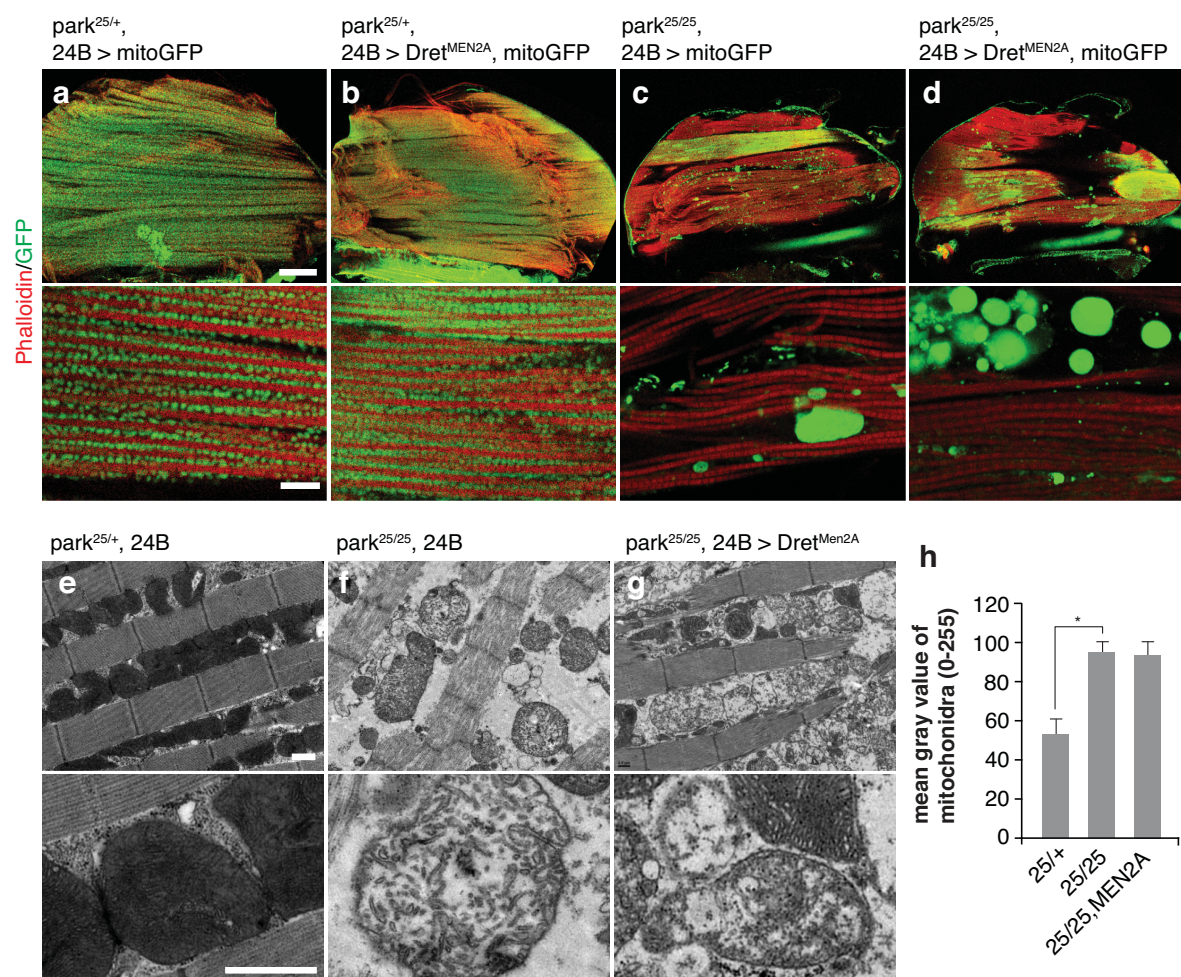
Figure 2-14 _24B-GAL4_ > Dret^MEN2A does not rescue mitochondrial morphology in _park_ mutant flies. (a-d) Photomicrographs of hemi-thoraces stained with phalloidin-alexa568, mitochondria labeled with UAS-mitoGFP, DL-IFMs at low magnification (upper panels) and individual myofibrils at high magnification (lower panels) of 2-5 day old flies with indicated genotypes, n=3-4 flies per genotype, (e-g) Transmission electromicrographs of sarcomeres and mitochondria from ultrathin sections of DL-IFMs from 5-7 day old flies at lower magnification (upper panel) and higher magnification (lower panel) (h) optical density measurement of mitochondria TEM captured mitochondria, averages of 46-199 number of mitochondria per fly, n=3-4 flies per genotype, means ± SEM, * p<0.01, student's t-test. Scale bars: (a, upper panel) 100 μm, (a, lower panel) 10 μm, (e, upper and lower panels) 1 μm. Complete genotypes: _(a) UAS-mitoGFP/+;park^25::24B-GAL4/TM3, (b) UAS-Dret^MEN2A/UAS-mitoGFP;park^25::24B-GAL4/TM6, (c) UAS-mitoGFP/+;park^25::24B-GAL4/park^25, (d) UAS-Dret^MEN2A/UAS-mitoGFP;park^25::24B-GAL4/park^25, (e) +/+;park^25::24B-GAL4/TM3, (f) +/+;park^25::24B-GAL4/park^25, (g) UAS-Dret^MEN2A/+;park^25::24B-GAL4/park^25. TEM sample preparation and imaging was performed by Marianna Braun, EM-Histo facility, MPIN._

sarcomeres with altered morphology, significantly shorter, with a missing Z-line and an enlarged M-line, hereafter referred to as "short". The different muscle phenotypes are, however, not fully penetrant and vary to a high degree in their expressions. In addition to degenerated myofibrils, the mitochondria of the muscles are severely distorted as discussed in section 2.4.3. These phenotypes appear to become more severe in older flies, which is why it is considered a degenerative phenotype, rather than developmental. We decided to use the indirect flight

Pink1^{B9/+}, mef2   mef2 > Dret^{MEN2A}   Pink1^{B9/Y}, mef2   Pink1^{B9/Y}, mef2 > , Dret^{MEN2A}

FM6   mef2 > Dret^{MEN2A}
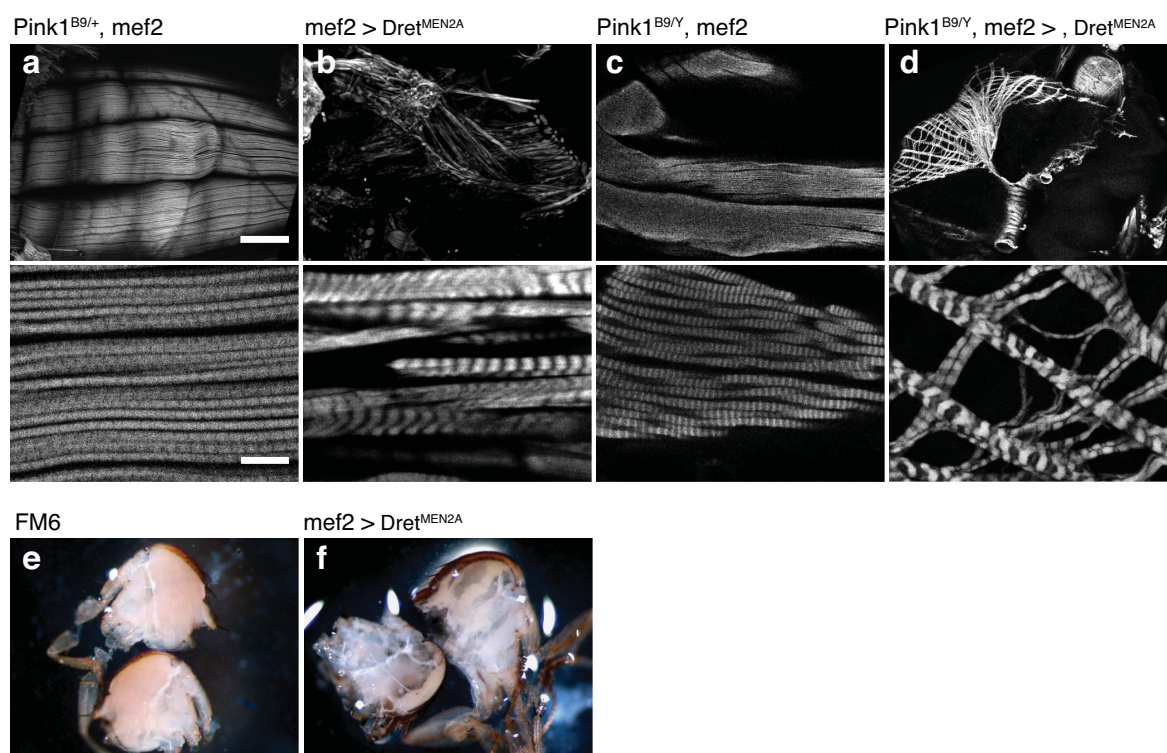
Figure 2-15 *mef2-GAL4* > Dret^{MEN2A} overexpression causes severe muscle phenotype – no interaction with *Pink1* loss of function. (a-d) Photomicrographs of hemi-thoraces stained with phalloidin-alexa568, with DL-IFMs at low magnification (upper panels) and individual myofibrils at high magnification (lower panels) of 1-2 day old flies with indicated genotypes, n=6-8 flies per genotype, (e,f) photomicrographs of hemi-thoraces under halogen illumination. Scale bars: (upper panel) 100 µm, (lower panel) 10 µm. Complete genotypes*: (a) Pink1^{B9}::mef2-GAL4/+, (b) Pink1^{B9}::mef2-GAL4/Y, (c) UAS-Dret^{MEN2A}/+;mef2-GAL4/+, (d) Pink1^{B9}::mef2-GAL4/Y;UAS-Dret^{MEN2A}/+, FM6/+.*

muscles as a system to study genetic epistasis between Dret and *park/Pink1* and hypothesized that active Dret overexpression can rescue the phenotypes of the *park* and *Pink1* mutants. No rescue of muscle or muscle- mitochondrial morphology in *park²⁵* mutants by *24B* > Dret^{MEN2A}

To test whether Dret^{MEN2A} can rescue the muscle degeneration, I used the driver line *24B-GAL4*, which is expressed in all mesodermal tissue including muscle from the embryonic stage through adulthood, to overexpress UAS-Dret^{MEN2A} in the *park²⁵* mutant line. From this cross, only a small fraction of the offspring carried both the UAS-Dret^{MEN2A} and the *24B* alleles, approximately 1:1000 flies, suggesting that the Dret^{MEN2A} expression in mesoderm may be lethal during development. The escapers, together with controls and *park²⁵* mutant flies were dissected and stained for f-actin using a fluorescent phalloidin conjugate to visualize the myofibrils (figure 13a-d). Among the different muscle abnormalities, I chose the characteristic sarcomere morphology of the park mutant files ('short') to score whether this phenotype was rescued (figure 2-13e). Approximately 50 % of the *park²⁵* mutant flies displayed this morphology (13c,f), and in the *park^{25/25}*, *24B* > Dret^{MEN2A} flies, this ratio was not significantly different (figure 13d,f). It still

remained possible that even though the myofibril morphology was not rescued, the mitochondria would be. To investigate this, I again used UAS-mitoGFP to fluorescently label the mitochondria. Wild type muscle showed small round mitochondria aligned between the myofibrils in a dense row, homogenously spread over the muscle tissue (figure 2-14a). The appearance was not changed with Dret^{MEN2A} overexpression (figure 2-14b). In the *park^{25}* mutant flies, the mitochondria were severely enlarged (figure 2-14c), and this was not altered by 24B > Dret^{MEN2A} overexpression. Transmission electron microscopy (TEM) was also performed to examine whether the ultrastructure appearance of the mitochondria was rescued. Wild type mitochondria showed densely packed cristae, giving a dark appearance in TEM (figure 2-14e), which was quantified by optical density (2-14h). In the *park^{25}* mutants, the cristae density was significantly decreased and the cristae appear broken (figure 2-14f,h). This morphology was again not altered in Dret^{MEN2A} expressing mutants (figure 2-14g,h). In conclusion, there was no evidence that *24B* driven Dret^{MEN2A} expression could reduce the phenotypes of the *park* mutants. It should be noted that the flies analyzed were rare escapers from the overall high embryonic lethality of the Dret^{MEN2A} expression, and it is possible that these flies do not fully represent the general population, perhaps due to some genetic compensation.

2.4.5. Severe muscle degeneration from *mef2* > Dret^{MEN2A} overexpression

Since *24B* > Dret^{MEN2A} expression (1) caused high lethality and (2) did not rescue the *park^{25}* phenotypes, I decided to test another driver line, the *myocyte enhancer factor 2 (mef2)-GAL4*, in which expression is restricted to muscle tissue. *Mef2* > Dret^{MEN2A} expression in control flies caused a severe loss of muscle tissue with remaining myofibrils being abnormally thick, and having a completely distorted appearance compared to controls (figures 2-15a,c,e,f). Expressing Dret^{MEN2A} in the *park^{25}* line also caused embryonic lethality. To test if the situation would be similar in a *Pink1* mutant background, I also examined the *Pink1* null mutant line *B9*. *Pink1^{B9}* flies have highly similar muscle and mitochondrial phenotypes to the *park* mutant flies, with about 60 % of the flies showing the typical "short" myofibril morphology (figure 2-15c). Expressing Dret^{MEN2A} with *mef2-GAL4* in a *Pink1* mutant background did not modify the severe Dret^{MEN2A} phenotype (figure 2-15d).

Pink1$^{B9/+}$, mef2

mef2 > Dret^{MEN2B}

Phalloidin

Pink1$^{B9/Y}$, mef2

Pink1$^{B9/+}$, mef2 > Dret^{MEN2B}

Pink1$^{B9/Y}$, mef2 > Dret^{MEN2B}

Phalloidin

f

wild type

short

thick/actin blobs

g

% of flies

wild type
short
thick/actin blobs

B9/+
B9/Y
mef2 > MEN2B
B9/+, mef2 > MEN2B
B9/Y, mef2 > MEN2B
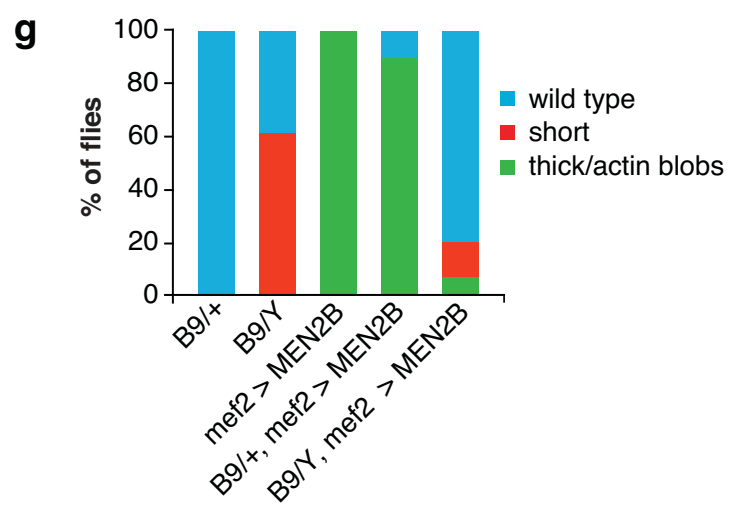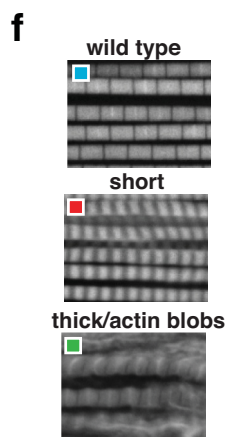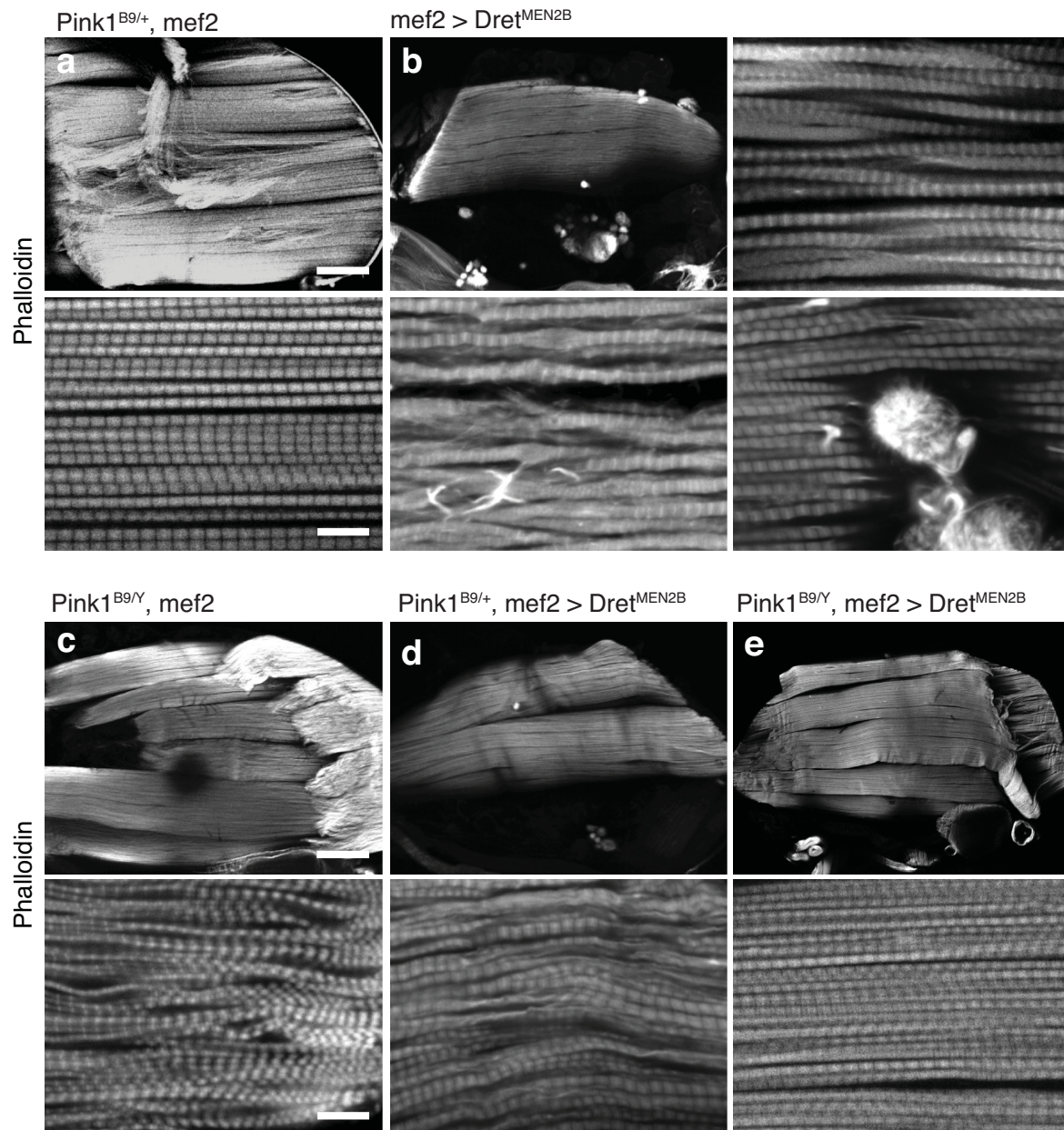
Figure 2-16 *mef2-GAL4* > Dret^MEN2B interacts genetically with *Pink1* loss of function in regulating myofibril morphology. (a-e) Photomicrographs of hemi-thoraces stained with phalloidin-alexa568, with DL-IFMs at low magnification (upper panels) and individual myofibrils at high magnification (lower panels) of 2-5 day old flies with indicated genotypes, photomicrographs of typical wild type, short or thick/frayed myofibrils, in (b) 3 example high magnification images illustrate different morphologies, (f) example images of typical wild type, 'short', or 'thick/actin blobs' myofibril morphologies, (g) percentage of flies with wild type (blue bars), short (red bars) or thick/actin blobs (green bars) sarcomeres. n=8-20 flies per genotype, scale bars: (upper panel) 100 μm, (lower panel) 10 μm. Complete genotypes: *(a) Pink1^B9::mef2-GAL4/+, (b) Pink1^B9::mef2-GAL4/Y, (c) UAS-Dret^MEN2B/+;mef2-GAL4/+, (d) Pink1^B9::mef2-GAL4/+;UAS-Dret^MEN2B/+, (e) Pink1^B9::mef2-GAL4/Y;UAS-Dret^MEN2B/+.*

2.4.6. Genetic interaction between *mef2* > Dret^MEN2B and *Pink1* in regulating muscle morphology

The experiment using *mef2* > Dret^MEN2A demonstrated that activated Dret signaling can regulate muscle morphology in a powerful manner. The other version of constitutively active Dret, MEN2B, previously gave a milder phenotype as compared to MEN2A in eye development (Aron *et al.* 2010). To test the effect of MEN2B in the muscle system, I overexpressed Dret^MEN2B using *mef2-GAL4*. The flies were viable, but showed muscle morphology with several abnormalities, commonly including thicker myofibrils of irregular shape, often with large actin deposits (figure 2-16a). To investigate whether Dret^MEN2B interacts genetically with *Pink1*, I overexpressed it in a *Pink1^B9* mutant background (figure 2-16b-e) and scored the flies for the myofibril appearances 'short', 'thick/actin blobs', or 'wild type' (figure 2-16f). Of the *Pink1^B9* mutants, 65% displayed
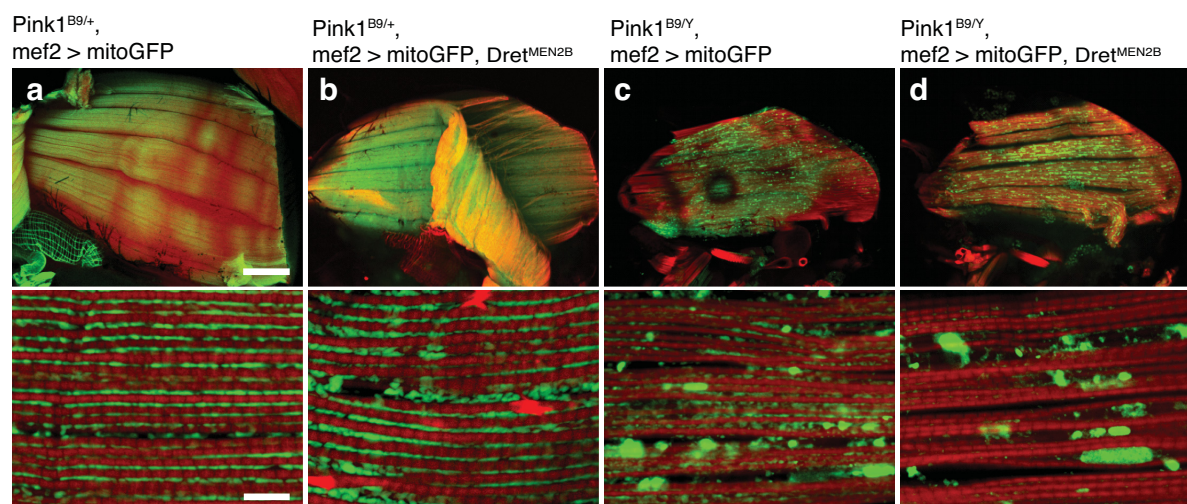
Figure 2-17 *mef2-GAL4* > Dret^MEN2B overexpression does not rescue mitochondrial morphology phenotype of *Pink1* mutants. (a-d) Photomicrographs of hemi-thoraces stained with phalloidin-alexa568, mitochondria labeled with UAS-mitoGFP, DL-IFMs at low magnification (upper panels) and individual myofibrils at high magnification (lower panels) of 2-5 day old flies with indicated genotypes, n=8-10 flies per genotype, scale bars: (upper panel) 100 μm, (lower panel) 10 μm Complete genotypes: *(a) Pink1^B9::mef2-GAL4/+;UAS-mitoGFP/+, (b) Pink1^B9::mef2-GAL4/Y;UAS-mitoGFP/+, (c) Pink1^B9::mef2-GAL4/+;UAS-Dret^MEN2B/UAS-mitoGFP, (d) Pink1^B9::mef2-GAL4/Y;UAS-Dret^MEN2B/UAS-mitoGFP.*

the 'short' phenotype, the remainder had wild type-like myofibrils (figure 2-16g). Overexpressing Dret^{MEN2B} in flies heterozygous for *Pink1^{B9}* led to 92 % displaying 'thick/actin blobs' myofibrils. In *Pink1^{B9}* mutants overexpressing Dret^{MEN2B}, 80 % instead displayed wildtype-like myofibrils, with the remaining showing either the "short" phenotype (13 %) or the "thick/actin blob" phenotype (7 %). These results indicate that Dret^{MEN2B} under control of the *mef2-GAL4* driver interacts genetically with Pink1 in regulating muscle morphology.

2.4.7. No rescue of Pink1 mitochondrial phenotype by *mef2* > Dret^{MEN2B} overexpression

To test whether Dret^{MEN2B} overexpression could rescue mitochondrial abnormalities in the *Pink1* mutants, I used the UAS-mitoGFP allele to genetically label mitochondria in *Pink1^{B9}, mef2 >* Dret^{MEN2B} flies. The analysis showed that Pink1 heterozygous controls expressing Dret^{MEN2B} had normal mitochondrial morphology compared to controls (figure 2-17a,b). *Pink1^{B9}* mutants showed a mitochondrial phenotype highly similar to the park mutants as reported previously (figure 2-17c). In Dret^{MEN2B} expressing *Pink1^{B9}* mutants, no difference was seen as compared to *Pink1^{B9}* alone (2-17-d).

2.5. Function of combined *Ret* and *PINK1/Parkin* activity in nigrostriatal dopamine neurons of aged mice

2.5.1. Generation of *Ret/PINK1* and *Ret/Parkin* double mutant mice

We previously showed that *Ret* interacted genetically with *DJ-1* in the dopamine neurons of the SNpc during aging in mice, where 18 month old *Ret/DJ-1* double mutant mice had lost a higher number of neurons than those of *Ret* and *DJ-1* single mutants combined. Knockout mouse models for the two other common genes causing ARPD, *Parkin* and *PINK1*, have previously been characterized by several different groups, and show no neurodegenerative phenotypes, similar to *DJ-1* mutants. We now asked whether the genetic interaction between *DJ-1* and *Ret* was specific for *DJ-1* or also present between *Ret* and *Parkin* and/or *PINK1*. To this end, the *Dat-Cre;Ret^{lx}* mice ("*Ret*") were crossed to mice with *PINK1^{lx}* and *Parkin$^-$* alleles. The use of a conditional *PINK1* allele would allow us to conclude that a hypothetical genetic interaction would be cell autonomous. To be able to directly compare it with results from the *Ret/Parkin* and *Ret/DJ-1* situations that are null alleles, we also generated a *PINK1$^-$* allele by recombining the *PINK1^{lx}* allele in the germ line, mediated by the *DAT-Cre* recombinase.

2.5.2. Normal development of *Ret/PINK1* double mutant mice and absence of early neurodegeneration

Ret/PINK1^{lx}, *Ret/PINK1$^-$* and *Ret/Parkin* double mutant mice were all viable and did not present apparent phenotypes at birth. To assess whether young mice would already show the onset of an early neurodegenerative phenotype, a cohort of *Ret/PINK1^{lx}* and littermate controls were sacrificed at 3 months of age. We performed stereological quantifications of TH+ neurons in the SNpc and measured the density of TH+ fibers in the striatum but the results showed no signs of early neurodegeneration, with equal numbers of TH+ neurons and striatal fibers in controls and double mutants (figures 2-18a,b, 2-19a,b).

2.5.3. No behavioral alterations or neuronal loss in aged *Ret* single, *Ret/PINK1*, and *Ret/Parkin* double mutant mice

At 18 months, we performed a behavioral assessment by measuring activity in an open field arena as described previously (see section 2.1.4). The results confirmed that mice carrying the *DAT-Cre* allele are hyperactive compared to controls, but we did not see a difference between *PINK1^{lx}* and *Ret* or *Ret/PINK1^{lx}* as in the case of the *Ret/DJ-1* analysis (figure 2-18c). Next, we performed stereological quantifications of TH+ neurons in the SNpc and unexpectedly, there was no reduction in the number of TH+ neurons in Ret single mutant mice compared to controls (figure 2-18d). In *Ret/PINK1^{lx}* double mutants there was a small (21%) but significant reduction of TH+ neurons compared to *PINK1^{lx}* single mutants. Due to delays in the breeding of the *Ret/Parkin* and *Ret/PINK1$^-$* mice, we did not have more than two mice per group of these double mutant lines, however we decided to analyze them to see whether there were any clear tendencies.

2.5.4. Normal density of striatal TH+ fibers in aged *Ret* and *Ret/PINK1* double mutant mice

Stereological quantifications of *Ret*, *Ret/PINK1$^-$* and *Ret/Parkin* double mutant lines did not however indicate any tendencies of loss of DA neurons in these mice (figure 2-18e). To quantify the density of striatal TH+ fibers, we developed a new image analysis method based on automated recognition of the fibers to measure the image area covered by fibers, divided by the total image area, with the striosomal compartment excluded. This method does not require manual thresholding of the images, which makes it more unbiased and less time consuming. To test the method, 18 month old mice from the previous *DJ-1* and *DJ-1/Ret* colony were analyzed. The results were in agreement with the previous data and indicated a 48 % decrease in fiber density in *DJ-1/Ret* compared to *DJ-1* alone (figure 2-19c,d). Thus, these results validated that
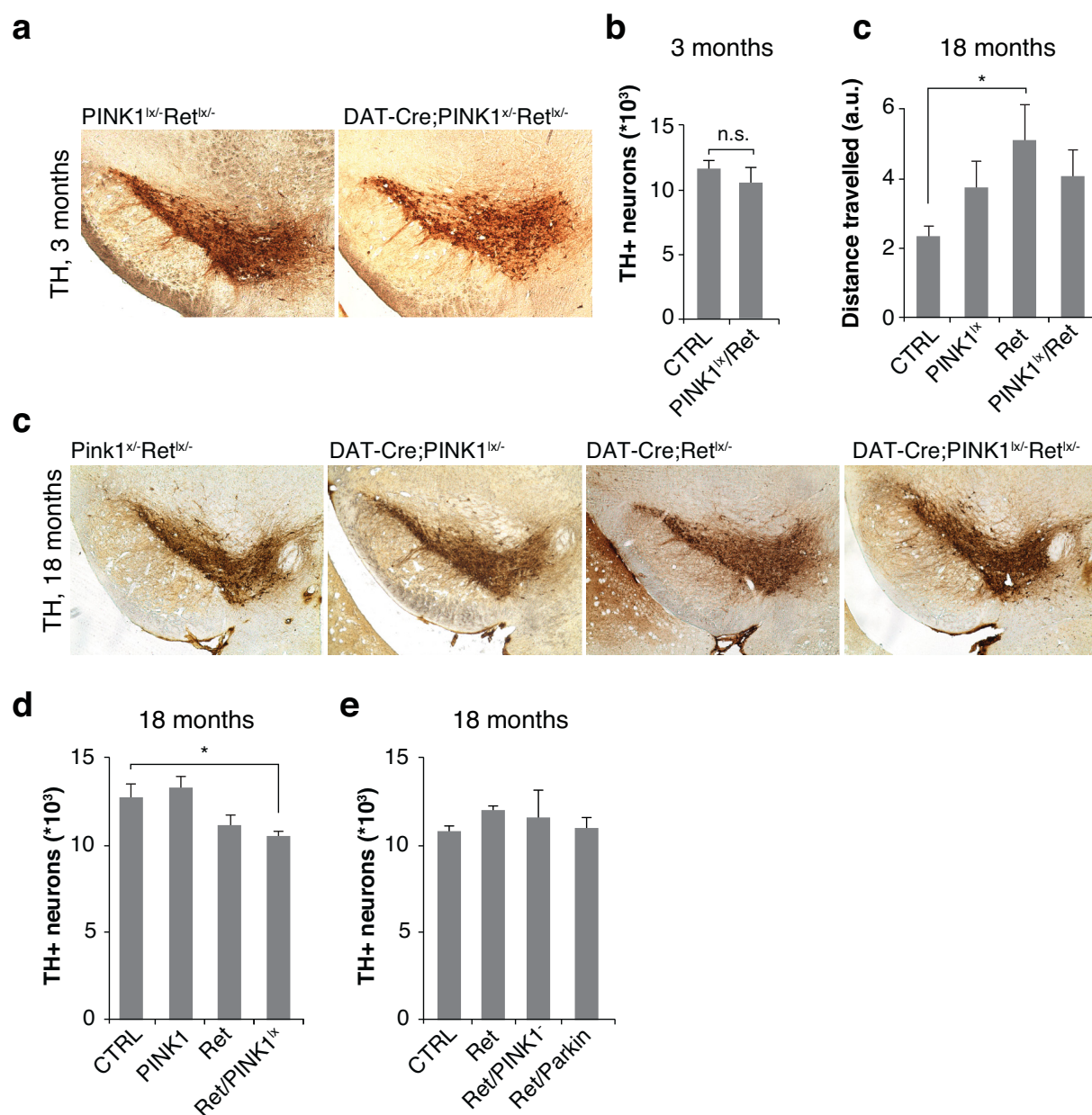
Figure 2-18 No behavioral deficits or loss of TH+ neurons in aged *Ret* single, *Ret/PINK1* or *Ret/Parkin* double mutant mice. (a,d) Photomicrographs of coronal brain sections from 18 months old control, *PINK1^lx^*, *Ret*, and *Ret/PINK1^lx^* mutant mice showing dopamine neurons in the substantia nigra (SNpc) for the DA markers TH. (b,e,f) Stereological quantifications of DA neurons in SNpc: (b) 3 month old control and *Ret/PINK1^lx^* mice, n= 3 mice per genotype, (e) 18 month old control*, PINK1^lx^, Ret, Ret/PINK1^lx^* mice, n=4-8 mice per genotype, (f) 18 month old control, *Ret, Ret/ PINK1^-^, Ret/Parkin* mice, n=2-3 mice per genotype, (c) behavioral assessment of control*, PINK1^lx^, Ret* and *Ret/PINK1^lx^* mice in an open-field arena where horizontal movement was automatically tracked during 20 min, n=4-9 mice per genotype means ± SEM, * p<0.05, one-way ANOVA with Bonferroni's post hoc test (stereology), student's t-test (open-field), n.s. = not significant. Scale bars: (a,d) 250 μm. Complete genotypes: *mixed controls, DAT-Cre;PINK1^lx/-^, DAT-Cre;Ret^lx/-^, DAT-Cre;Ret^lx/-^;PINK1^lx/-^, DAT-Cre;Ret^lx/-^;PINK1^-/-^, DAT-Cre;Ret^lx/-^;Parkin^-/-^*. Mice were bred by P. Klein, behavioral testing and perfusion was performed by P. Klein and Daniel Nagel, histological preparations, immunostainings and stereological quantifications were performed by D. Nagel.

the new method could detect a decrease in fiber density, while at the same time confirming previous results of the requirement of *Ret* for maintaining striatal fibers. Next, we analyzed the fiber density of the 18 month old control, *Ret*, *PINK1^{lx}* and *Ret/PINK1^{lx}* double mutants. In striking contrast to previous results, we did not observe any decrease of fibers in *Ret* single or *Ret/PINK1^{lx}* double mutants compared to *PINK1^{lx}* or heterozygous controls (figure 2-19c,e). Finally, we analyzed the TH+ fiber density in 24 month old control, *PINK1^{lx}*, *Ret* and *Ret/PINK1^{lx}* mice. As expected, the results showed no reduction of fiber density in the *Ret* or *Ret/PINK1^{lx}* compared to controls or *PINK1* mutants, similar to results at 18 months (figure 2-19f,g). At this point, we can only conclude that the original Ret and Ret/DJ-1 mouse colonies responded highly differently to conditional ablation of Ret in terms of the integrity of the nigrostriatal system, than the new Ret, Ret/Pink1, and Ret/Parkin mouse colony.
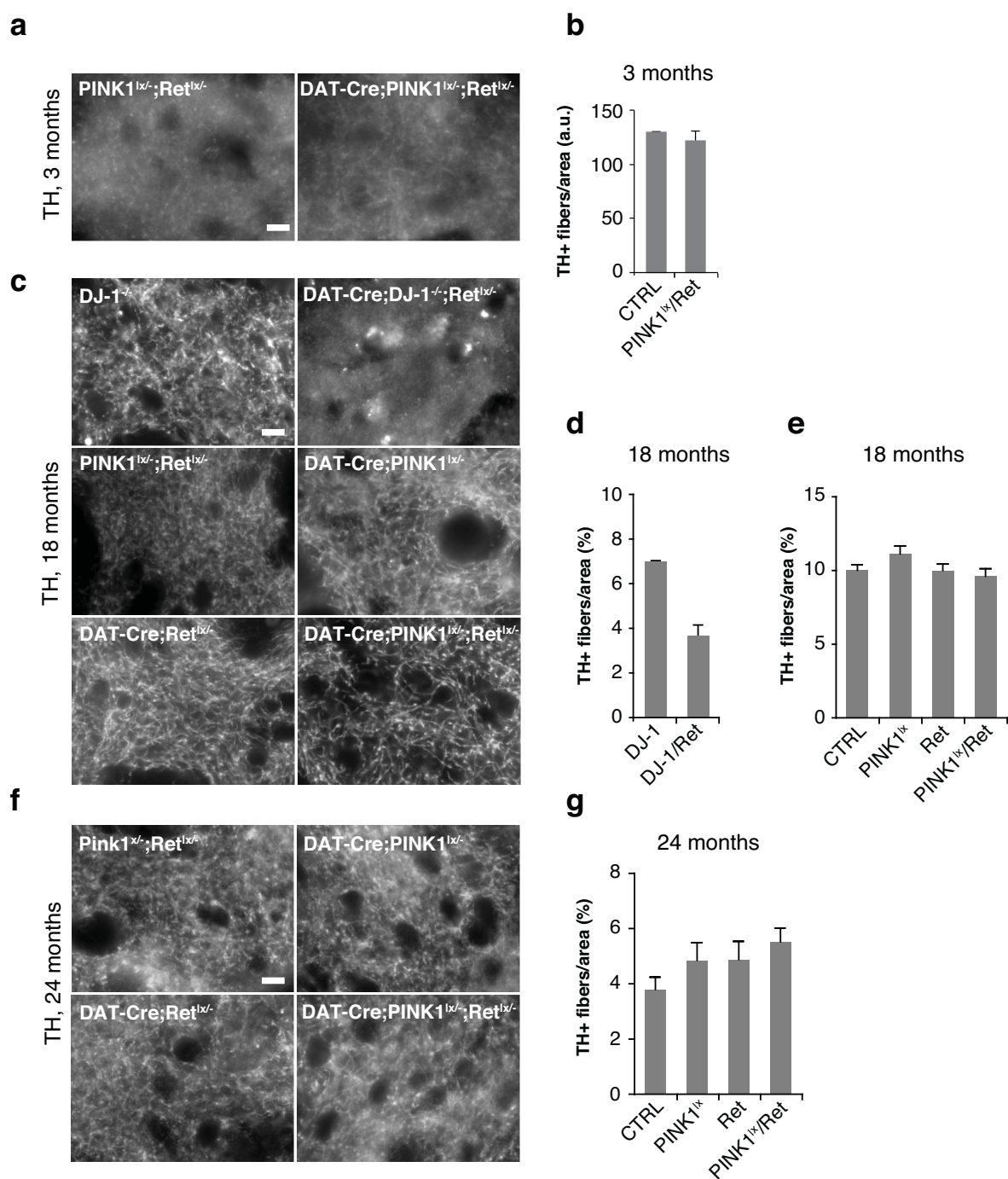
Figure 2-19 No loss of TH+ fibers in aged *Ret* single or *Ret/PINK1*^{lx} double mutant mice. (a,c) Photomicrographs of coronal brain sections from (a) 3 month old control and Ret/Pink1 double mutant mice, (c) 18 month old *DJ-1, Ret/DJ-1*, control, *PINK1*^{lx}*, Ret,* and *Ret/PINK1*^{lx} mice and, (e) 24 months old control, *PINK1*^{lx}*, Ret,* and *Ret/ PINK1*^{lx} mice showing axonal fibers of the dorsal striatum stained for the DA marker TH, (b) quantifications of fiber density using the counting grid method, n=3 mice per genotype, (d,e,f) quantifications of fiber density using the automated fiber area method, (d) n=2 mice per genotype, (e) n=5-8 mice per genotype, (g) n=3-5 mice per genotype means ± SEM, Scale bars: (a,b) 10 µm. Complete genotypes: *mixed controls, DAT-Cre;PINK1*$^{lx/-}$*, DAT-Cre;Ret*$^{lx/-}$*, DAT-Cre;Ret*$^{lx/-}$*;PINK1*$^{lx/-}$*, DJ-1*$^{-/-}$*, DAT-Cre;Ret*$^{lx/-}$*;DJ-1*$^{-/-}$*.* Mice were bred by P. Klein, perfusions and histological preparations were performed by P. Klein and D. Nagel, immunostainings by D. Nagel, microscopy and image analysis in (e) by D. Nagel and in (d,g) by P. Klein.

3. Discussion

The neurotrophic factor GDNF and its receptor Ret have proven to be required for the survival of nigrostriatal dopamine neurons during aging in mice, and therefore provide a target for PD therapy, currently under clinical development. Although they evidently have a critical function in dopamine neurons, the nature of this function remains largely unknown. In this project, we investigated whether Ret signaling cooperates with three ARPD-associated genes in maintaining critical cellular functions during aging and cellular stress. For this purpose, we have used mouse genetics to analyse how double loss-of-function affects dopamine neurons during aging. Furthermore, we studied cellular signaling and mitochondrial dynamics in cultured cells, and finally, genetic epistatis in *Drosophila*. We found that combined activity of Ret and DJ-1 is required for survival of a population of SNpc dopamine neurons during aging, indicating a genetic interaction between the two genes. In biochemical analysis using cultured cells, I found no evidence for a function of DJ-1 in regulating either PI3K-Akt, or Ras-Erk signaling pathways, in opposition to previously published reports. I also asked whether Ret signaling can compensate for loss of Parkin and PINK1, and found a novel function of Ret in reversing mitochondrial fragmentation after PINK1 or Parkin knockdown. In *Drosophila,* I found that constitutively active Dret can strongly modify muscle development and can, to some extent compensate, for *Pink1* loss-of-function in terms of myofibril morphology. However, Dret did not rescue mitochondrial impairment of *park* or *Pink1* mutants. Lastly, I investigated how combined loss of *Ret* and *PINK1* or Parkin affects the survival of dopamine neurons in aging mice. Unexpectedly, I found no signs of neurodegeneration, either in Ret single, or in Ret/PINK1 and Ret/Parkin double mutants, suggesting that unknown factors, possibly genetic background, are critical for the development of a neurodegenerative phenotype in mice lacking Ret function.

3.1. DJ-1 is required for survival of a subset of neurons lacking Ret during aging

To test whether *Ret* and *DJ-1* interact genetically, we generated double mutant mice that lack *Ret* in DA neurons, and *DJ-1* in all cells, and followed these mice during aging. Intriguingly, these

mice showed increased neurodegeneration of nigrostriatal DA neurons compared to *Ret* single mutant mice, which at two years had lost approximately 26 % of their SNpc DA neurons, while the double mutant mice had lost 41 %, indicating a strong interaction between the two genes. *DJ-1* single mutant mice showed no loss of neurons, so it appears that DJ-1 is not critical for survival of DA in mice without further insults. However, when the neurons are impaired in receiving trophic signaling via the Ret receptor, DJ-1 becomes critical for survival of a subset of neurons. When we studied the axonal projections of the nigral neurons in the target area, the dorsal striatum, we found that the density of fibers in Ret single mutants was reduced by about 50 % compared to controls, and interestingly this difference was repeatead in the *Ret/DJ-1* double mutants. The fact that the loss of fibers exceeded the loss of cell bodies in *Ret* mutants was previously known, and indicates that Ret has a critical function in maintaining axons. The finding that *Ret/DJ-1* double mutants did not lose additional fibers, indicates that DJ-1 does not have a function in axon maintenance, but protects against cell death via other mechanisms.

The two datasets of striatal innervation and SNpc cell body numbers create an interesting implication: When a neuron dies, its axon usually degenerates with it. Since more cell bodies were lost in *Ret/DJ-1* double mutants than in Ret single mutants, we would intuitively expect a corresponding decrease in fibers. As this was found not to be the case, there are two hypothetical models that can explain this data. One possibility is that the remaining neurons in the *Ret/DJ-1* double mutants compensate for the loss of striatal DA fibers by resprouting, thereby increasing the number of fibers per neuron (figure 3-1, model A). Alternatively, there could be a population of surviving neurons in the *Ret* mutants that have lost most of their striatal fibers. These neurons would be sensitized, and in mice lacking also *DJ-1*, this population would succumb to a higher extent than neurons richer in axonal projections (figure 3-1, model B). We regard the first theory of resprouting as more improbable, since it was shown that Ret is required for resprouting after MPTP lesions (Kowsky *et al.* 2007), however, as this is a different genetic model, we cannot exclude this theory. We elaborated on the second theory, and further hypothesized that if some neurons have lost most of their target innervation, they would be smaller and atrophic, compared to the others, as they would have received less trophic support with smaller axonal arbors. If this indeed were the case, we would predict a decrease in average cell body size in the *Ret* mutants compared to controls, with an increase in the average size in *Ret/DJ-1* double mutants, as the atrophic neurons succumb. To test this theory, I measured the cell body size of SNpc DA
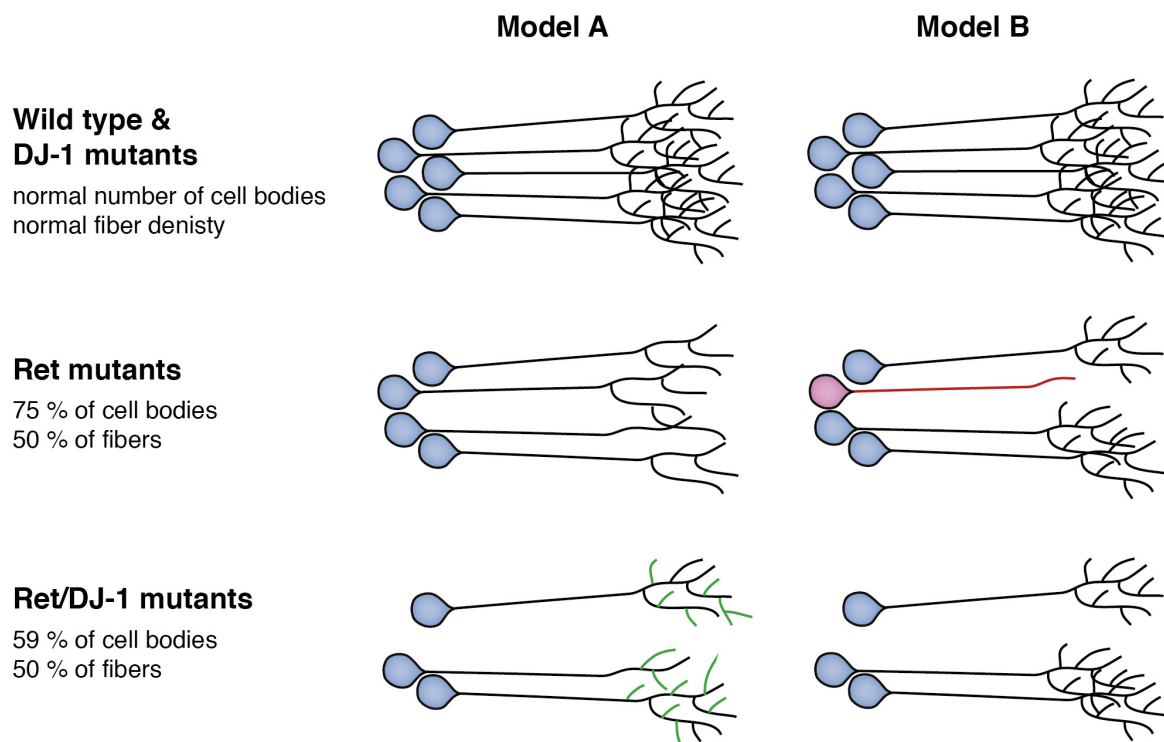
Figure 3-1 Two models of neurodegeneration of nigrostriatal neurons in *Ret* single and *Ret/DJ-1* double mutant mice. 24 month old *Ret* mutant mice showed a reduction of approximately 25 % of the TH+ SNpc cell bodies and 50 % of the striatal fibers as compared to wild type of *DJ-1* mutants (unaffected). *Ret/DJ-1* double mutants showed, as compared to *Ret* alone, an increased 41 % reduction of TH+ SNpc neurons, while the density of striatal fibers remained unchanged as compared to *Ret*. Two theoretical models can explain the numbers: In model A, the remaining neurons in *Ret/DJ-1* double mutants resprout, to compensate for the neuronal loss, (green indicating new fibers). In model B, a population of neurons has lost most of its fibers and is sensitized (pink), while remaining neurons have more intact fibers. In *Ret/DJ-1* double mutants, the sensitized population is preferentially lost.

neurons, and results showed that it was slightly decreased in *Ret* mutants as compared to controls, as predicted. However, in *Ret/DJ-1* double mutants, there was no significant decrease compared to controls, but also no significant increase compared to *Ret* mutants, due to variation between animals and the small magnitude of difference in the *Ret* mutants. Because of this, we were, unfortunately, not able to conclude from this experiment whether the theory was correct or not.

The behavioral assessment showed that mice carrying the *DAT-Cre* knock-in allele were hyperactive compared to controls, but there was no reduction in Ret single or *Ret/DJ-1* double mutants as compared to *DAT-Cre* controls. With only one functional copy of the *DAT* gene, neurons are deficient in dopamine-reuptake at the synapse, which causes increased synaptic dopamine levels, similar to the effects of pharmacological DAT inhibitors, such as cocaine. It is

possible that this effect masks functional impairments that otherwise would be present in the double mutants. In fact, the *DJ-1* single mutants were hypoactive, while the *DAT-Cre* carrying *Ret/DJ-1* double mutants were hyperactive. Measurements of striatal dopamine content showed elevated levels in *DAT-Cre*, *Ret* single and *Ret/DJ-1* double mutants compared to controls, likely due to a compensatory upregulation in response to the reuptake deficiency. The fact that dopamine content in 18 month old mice was at a similar level in *DAT-Cre*, *Ret* single and *Ret/DJ-1* double mutants, despite approximately 50 % less striatal fibers in the latter two, suggests that dopamine synthesis may have been even further upregulated in the mutants. Western blot analysis of the rate-limiting dopamine synthesis enzyme TH could not, however, confirm this theory, although the analysis, for technical reasons had to be performed in 24 month-mice, which cannot exclude a down-regulation of TH between 18 and 24 months.

It remains unclear why combined activity of *Ret* and *DJ-1* is required for maintaining a population of dopamine neurons. One possibility is that the Ret and DJ-1 proteins perform relatively independent functions in the cell, although the meaning of independence in a cell's physiology is, of course, a matter of definition. Deficiency of one of these functions could sensitize the cell, and additional impairment of the second function, could cause cell death. Another possibility is that Ret and DJ-1 cooperate in a much more direct way, by regulating the same function, for example a particular signal transduction pathway. It is important to note that the combined activity of *Ret* and *DJ-1* is not required for cell survival in young mice, as three month old double mutants showed normal numbers of neurons – it is only upon aging that their functions become critical. Because of this fact, we can narrow down the possible functions of both DJ-1 and Ret to aging-dependent processes.

Following this argument, it is of importance to understand what occurs during aging of a DA neuron. Aging is a process that involves molecular damage to the cell's proteome, genome and lipids – damage that cannot be fully repaired and therefore, accumulates. DNA damage and oxidative stress are two events widely accepted to play a central role in the aging process. Superoxide and reactive oxygen species are generated by the electron transport chain of the mitochondria, and can cause somatic DNA mutations, modifications of proteins and lipids, protein misfolding and aggregation – other processes that are believed to be involved in the aging process. Mitochondrial DNA could be particularly vulnerable to oxidative stress due to its close physical proximity to the electron transport chain, and indeed mice lacking a mitochondrial

DNA transcription factor, have reduced efficiency of mitochondrial biogenesis (Ekstrand *et al.* 2007). In addition to producing ATP, mitochondria play a critical role in buffering cellular calcium, together with the ER. SNpc DA neurons are unusual in that they rely on the L-type voltage gated calcium channel, Ca(v)1.3, for autonomous pacemaking, which causes bigger calcium transients than in other cell types. Mitochondria are critical for buffering the calcium influx, thus avoiding calcium overload (C. S. Chan *et al.* 2007). It was recently found that the calcium buffering function was impaired in *DJ-1* null mice, which was due to decreased expression of mitochondrial uncoupling proteins, causing increased oxidative stress and cell death (Guzman *et al.* 2010). It is possible that regulating the expression of mitochondrial proteins, required for calcium buffering, is a critical function of DJ-1 during aging. Interestingly, a study found that Ret regulates several different types of voltage-gated calcium channels in dorsal root ganglionic neurons, specifically via Ras-Erk signaling (Woodall *et al.* 2008). In addition, GDNF was found to regulate A-type potassium channels in midbrain DA neurons, also via Ras-Erk signaling (F. Yang *et al.* 2001). One hypothesis is, therefore, that both Ret and DJ-1 are required for controlling calcium homeostasis – Ret controls one or several cation channels via Erk signaling, while DJ-1 promotes mitochondrial calcium buffering via upregulation of uncoupling proteins. This hypothesis would fit well with the fact that the type of neurons preferentially lost in *Ret/DJ-1* double mutants have very special calcium/potassium signaling properties as they express GIRK2 but not calbindin, and are dependent on Ca(v)1.3 pacemaking.

3.2.   DJ-1 does not regulate Akt or Erk activation *in vitro*

Two studies reported that *DJ-1* interacts genetically with the PI3K/Akt pathway in *Drosophila*, the second of which, by Mak and colleagues further showed that *DJ-1* interacts genetically with the phosphatase *PTEN*. Furthermore, in mammalian cell culture, they found that DJ-1 dramatically upregulates Akt phosophorylation in COS7, A549, NIH-3T3 and MEF cells. In this study, a modest RNAi depletion of DJ-1 caused the normally high levels of Akt phosphorylation to decrease to almost undetectable levels (R. H. Kim, Peters, *et al.* 2005). Such a function of DJ-1 creates an interesting direct link to Ret signaling, which is a strong activator of PI3K. It would also suggest a mechanism by which DJ-1 and Ret may promote cell survival, as Akt is a key regulator of apoptosis and metabolism among other things. Unexpectedly, I found no evidence of DJ-1 regulating Akt phosphorylation, although I used similar methods and several cell types common to the previous report. The reason the results of our studies differ is unclear.

In parallel work from our group in *Drosophila*, no evidence was found for *DJ-1A/B* being a strong genetic interactor of *Akt* or *PI3K* (Aron *et al.* 2010)*,* again contradicting previous studies. Later, a follow up study by Mak and colleagues reported that DJ-1 regulates Akt specifically under hypoxic conditions, but in this report the effect under standard oxygen conditions was modest (Vasseur *et al.* 2009).

In work by our group, it was found that DJ-1 interacts genetically with the Ras-Erk pathway in *Drosophila* and later, another group reported that DJ-1 increased Erk1/2 phosphorylation in COS7 cells (Aron *et al.* 2010; L. Gu *et al.* 2009). In my experiments, I found no evidence for DJ-1 as a regulator of Erk1/2 phosphorylation in mammalian cell lines. It remains possible that DJ-1 converges with the Ras-Erk pathway downstream of the Erk signaling cascade, but we were unable to pinpoint the exact nature of the genetic interaction. Erk1/2 activates major transcription factors, such as c-myc and the Cre-binding protein (CREB), and these could be possible targets of DJ-1 activity or a DJ-1 regulated pathway. Erk1/2 also regulates translation via map-kinase interacting kinase 1/2 (Mnk1/2) and the ribosomal S6-kinases, and DJ-1 has been suggested to regulate protein translation in general (van der Brug *et al.* 2008).

It was previously reported that serum treatment induces DJ-1 expression in HeLa cells, and indirect evidence suggested that the effect was mediated via the Ras-Erk pathway (Nagakubo *et al.* 1997). To test whether the same was true for Ret signaling, I used the SH-SY5Y cell line, which expresses endogenous Ret, but saw no effect on DJ-1 levels, either after GDNF/GFRα1, or serum treatment. I also investigated whether GDNF or oxidative stress could cause DJ-1 to translocate between subcellular compartments, as DJ-1 had been reported to localize to the cytosol, nucleus, and mitochondria. In my experiments, I conversely found no evidence for a significant translocation with 3 or 24 hours of treatment, although the results were somewhat difficult to interpret. However, even if such an effect of Ret – regulating either DJ-1 expression, or localization – had been present, this type of linear pathway would not fit well with the genetic findings from the mouse experiment, where double loss-of-function caused an increased phenotype. This type of synergism is rare in genetics and is typically observed by modifying two genes that regulate a common target. In such a case, disrupting the function one gene causes either a mild, or no phenotype, as the other gene compensates, maintaining the target function. However, when disrupting the second gene, the common target is impaired to a greater extent,

whereupon a phenotype appears. The recent finding that DJ-1 is required for protecting against oxidative stress, by increasing the mitochondrial calcium buffering capacity (Guzman *et al.* 2010), would serve as such a candidate target function, and remains to be investigated, particularly in the light of our later finding that Ret can control mitochondrial integrity.

3.3. GDNF/Ret reverses mitochondrial fragmentation after Parkin or Pink1 depletion – a novel function of neurotrophic factor signaling

We were interested in studying if Ret signaling converges with the functions of Parkin and Pink1, in addition to DJ-1. It had recently been shown that *Pink1* and *park* mutant *Drosophila* have swollen, functionally impaired mitochondria, and that PINK1 or Parkin depleted mammalian cells displayed fragmented mitochondrial networks. We decided to test whether GDNF stimulation could regulate mitochondrial dynamics in the neuroblastoma cell line SH-SY5Y after Parkin depletion. Even though the experiments did not fully recapitulate the mitochondrial fragmentation after Parkin depletion, it was evident that GDNF/GFRα1 treatment shifted the balance towards fusion, as both control and Parkin siRNA cells had less fragmented mitochondria after the treatment. Using Ret9 transfected HeLa cells, I could further show that PINK1 knockdown caused robust mitochondrial fragmentation, which was rescued by GDNF/GFRα1 treatment. Since HeLa cells do not express the alternative GDNF receptor NCAM, we concluded that the effect is mediated by Ret. To begin dissecting the pathway by which Ret reverses mitochondrial fragmentation, the natural starting point was to test which of the canonical pathways activated by Ret is required. In order to do this, I first used Ret9 signaling mutants, Ret9^{Shc+} and Ret9^{Dok+}, which have altered affinity to the adaptor proteins that activated Ret recruits. Ret9^{Shc+} was reported to increase PI3K activation, while Ret9^{Dok+} was reported to increase Ras activation with significantly decreased PI3K activation (Stenqvist *et al.* 2008; Lundgren *et al.* 2006). The experiment showed that both constructs rescued the mitochondrial fragmentation, suggesting that the effect is independent of PI3K/Akt, but western blot analysis for phospho-Akt unfortunately showed residual Akt activation by Ret9^{Dok+}. Akt phosphorylation was reduced as compared to the Ret9^{WT}, but not fully abolished, and for this reason involvement of the Akt pathway cannot be ruled out by this experiment. Another way to address the question was to use pharmacological kinase inhibitors. The results indicated that when inhibiting PI3K, Ret was still able to rescue mitochondrial fragmentation. On the other hand, when inhibiting Mek1/2 in the Ras-Erk pathway, rescue was abrogated. A problem with

this approach is that applying pharmacological compounds interfere with the basic physiological signaling of the cell, whereas the signaling mutant constructs only modulate the signaling added by Ret overexpression. High concentrations of kinase inhibitors are toxic, while low concentrations leave residual signaling. In these experiments, even though Akt phosphorylation was significantly reduced by the PI3K inhibitor, it cannot be ruled out that a low level of activation is sufficient to mediate the rescue. Conversely, it is possible that a high concentration of the Mek1/2 inhibitor is toxic, causing fragmentation by a different pathway, and masking the rescue. For these reasons, further experiments using independent methods are required to characterize the pathway of rescue in detail.

To understand how Ret signaling could reverse mitochondrial fragmentation after PINK1 or Parkin depletion, we should first recognize that at least two general scenarios are imaginable: (i) Mitochondria could fragment as a secondary consequence of different impairments, such as oxidative damage, deficient mitophagy, or other stress factors. It is possible that Ret signaling counteracts one of these primary causes, without directly regulating fusion or fission. (ii) On the other hand, the opposite scenario is also possible – that Ret signaling targets the physiological mechanisms controlling fusion and fission, and by activating Ret, the balance is shifted in the direction of fusion irrespective of mitochondrial impairments, or Parkin and PINK1 activity.

If we consider the first scenario, little is known about how Ret signaling may regulate these events. It is known that GDNF treatment reduces oxidative stress in rodent models of PD, but little is known about the mechanism (M. P. Smith & Cass 2007). It is possible that one of the pathways downstream of Ret activates transcription factors, such as Nrf1/2, which are important for protection against oxidative stress, and activate mitochondrial biogenesis to replenish the mitochondrial pool. Interestingly, Erk1/2 were found to localize to mitochondria in DA neurons of Parkinson's disease brains, and recently, it was shown by the same group that overexpression of a constitutively active version of Erk2 was sufficient to induce mitophagy in SH-SY5Y cells (J.-H. Zhu *et al.* 2003; Dagda *et al.* 2008). From these findings we can hypothesize that Ret signaling via the Erk pathway may compensate for loss of the PINK1-Parkin pathway by promoting clearance of damaged mitochondria by mitophagy.

If we instead consider the second scenario, it is known that activities of fission and fusion proteins are tightly regulated, and a number of regulatory factors have been identified. The E3 ubiquitin ligase MARCH5 ubiquitinates all three of the core fusion and fission proteins Drp1, Mfn1/2 and Opa1, shifting the balance towards fission. Mitochondrial-anchored protein ligase (MAPL) mediated ligation of small ubiquitin-like modifier (SUMO) to Drp1 also promotes fission (Westermann 2010). Also the Bcl2-family proteins Bax and Bak were found to regulate Drp1 SUMOylation, which is interesting since Bax and several other Bcl2-family proteins are regulated by Ret-activated pathways. Bax and Bak associate with Drp1 at fission sites, and this was linked to mitochondrial outer membrane permeabilization and apoptosis (Montessuit *et al.* 2010; Martinou & Youle 2011). Interestingly however, Bax and Bak were also found to promote fusion via Mfn1/2 during physiological conditions (Hoppins *et al.* 2011; Cleland *et al.* 2011). Furthermore, Drp1 is also regulated by phosphorylation at different positions, which are mediated by cAMP dependent kinase (PKA), Ca^{2+}/calmodulin-dependent protein kinase 1 alpha (CaMK1alpha) and cyclin-dependent kinase 1 (CDK1). However, Drp1 can also be dephosporylated by the protein phosphatase calcineurin, which is activated by Ca^{2+} (Cribbs & Strack 2007; Merrill *et al.* 2011; Taguchi *et al.* 2007). One possibility is that Ret signaling regulates one of these pathways or, thus far unknown modifiers of the Drp1/Mfn/Opa1 activity.

3.4. Ret overexpression regulates muscle development in *Drosophila* but is not a strong interactor of *Pink1* and *park*

Previously, our group has shown that the two *Drosophila* homologs of *DJ-1* interact strongly with Dret[MEN2] and the Ras-Erk pathway during eye development. As an example of this, combined overexpression of DJ-1A and Dret[MEN2A] in the compound eye caused a considerably stronger phenotype than overexpression of Dret[MEN2A] alone, while DJ-1A alone did not cause any phenotype. Here, I asked whether *park* interacts with Dret[MEN2A], in a manner analogous to that of DJ-1, and to test this, I overexpressed parkin using the same eye-specific driver and the Dret[MEN2A] allele. The results revealed no enhanced phenotype with Parkin overexpression, indicating that the function of modulating Dret signaling in eye development is specific to DJ-1 and not present in all ARPD-associated genes. However, in mammalian cell lines, I found a link under a different genetic situation - Ret signaling (gain-of-function) modulated phenotypes of Parkin and PINK1 loss-of-function. I tested whether this function of Ret is conserved in *Drosophila*, and specifically if Dret[MEN2A] overexpression could rescue some of the phenotypes in

park and *Pink1* mutants. I first analyzed the dopamine neurons in the PPL1 cluster for their relevance in PD, with respect to cell numbers and mitochondrial size. I found the loss of dopamine neurons to be smaller than previously reported, as the *park* mutants showed only loss of one out of twelve cells, while *Pink1* mutants had a normal number of cells. It is possible that a modifier in the genetic background, or increased stress due to particular housing conditions, is required to sensitize the flies enough to induce cell death. On the other hand, the reported mitochondrial phenotype of the *park* mutants was well reproduced in my experiment. However, overexpressing Dret^{MEN2A} using *TH-GAL4*, did not change mitochondrial size, either in a wild-type background, or in *park* mutants.

The indirect flight muscles of *park* and *Pink1* mutants have severely enlarged and dysfunctional mitochondria, and in addition, the myofibrils themselves are affected with abnormal sarcomere structure. When overexpressing Dret^{MEN2A}, driven by the broad mesodermal driver *24B-GAL4*, the eclosion ratio was very low, indicating that Dret^{MEN2A} is likely toxic to one of the targeted organs during development. The flies that were analyzed did not show any phenotype as adults, but the overexpression also did not modulate the *park* mutant phenotype. However, being such rare escapers, it is likely that these flies do not well represent the true nature of this genotype and should perhaps be regarded as abnormal. When instead expressing Dret^{MEN2A} using a driver that is restricted to somatic muscle cells (*mef2-GAL4*), the flies displayed highly severe muscle degeneration, much stronger than that of *park* and *Pink1* mutants. No genetic interaction between Dret^{MEN2A} and *Pink1* was seen, however with such a strong overexpression phenotype, a weak effect of the *Pink1* mutant allele may be hard to discern. Overexpression of the other constitutively-active allele, Dret^{MEN2B}, in the eye causes a milder phenotype than MEN2A, suggesting differences between the versions, either in substrate-specificity, or in activity. Expressing Dret^{MEN2B} alone using the *mef2-GAL4* driver caused a weaker phenotype than *mef2*>Dret^{MEN2A}, also in the indirect flight muscles, with wider, irregular myofibrils, and frequent actin blobs – a phenotype qualitatively different than the *park* and *Pink1* null phenotypes. Interestingly, I found that overexpressing Dret^{MEN2B} in *Pink1^{B9}* mutants largely eradicated both phenotypes, producing flies with largely normal myofibril morphology, suggesting partly epistatic function. However, there was no rescue of the gross mitochondrial morphology from what could be observed by mitoGFP labeling and fluorescence microscopy. It remains possible

that Dret^{MEN2B} overexpression generates a subtle rescue detectable by ultrastructural analysis, or readouts of mitochondrial activity, this possibility remains to be investigated.

It is generally assumed that the myofibril phenotype of *Pink1* mutants is caused by events downstream of the mitochondrial deficiency, and it is conceivable that it is rescued by Dret^{MEN2B} without rescuing the mitochondria *per se*. Another, although unlikely, possibility is that the myofibril and mitochondrial phenotypes are due to different functions of Pink1, of which Dret^{MEN2B} rescues only one. We have not yet found any evidence supporting the hypothesis that Dret controls mitochondrial integrity in *Drosophila*, which is in contrast to the results from cultured mammalian cells. However, there are several reasons why this could be the case, as the systems are different at several levels. First, the mitochondrial phenotypes of Parkin and Pink1 loss-of-function are opposite in RNAi treated cultured mammalian cells and in mutant *Drosophila*, in terms of their relation to fusion and fission proteins (see section 1.2.5). If mammalian Ret rescues increased fission, but not increased fusion, the results are perhaps expected. If, for example, Ret promotes fusion in general, we would actually expect a more severe phenotype when overexpressing Dret in the fly. However, I found no notable hyperfusion with Dret$^{MEN2A/B}$ overexpression in heterozygous control flies, and also no increased mitochondrial size in *park* and *Pink1* mutants. Another possible explanation is that Ret protects mitochondrial integrity only on a transient timescale after RNAi knockdown followed by GDNF treatment, as I did in cell culture, while the genetic modifications in *Drosophila* may be compensated for on a longer timescale. A third possibility is that functional differences between mammalian and Drosophila Ret produce the difference. Knowledge of the physiological function of *Dret* is limited and sequence conservation between *Dret* and mammalian *Ret* is moderate. Hence, it is possible that the function of *Dret* differs from the mammalian version.

The results from *mef2-GAL4* driven overexpression of both Dret^{MEN2} alleles indicate that high levels of Dret signaling can strongly regulate muscle development or maintenance. It is unclear whether Dret is physiologically expressed in muscle, but in previous expression studies, muscle was not mentioned as a tissue with Dret expression, and thus, Dret is likely not a physiological regulator of muscle development. However, in overexpression conditions, Dret$^{MEN2A/B}$ acts as a strong modifier, highlighting the importance of Dret-activated signaling pathways in the muscle system.

It was recently reported that two translational regulators with opposing functions, Eukaryotic translation initiation factor 4E-binding protein (4E-BP) and S6-kinase (S6K), both downstream of target of rapamycin (TOR), interact genetically with *Pink1* and *park*. Overexpression of 4E-BP, or removing its inhibition by TOR by blocking TOR with rapamycin, suppressed *Pink1* and *park* phenotypes, by promoting 5' cap-independent translation (Tain, Mortiboys, *et al.* 2009). Conversely, overexpression of S6K or TOR enhanced *Pink1* and *park* phenotypes, by promoting 5' cap-dependent translation (S. Liu & Bingwei Lu 2010). Along the same line, a recently published genome-wide screen showed that deficiency of PI3K21B suppressed *park and Pink1* wing posture phenotypes (Fernandes & Rao 2011). PI3K21B is an SH2 adaptor protein of the *Drosophila* PI3K complex, and since TOR is a downstream target of Akt, these three studies together suggest that reducing signaling via the PI3K-Akt-TOR pathway suppresses *park* and *Pink1* phenotypes by triggering a switch from 5'cap-dependent to 5'cap-independent translation, important in stress responses (Holcik & Sonenberg 2005). Since Dret activates PI3K, we could, based on these reports, predict that Dret overexpression would enhance the *Pink1* and *park* phenotypes. However, this was not the case, since Dret^MEN2B driven by *mef2-GAL4* suppressed the myofibril phenotype, and Dret^MEN2A expressed in DA neurons did not exacerbate the phenotype. In a recent genome-wide RNAi screen of regulators of muscle morphogenesis, myofibril phenotypes were categorized into a number of classes, and the classes described as "Trapezoid" and "Actin blob" had a similar appearance as compared to the Dret^MEN2B phenotype described here. These two classes contain a large number of genes of highly diverse functions, including many transcription factors, other DNA binding proteins, and interestingly, regulators of metabolism and insulin receptor signaling.

3.5.   Absence of neurodegeneration – importance of genetic background in transgenic mouse models

To determine whether *Ret* interacts genetically with *Parkin* and *PINK1* in mouse nigrostriatal dopamine neurons, we generated compound mice, lacking either *Ret* and *PINK1,* or *Ret* and *Parkin* in dopamine neurons. After the initial study describing mild neurodegeneration after conditional ablation of *Ret al*one, and the finding of increased degeneration in *DJ-1/Ret* double mutants, we were interested to know whether deleting other ARPD genes would also intensify the *Ret* phenotype. We expected one of three outcomes: (i) No enhanced degeneration compared

to R*et al*one, i.e. loss of approximately 25-30 % of SNpc cell bodies and 50 % striatal fibers at 24 months. This result would indicate that the interaction with *DJ-1* is quite specific. (ii) A similar phenotype as compared to *Ret/DJ-1*, i.e. loss of approximately 40 % neurons and 50 % striatal fibers. Such a scenario would suggest that Ret functions synergistically with Pink1 and Parkin with the same level of functional significance as with DJ-1, or that any additional stress factor is sufficient to cause a mild increased cell death. The last predicted outcome (iii), would be a stronger, or qualitatively different phenotype than with *DJ-1*, e.g. increased loss of cell bodies or striatal fibers. This would suggest that *Ret* interacts genetically with *PINK1* and/or *Parkin* through a pathway different to that of *Ret/DJ-1*. All of these predicted scenarios were of course only speculative, as the result of the experiment gave a different conclusion. The outcome was instead, that by crossing the *Dat-Cre;Ret^lx* mice to *Parkin^-* and *PINK1^lx* lines, it completely abrogated the previous neurodegenerative phenotype of the *Ret* mutants. Importantly, it is not a rescue effect of the additional mutations, since *Ret* single mutants derived from the new *Ret/PINK1* and *Ret/Parkin* lines, also did not show neurodegenerative phenotypes.

This leads to the obvious question, why the *Ret* phenotype is so strikingly different between the two experiments? The animals of both colonies were housed in the same animal facility and analyzed with genotypes blinded using similar methods, reagents and experimental setups. A small group of *Ret/DJ-1* mice was reanalyzed together with the *Ret/PINK1* mice, and the phenotype in the *Ret/DJ-1 mice* was reproduced as previously described, indicating that technical problems of the analysis are unlikely. A possible explanation may instead be found in the genetic background. The original *DJ-1*, *Parkin* and *PINK1* alleles were generated in the Sv129J strain, after which they were embryo-rederived into the C57BL/6J strain, crossed to the *Dat-Cre* and *Ret* *al*leles, and then intercrossed in a series of breedings. The original *Dat-Cre* allele was generated and kept in the Sv129J background, while the *Ret^lx* allele was maintained in a mix of Sv129J and C57BL/6J. The complexity of the situation, unfortunately, does not allow a feasible analysis of the contribution of each parental strain to the mice that were analyzed. However, it appeared from the coat color as if the *Ret/DJ-1* line had a higher contribution of Sv129J, as they, in general, had brown coats, while the *Ret/ PINK1* and *Ret/Parkin* lines appeared to have comparably higher contribution of C57BL/6J, as they typically had black coats.

Mouse genetic backgrounds can have profound effects on phenotypic expression of transgenic mouse models (Sanford *et al.* 2001). As an example, *EGFR* knockout mice in a CF-1 background die in the peri-implantation stage due to inner mass degeneration, while in the Sv129 background, they instead die in the mid-gestation phase due to placental defects. However, in a CD-1 background, EGFR knockout mice live up to three weeks after birth, but die due to dysfunction in multiple systems (Threadgill *et al.* 1995). Also, mice mutant for *TGF-β*, a distant homolog to *Ret*, were demonstrated to display different phenotypes depending on the genetic background (Bonyadi *et al.* 1997). A recent genomic study compared whole genome sequences of seventeen common laboratory mouse strains, and found 56 million unique sites of differences between all the strains (Keane *et al.* 2011). Furthermore, by performing a single cross between two of the strains, they could show how the two allelic variants were expressed in highly different ratios between different tissues, which suggests that gene expression may be one mechanism, by which allelic variants can give rise to different phenotypes

Expression of traits is not only determined by genetic variants - also epigenetic variation can be inherited, and modify the expression of traits. The suggested implication from this study, that genetic or epigenetic background modifiers can cause such a dramatic difference in the neurodegenerative phenotype of *Ret* mutant mice, is interesting. As of today, this is of course highly speculative, as direct evidence is missing. However, it is possible that these types of differences may play an important role for the risk of humans developing PD. Dissecting the background variations between the strains analyzed here, with the goal of identifying critical modifiers, is theoretically interesting, but unfortunately a highly extensive experiment and beyond the scope of this project.

3.6.   Concluding remarks and future perspectives

In this thesis, I present evidence that the neurotrophic factor receptor Ret may converge with the functions of ARPD-associated proteins. Conditional ablation of *Ret* in dopamine neurons of mice sensitizes a population of neurons, making *DJ-1* critical for survival. When also the *DJ-1* gene is deleted, this population of sensitized neurons succumbs during aging. To understand which critical cellular functions Ret and DJ-1 maintain, understanding of the aging process is of central importance, since aging is an absolute requirement for DA neuron cell death in *Ret* and *Ret/DJ-1* double mutant mice. Aging is also the number one risk factor for developing PD, but

our knowledge of the underlying mechanisms, is limited. Connecting the aging process with the functions of PD-associated genes and neurotrophic factor receptors may identify novel targets for therapeutic development.

In the second part of my project, I found that Ret signaling can regulate mitochondrial dynamics in cultured cells. Mitochondria play an important role in normal cellular aging. They have physiological functions in ATP production, calcium-buffering capacity, and in the initiation of programmed cell death. When impaired, they generate undesirable reactive oxygen species, which damage the cell. The PD-associated proteins Parkin and PINK1 have been shown to help the cell maintain a healthy pool of mitochondria, by clearing damaged ones through mitophagy, and promoting the generation of new ones by increasing transcription of mitochondrial proteins. If Ret signaling, also under physiological conditions in DA neurons, helps in maintaining a healthy pool of mitochondria, it would explain why DA neurons in *Ret* mutant mice slowly degenerate. It would also explain why Ret stimulation by GDNF protects DA neurons in PD models, although the effect of reversing mitochondrial fragmentation in cultured cells may be something that is only seen in this rather artificial system. It would be highly interesting to learn whether GDNF treatment in mouse models of PD, with mitochondrial defects, also protects against mitochondrial pathology. Moreover, our knowledge of the pathway by which Ret targets mitochondria is at this point very limited. Studying changes in the mitochondrial proteome and phosphoproteome after GDNF treatment may give interesting leads into the mechanism.

4. *Materials and Methods*

4.1.   Buffers, media and reagents

Table 4-1 General purpose buffers

PBS	10 mM Na2HPO4 pH 7.4
	2 mM KH2PO4
	0,137 M NaCl
	2,7 mM KCl
TBS	50 mM Tris pH 7.4
	150 mM NaCl
TBST (biochemistry)	1X TBS
	0,1% TritonX-100
TBST (histology)	1X TBS
	0,1% Tween
PFA 4%	1L: 40 g paraformaldehyde in 900 ml H2O, heat to 65°C. Add 400 µL NaOH 5M, then neutralize with 150 µL HCl 37 %. Add 100 ml 10X PBS.

Table 4-2 Solutions for mouse histology and genotyping

Chloral hydrate	8 % chloral hydrate (Roth, Germany) in PBS
Sucrose solutions	15 % and 30 % sucrose in PBS
	used for brain immersion
Cryoprotection solution (1L)	300 mL distilled water
	300 mL glycerol
	300 mL Ethyleneglycol
	100 mL PBS
	used to store mouse brain sections at -20 ^{0}C
Egg embedding	mix egg yelow and sucrose 10 : 1 (g/g)
	use cold mix for embedding (4 ^{0}C)
	to polymeraze, add 1 mL glyceraldehyde 25 % to
	20 mL egg mix; mix well and allow 45 min for
	after polymerization at r.t., store at -80^{0}C
Tail lysis	25 mM NaOH, 0.2 mM EDTA
	Neutralization: Tris HCl 1,5M pH 8.8
Blocking buffer	1X PBS
	5% bovine serum albumin (BSA)
Antibody incubation buffer	1X PBS
	2% BSA
	0,1% Triton-X100
Mounting medium (1L)	Add Celvol205 (Calvanese Chemicals) to 800 ml 1XPBS, adjust to pH 7.2. Stir for 24 hours at RT, add 400ml glycerol and stir another 24 hours at RT. Remove undissolved Celvol by centrifugation at 12000rpm for 30 min. Add H20 to adjust to preferred viscosity. Keep aliquots at -20°C for long-term storage.

Table 4-3 Solutions for SDS-PAGE/Western blot analysis

Cell lysis buffer	1% Triton X-100
	150 mM NaCl
	1mM EDTA
	10 mM Tris-HCl (pH 7.5)
	100 mM NaF
	1 mM NaVO3
	10 mM Na4P2O7
Brain lysis buffer	150 mM NaCl
	50 mM Tris_HCl, pH 7.4
	2 mM EDTA
	1% Nonidet P-40
	1% SDS
Reducing sample buffer for SDS PAGE	300mM Tris·HCl pH 6.8
	12% SDS
	600mM DTT
	0.6% (w/v) Bromophenol-blue
	60% glycerol
Blocking solution	5% non-fat dry milk in TBST
Stripping solution	1x PBS
	2% SDS
	0,14% β-Mercaptoethanol

Table 4-4 Solutions for fly histology and genetics

Standard fly food (1L)	15 g yeast
	11.7 g agar
	80 g molasses
	60 g corn flower
	6.3 ml propionic acid
	2.4 g methylparaben
	yeast paste (yeast granules
Longevity assay fly food (1L)	70 g sucrose
	35 g cornmeal
	5 g agar
	50 g yeast
	4,5 ml propprionic acid
Squishing buffer	10 mM Tris-HCl pH8
	1 mM EDTA
	25 mM NaCl
	200 g/ml Proteinase K
Blocking buffer	1X PBS
	5% fetal calf serum
	0,1% Triton-X100
PFA fixative solution	1X PBS
	4 % PFA
	0,1% Triton-X100
Phalloidin staining	1X PBS
	0,1% Triton-X100
	Phalloidin-Alexa568, 1:1000 (Invitrogen)
Mounting medium	Vectashield mounting medium H-1000 (Vector Laboratories)

Table 4-5 Buffers for molecular biology

Tris/EDTA (TE) buffer	10 mM Tris·Cl, pH 8.0
	1mM EDTA, pH 8.0

Tric/acetate/EDTA (TAE) buffer	50× stock solution (1L): 242 g Tris base 40 mM Tris·acetate 57.1 ml glacial acetic acid 2 mM Na2EDTA·2H2O H2O up to 1 liter
Gel loading buffer	25 ml Glycerol 1 ml 50X TAE 0.1 g Orange G 24 ml H2O

Table 4-6 Cell culture media a reagents

Cell culture media	
Embryo suspension medium (1L)	Dulbecco's modified Eagle's medium (DMEM) high glucose, Hepes+ (Invitrogen) 1ml Penicillin/Streptamycin 10,000 units (Penstrep)
MEF-P0 medium (1L)	DMEM 15% fetal calf serum 1% 1x non-essential amino acids 1 ml 1x penstrep
MEF culture medium (1L)	DMEM 9% fetal calf serum 1% 1x non-essential amino acids 1% 1x penstrep
DMEM culture medium	DMEM 10% fetal calf serum 1% L-Glutamine 1% pen/strep
SH-SY5Y medium	DMEM/F12 (1:1) with GlutaMAX (Invitrogen) 10% fetal calf serum 1% pen/strep
Transfection reagents	
Calcium Phosphate Transfection Kit	K2780-01, Invitrogen
Lipofectamine 2000	11668-019, Invitrogen
Lipofectamine RNAiMAX	13778-150, Invitrogen
Cell viability assay	
CellTiter-Glo Luminescent Cell Viability Assay	G7571, Promega

Table 4-7 PCR primers

Primer name	Sequence (5' to 3')
DJ-1 Forward	AGG CAG TGG AGA AGT CCA TC
DJ-1 Reverse WT	AAC ATA CAG ACC CGG GAT GA
DJ-1 Reverse mutant	CGG TAC CAG ACT CTC CCA TC

Pink1 wt forward	ACC CCA GAA ACC AAC AAG TG
Pink1 lx reverse	TGG CCT GAG ACC TTG TCT TT
Pink1 reverse	AAG GAG CAG AGT CCG AGG TT
NeoR forward	TGA ATG AAC TGC AGG ACG AG
NeoR reverse	AAT ATC ACG GGT AGC CAA CG
Parkin wt forward	TGC TCT GGG GTT CGT C
Parkin ko forward	TTG TTT TGC CAA GTT CTA AT
Parkin ko reverse	TCC ACT GGC AGA GTA AAT GT
Retlx Forward	CCA ACA GTA GCC TCT GTG TAA CCC C
Retlx Reverse	GCA GTC TCT CCA TGG ACA TGG TAG
Retrec Forward	CGA GTA GAG AAT GGA CTG CCA TCT CCC
Retrec Reverse	ATG AGC CTA TGG GGG GGT GGG CAC
Cre Forward	GCC TGC ATT ACC GGT CGA TGC AAC GA
Cre Reverse	GTG GCA GAT GGC GCG GCA ACA CCA TT
h PINK1 RT forward	TGG CCC CAG AGG TGT CCA CG
h PINK1 RT reverse	CGC TGG AGC AGT GCC CTC AC
hGAPDH RT forward	GTC GCC AGC CGA GCC ACA TC
hGAPDH RT reverse	TGA CCT TGG CCA GGG GTG CT

Table 4-8 Plasmids

DJ-1 (pCMV-myc)	Phillip Kahle, Hertie Institute, Tübingen
pCMV Myc empty vector	Phillip Kahle, Hertie Institute, Tübingen
hrGFP (pCDNA3)	Edgar Kramer, Universität Hamburg, Hamburg
Ret9 (pJ7omgea)	Patrik Ernfors, Karolinska Institutet, Stockoholm
Ret9-Shc+ (pJ7omgea)	Patrik Ernfors, Karolinska Institutet, Stockoholm
Ret9-Dok+ (pJ7omgea)	Patrik Ernfors, Karolinska Institutet, Stockoholm

Table 4-8 siRNA oligos

DJ-1	AGGAAAUGGAGACGGUCAUCCCUGU	Stealth RNAi, Invitrogen
DJ-1 CTRL	ACAGGGAUGACCGUCUCCAUUUCCU	Stealth RNAi, Invitrogen
Parkin	GGAGAGAACCUCAACCGCUAGGAUA	Stealth RNAi, Invitrogen
Parkin scrambled	UAUCCUAGCGGUUGAGGUUCUCUCC	Stealth RNAi, Invitrogen
PINK1	#VHS50790	Validated Stealth RNAi, Invitrogen (set of 3)
Medium GC negative control	#12935-300	Stealth RNAi, Invitrogen

Table 4-9 Recombinant proteins

Mouse Insulin-like growth factor 1 (IGF-1)	Shenandoah Biotechnology
Human Glia cell line-derived neurotrophic factor (GDNF)	Shenandoah Biotechnology
Human GDNF family receptor 1 (GFRα1)	R&D Systems

Table 4-10 Antibodies

Antibody	Species	Source	Dilution	Application
Primary antibodies				
AKT	rabbit	#9272, Cell Signaling Technology	1:1 000	WB
phospho-AKT S473	rabbit	#9271, Cell Signaling Technology	1:1 000	WB
phospho-AKT S473	rabbit	#4060, Cell Signaling Technology	1:5 000	WB
p42/p44 MAPK	rabbit	#9102, Cell Signaling Technology	1:1 000	WB
phospho-p42/p44 MAPK	rabbit	#4376, Cell Signaling Technology	1:1 000	WB
phospho-p42/p44 MAPK	rabbit	#4370, Cell Signaling Technology	1:3 000	WB
Ret	goat	#70R-RG002, Fitzgerald	1:1 000	WB
DJ-1	goat	# ab4150, Abcam	1:1 000	WB
PTEN	rabbit	#9559, Cell Signaling Technology	1:1 000	WB
Tyrosine hydroxylase	mouse	# 22941, Immunostar	1:2 000	IHC
Tyrosine hydroxylase	rabbit	# ab152, Millipore	1:1 000	IHC
GIRK2	rabbit	#APC-006, Alamone Labs	1:80	IHC
COX IV	rabbit	#4850, Cell Signaling Technology	1:5 000	WB
Lamin	rabbit	#ab2559, Abcam	1:1 000	WB
Parkin	mouse	#4211, Cell Signaling Technology	1:1 000	WB
β-actin	mouse	#A5316, Sigma	1:20 000	WB
β-tubulin (T-8660, Sigma).	mouse	#T-8660, Sigma	1:20 000	WB
GFP	rabbit	#A11122, Invitrogen	1:2 000	IHC
Secondary antibodies				
anti-mouse HRP	sheep	GE Life Sciences	1:5 000	WB
anti-rabbit HRP	goat	GE Life Sciences	1:5 000	WB
anti-goat HRP	rabbit	DAKO	1:5 000	WB
anti-rabbit-alexa488	goat	Molecular probes	1:1 000	IHC
anti-mouse-Cy3	donkey	Jackson Immunoresearch	1:1 000	IHC
anti-rabbit-biotin	donkey	Vectorlabs	1:500	IHC
Streptavidin-Cy3		Sigma-Aldrich	1:1 000	IHC

4.2.   Molecular biology

4.2.1.   Tail DNA preparation and genotyping

Tail biopsies (1-3 mm) were taken from mice and incubated at 95 °C three times for 15 min in 100 µl of 50 mM NaOH and vortexed thoroughly between heating steps. Samples were then centrifuged to precipitate the remaining debris and the mix was neutralized with the addition of 10 µl 1.5 M Tris-HCl, pH 8.8 and stored at 4 °C. PCR was carried out in a total volume of 25 µl and contained 2.5 mM dNTPs, 200 nM specific primers, 1X PCR buffer (NEB), 0.1 µl of Taq polymerase (NEB) and 2 µl of tail DNA lysates. PCR samples were analyzed by agarose gel electrophoresis in gels of 2% agarose in TAE buffer with 30 µl ethidium bromide per liter gel solution.

4.2.2. Preparation of plasmid DNA

Plasmid DNA was purified from 500 ml bacterial cultures. Single colonies of transformed bacteria were picked from LB plates containing ampicillin and inoculated into flasks containing LB medium with 100 µg/ml ampicillin and grown overnight shacking at 37 °C. Harvesting and purification of maxipreparation was carried out according to Qiagen protocol using Qiagen buffers. The DNA concentration was measured in a UV spectrometer at 260 nm.

4.2.3. Preparation of RNA and quantification by RT-PCR

RNA from HeLa cells was prepared using RNeasy Mini Kit (Qiagen). Briefly, cells were scraped on ice in lysis buffer RLT, passaged through a Qiashredder column for homogenization. One volume of 70 % ethanol was added to the lysates and the solution was transferred to an RNeasy spin column, which binds the RNA on centrifugation. The column was washed with RPE buffer, after which the RNA was eluted in H2O and the RNA concentration was measured with a UV spectrophotometer at 260 nm. For the reverse-transcriptase PCR (RT-PCR) analysis, the OneStep RT-PCR kit (Qiagen) was used according to the manufacturer's instruction. For each reaction, 100 ng of RNA, 6 µM specific primers and 1 µl enzyme mix was used in a 25 µl reaction volume. After reverse transcription, cDNA was amplified by 30 PCR cycles.

4.3. Cell culture, in vitro assays and biochemistry

4.3.1. Preparation of mouse embryonic fibroblasts and transfection

14,5 days pregnant C57BL/6 mice were sacrificed, and the uterus extracted was placed in cold PBS. The embryos were extracted and placed in cold embryo suspension medium. The head and abdominal/thoracic organs were removed; the remaining tissue was minced using a scalpel and further homogenated by passing through hypodermic needles of decreasing diameters. The tissue homogenate was digested by incubating with trypsin for 10 minutes in a 1:1 ratio of cell suspension to trypsin. Trypsin digestion was repeated with a second volume, the mixture was left to settle for 2 min, after which the cell fraction was recovered by decanting. Cell suspension was plated at a density of 5×10^6 cells in one 15 cm tissue culture dish in MEF-P0 medium. After 4 days in culture, cell were passaged and cultured up to 6 passages in MEF culture medium. Cells were transfected using the standard Calcium phosphate-precipitate method.

4.3.2. Transfection of cell lines

HeLa cells were transfected using Lipofectamine 2000 for plasmids and Lipofectamine RNAiMAX for siRNA by the forward transfection method, according to manufacturer's instructions. SH-SY5Y and A549 cells were transfected using Lipofectamine 2000 for plasmids or Lipofectamine RNAiMAX by the reverse transfection method, according to the manufacturer's instructions. Plasmid overexpression experiments were incubated for 24 h after transfections before analysis for all cell types. For DJ-1 western blot experiments, siRNA knockdowns were incubated for 48 h after transfection for HeLa and A549 cells, while SH-SY5Y cells were incubated for 96 h after transfection before lysis.

4.3.3.   Western blotting

Cultured cell lines were harvested in lysis buffer with complete protease inhibitor mixture (Roche Diagnostics). Mouse brains were snap frozen, ventral midbrains and striata were dissected on ice, and homogenized in homogenizing buffer with complete protease inhibitor mixture (Roche Diagnostics) by 10 strokes using a dounce homogenizer. Cell lysates and brain homogenates were centrifuged at 1,000 g for 10 min, supernatants were saved, and the protein concentration was determined using the DC protein assay (BioRad). Samples were denatured by boiling in SDS-sample buffer; proteins were separated by SDS-PAGE according to standard procedures. Gels were transferred to nitrocellulose membranes (Protran, Schleicher&Schuell) by semi-dry blotting. Membranes were blocked for 45 minutes in non-fat dry milk solution, incubated with primary antibodies in blocking solution over night at 4ºC or for 1 hour at RT, washed 3 x 5 min in PBST, incubated with secondary antibodies in blocking solution for 1 hour at RT and again washed 3 x 5 min in PBST before incubation with ECL solution (GE Life Sciences) for 1min. To visualize signals, membranes were either exposed on X-ray films (GE Life Sciences), or imaged with a Fusion FX7 digital camera system (PeqLab). Membranes were stripped in stripping solution for 30min at 65ºC and washed 3 x for 10min each in PBST at RT, if subsequent detection of another protein was necessary. After stripping, membranes were again blocked and treated as described above.

4.3.4.   Cytotoxicity assay

SH-SY5Y cells were transfected with DJ-1 or CTRL siRNA, and cultured for 4 days for protein depletion. Next, cell were plated in 96 well plates at a density of 10 000 cells/well and cultured for another 8 hours. The medium was then exchanged to DMEM with 2% FCS, after which hydrogen peroxide in a series of concentration together with GDNF (50 ng/ml) and GFRα1 (50

ng/ml) or PBS was added. After 12 hours, viability was determined using the ATP/luminescence-based Celltiter Glo assay (Promega) according to the manufacturer's instructions.

4.3.5. Analysis of mitochondrial fragmentation

SH-SY5Y cells were transfected with Lipofectamine RNAiMAX with Parkin or a scrambled Ctrl siRNA over night by the reverse transfection method onto 13 mm glass coverslips. After transfection, the medium was changed to standard culture medium and incubated for 48 hours. GDNF (100 ng/ml) and GFRα1 (100 ng/ml) was added to the cell and incubated for another 24 hours. After this, Mitotracker Green FM (200 nm) (Invitrogen) was added to the cells and incubated for 15 minutes to label the mitochondria, and washed 3 x 10 minutes with culture medium. The coverslips were placed in metal holders with the cells covered in PBS with calcium and magnesium. The samples were blinded to the experimenter, and after this, the living cells could be image from underneath in a Zeiss Axioplan fluorescence microscope. Random fields were selected and within each field all cells were classified and counted by the morphology of the mitochondria as "tubular" or fragmented". HeLa cells were transfected with Pink1 or scrambled Ctrl siRNA in 6 cm plates. After 48 hours, the cells were resuspended and reverse-transfected with a Ret9-wt, Ret9-Shc+ or Ret9 Dok+ in a pJ7omega expression vector (Stenqvist *et al.* 2008; Lundgren *et al.* 2006). After 8 hours, the medium was changed to standard culture medium, GDNF (50 ng/ml) and GFRα1 (50 ng/ml) was added and incubated for another 18-22 hours. For kinase inhibitor experiments, GDNF/GFRα1 (50 ng/ml) together with the kinase inhibitors LY-294002 (PI3K), U0126 (Mek1) or DMSO was added 16 hours after Ret transfection and incubated for 3 hours. After GDNF/GFRα1 and/or inhibitors, cells were stained with Mitotracker Green FM and analyzed as described above.

4.4. Mouse genetics, histology and behavior

Table 4-11 Transgenic mouse lines

Allele	Description and reference
Ret^{lx}	The R*et al*lele was targeted with a construct with loxP sites flanking exon12 The FRT flanked neomycin selection cassette was excised with Flp recombinase (Kramer *et al.* 2006).
DJ-1$^-$	Gene trap targeting construct containing a splice acceptor, LacZ and neomycin recistance inserted between exons 6 and 7, creates a null allele (T.-T. Pham *et al.* 2010).
DAT-Cre	Knock-in of Cre recombinase into the 5' UTR of the DAT locus, expressing Cre specifically in dopaminergic neurons. Causes loss of function of the dopamine transporter gene.

PINK1^{lx}	Exon 2-3 flanked by loxP sites and a neomycin resistance cassette within, before exon 2, flanked by FRT sites (Wolfgang Wurst, unpublished).
PINK1^{-}	Cre mediated germ-line recombination of the Pink1lx alleles deletes exon 2-3 and creates a null allele.
Parkin^{-}	Gene targeting replaced exon 3 and parts of intron 3 with a neomycin resistance cassette, creating a null allele (Itier *et al.* 2003).

All lines were maintained in a mix of Sv129 x C57BL/6 background.

4.4.1. Cardiac perfusion, preparation of mouse brains and cryosectioning

Mice were anaesthetised with an intraperitoneal injection of 8% chloralhydrate. Skin and ribcage were cut open and the diaphragm was removed. A small incision was made into the right atrium and a needle connected to a peristaltic pump was inserted into the left ventricle and 25 ml of cold PBS was run through the animal's vascular system. This was followed by 25 ml of cold 4% PFA solution for fixation. Brains were removed from the scull and transferred to 4% PFA solution for post-fixation over night. Next, brains were treated for cyroprotection by incubation in 15 % and 30 % sucrose solutions. Left and right brain hemispheres were embedded separately in egg yolk with 10 % sucrose and 5 % glutaraldehyde, and kept frozen at –80°C until analyzed. 30 µm–thick coronal sections were cut on a cryostat, collected free floating, and used for immunohistological staining.

4.4.2. Immunostaining

Free floating sections were first incubated 1 hour in blocking buffer at RT. The primary antibody in antibody incubation buffer was added, and sections were incubated over-night at 4°C. After three washes in PBS (5 minutes each), the sections were incubated 1 hour at RT with biotin-coupled secondary antibodies (dilution 1:200 in antibody incubation buffer) from Vectastain ABC kits (Vector Laboratories). After another three washes in PBS, sections were incubated with a complex of avidin-biotin coupled to horseradish peroxisade (HRP; dilution 1:200 in PBS buffer; incubation 1 hour at RT). After three washes in PBS, the HRP substrate diaminobenzidine (DAB; Sigma-Aldrich, Germany) - diluted in tap water was added. Sections were incubated until a brown precipitate was formed.

4.4.3. Stereological quantification of neuron numbers

Stereological counts were performed with the StereoInvestigator software (MicroBrightField, Williston, Vermont, United States) on every sixth section of the SN or VTA. After immunolabeling of SN neurons, the exact order of sections spanning the midbrain area was

established. On each individual section, the area of the SN or VTA was delineated and an automated method allowed selection of smaller a 50 x 50 μm square, distributed on a grid with the dimension 125 x 125 μm. Within each automatically selected square, neurons were counted when there somas were in focus within a 10 μm segment on the Z-axis in the center of each section. By this method, a minimum of 200 cells per animal were counted. After all sections were processed, the program used the determined neuronal densities to extrapolate the total number of neurons found within the selected volume.

4.4.4. Quantification of striatal fiber density by counting grid

For every sixth 30 μm thick section, 4 images in dorsal striatum were aquired on 8 section, (a total of 32 images per mouse), using a Zeiss AxioVision 2 epifluorescence microscope with a 63X objective. In order to automatically delineate the fibers, the images were first thresholded and subsequently quantified with an automatic counting-grid macro implemented in the Metamorph software (Molecular Devices).

4.4.5. Quantification of striatal fiber density by fiber area measurement

For analyzing the striatal fiber density in the 18 and 24 months old Ret/Pink1/Parkin groups of mice, a new method for quantifying striatal fibers was developed, that does not require manual thresholding of the images, hence being more automated and unbiased. Images were acquired as described above. Using in series of algorithms in the CellProfiler 2.0 software (Broad Institute), striosomes were first automatically identified as objects using segmentation which takes into account their size, shape, and intensity, and were excluded from the area to be analysed. Next, the striatal fibers were identified using a similar approach as for the striosomes. Finally, the total area of fibers was measured and divided by the image area not occupied by striosomes. Average fiber area/total area per mouse was used for the statistical analysis.

4.4.6. Quantification of Soma Size of SN Neurons

GIRK2 immunostained coronal sections were analyzed using a bright field microscope with a 40× objective. Random cells were selected with stereological methods using the StereoInvestigator software. Five to seven animals per group were measured by circling cell soma of 149–275 cells per animal.

4.4.7. Measurements of Dopamine Levels by HPLC

18 months old mice were sacrificed, brains were removed, snap-frozen, and the striata were dissected. The tissue was homogenized in 0.1 M perchloric acid containing 0.5 mM disodium EDTA and 50 ng/ml, 3,4-dihydroxybenzylamine as an internal standard, centrifuged at 50,000 g for 30 min, and filtered through a 0.22 µM PVDF membrane. Monoamines and their metabolites were separated on a reverse-phase ODS column (YMC-Pack, S-3 µM, 120 A; Stagroma AG, Reinach, Switzerland). The column temperature was maintained at 33°C. The mobile phase was 34% citric acid 0.1 M, 48% Na2HPO4 0.1 M, 18% methanol, 50 mg/l EDTA, and 45 mg/l sodium octylsulfate, pH 4.5. The flow rate was set at 0.45 ml/min. The potential settings of the analytical cell (model 5011; ESA Inc.) were +0.45 V (first electrode) and –0.3 V (second electrode). Monoamines and their metabolites were read as second-electrode output signal.

4.4.8.   Open field behavioral analysis

Control and mutant mice, mice were subjected to open field behavioral assessment. 18 months old mice were housed individually in a room with 12 h/12 h reversed day-night cycle. All experiments were conducted during the night period in a quiet room with light of 12 lux. Mice were placed into a 59 cm×59 cm large arena for 20 min, they were filmed from above and their movement was tracked using EthoVision Pro 2.2. (Noldus, Sterling, USA). The experiment was repeated on the consecutive day and the average distance each mouse travelled during the two trials was determined. Experimental protocols were approved by the government of Oberbayern, Germany.

4.5.   *Drosophila* genetics and histology

Table 4-12 Transgenic drosophila lines

Allele	Chromosome	Description, source
park^{25}	3	Null allele by imprecise p-element excision, Leo Pallanck (USA)
park^{25}::24B-GAL4	3	park^{25} recombined with 24B-GAL4, Leo Pallanck (USA)
park^{25}::mef2-GAL4	3	park^{25} recombined with mef2-GAL4, Leo Pallanck (USA)
park^{25}::TH-GAL4	3	park^{25} recombined with TH-GAL4, Leo Pallanck (USA)
park^{1}	3	Null allele by imprecise p-element excision, Jongkyeong Chung (South Korea)
Pink1^{B9}	X	Null allele by imprecise p-element excision, Jongkyeong Chung (South Korea)
Pink1^{B9}::24B-GAL4	X	Pink1^{B9} recombined with 24B-GAL4, Alex Whitworth (UK)
Pink1^{B}::mef2-GAL4	X	Pink1^{B9} recombined with mef2-GAL4, Alex Whitworth (UK)

24B-GAL4	3	Mesoderm-specific driver, Bloomington stock center #1767
mef2-GAL4	3	Muscle-specific driver , Frank Schnorrer (Germany)
TH-GAL4	3	Dopamine neuron-specific driver, Hiromu Tanimoto (Germany)
UAS-Dret^{MEN2A}	2	Constitutively active Dret, Ross Cagan (USA)
UAS-Dret^{MEN2B}	3	Constitutively active Dret, Ross Cagan (USA)

4.5.1. Imaging and analysis of *Drosophila* eyes

1-5 days old flies were anaesthetized by CO_2, heads were removed and pictures of eyes were acquired using a Leica MZ 9.5 stereomicroscope equipped with a Leica DFC320 digital camera (LeicaMicrosystems, Wetzlar, Germany). Total eye area was determined using the ImageJ software (NIH, USA).

4.5.2. Dissection and analysis of flight muscles

Wings, head and abdomen were removed from CO_2 anaesthesized flies. The thoraces were placed in PFA fixative solution for 15 minutes. Thoraces were bisected sagitally along the midline using a razor blade (Gillette) and placed in phalloidin staining solution for 30 min to 1 hour. After staining, thoraces were washed in PST-tween 2 x 10 minutes and mounted in Vectashield mounting medium. The dorsal longitudinal indirect flight muscles were imaged in a Leica SP2 confocal laser scanning microscope using 20X and 63X objectives.

4.5.3. Whole-mount immunostaining of brains and analysis of PPL1 dopamine neuron numbers

Park25 mutant flies have reduced viability compared to wild type. To increase the survival, the flies were fed with food enriched with yeast and glucose and were flipped every 3-4 days. After 20-30 days, brains were dissected in PBS, fixed in PFA fixative solution for 1 hour and washed 3 x 5 minutes in PBST. After washing, the brains were incubated with a tyrosine hydroxylase antibody (ab152, Abcam) diluted 1:200 in PBST with 5 % FCS over night at 4 °C. After the primary antibody incubation, the brains were washed 3 x 5 min in PBST, and incubated with an alexa488-coupled secondary antibody diluted 1:200 in PBST with 5 % FCS for 2 hours at RT, and again washed 3 x 5 min in PBST. The brains were mounted on coverglass with the posterior side facing upwards in Vectashield. Confocal Z section were acquired every 1 µm using a Leica SP2 confocal laser scanning microscope with a 20x objective. After 3D reconstruction using the ImageJ software (NIH), the neurons in the PPL1 cluster were counted in a blinded manner.

4.5.4. Analysis of PPL1 neuron mitochondrial morphology

Brains of 2-4 day old flies were dissected and immunostained for tyrosine hydroxylase as described above, with the difference that a Cy3-coupled secondary antibody was used. The cells of the PPL1 cluster were imaged using a Zeiss spinning disc confocal microscope, Z-sections every 0,5 µm were acquired and deconvolved using Metmorph v7.6 software (Molecular Devices). The size of the mitochondria was measured by automated image analysis using Cell Profiler 2.0 (Broad Institute).

5. References

Abrescia, C. *et al.*, 2005. Drosophila RET contains an active tyrosine kinase and elicits neurotrophic activities in mammalian cells. *FEBS letters*, 579(17), p.3789-96.

Airaksinen, M.S. & Saarma, M., 2002. The GDNF family: signalling, biological functions and therapeutic value. *Nature reviews. Neuroscience*, 3(5), p.383-94.

Airaksinen, M.S., Holm, L. & Hätinen, T., 2006. Evolution of the GDNF family ligands and receptors. *Brain, behavior and evolution*, 68(3), p.181-90.

Akundi, R.S. *et al.*, 2011. Increased mitochondrial calcium sensitivity and abnormal expression of innate immunity genes precede dopaminergic defects in Pink1-deficient mice. *PloS one*, 6(1), p.e16038.

Andres-Mateos, E. *et al.*, 2007. DJ-1 gene deletion reveals that DJ-1 is an atypical peroxiredoxin-like peroxidase. *Proceedings of the National Academy of Sciences of the United States of America*, 104(37), p.14807-12.

Anvret, A. *et al.*, 2011. DJ-1 Mutations are Rare in a Swedish Parkinson Cohort. *The open neurology journal*, 5, p.8-11.

Arenas, E., 2010. Towards stem cell replacement therapies for Parkinson's disease. *Biochemical and biophysical research communications*, 396(1), p.152-6.

Aron, L. *et al.*, 2010. Pro-survival role for Parkinson's associated gene DJ-1 revealed in trophically impaired dopaminergic neurons. *PLoS biology*, 8(4), p.e1000349.

Bandyopadhyay, S. & Cookson, M.R., 2004. Evolutionary and functional relationships within the DJ1 superfamily. *BMC evolutionary biology*, 4, p.6.

Beilina, A. *et al.*, 2005. Mutations in PTEN-induced putative kinase 1 associated with recessive parkinsonism have differential effects on protein stability. *Proceedings of the National Academy of Sciences of the United States of America*, 102(16), p.5703-8.

Bernheimer, H. *et al.*, 1973. Brain dopamine and the syndromes of Parkinson and Huntington. Clinical, morphological and neurochemical correlations. *Journal of the neurological sciences*, 20(4), p.415-55.

Bespalov, M.M. & Saarma, M., 2007. GDNF family receptor complexes are emerging drug targets. *Trends in pharmacological sciences*, 28(2), p.68-74.

Besset, V., Scott, R.P. & Ibáñez, C.F., 2000. Signaling complexes and protein-protein interactions involved in the activation of the Ras and phosphatidylinositol 3-kinase

pathways by the c-Ret receptor tyrosine kinase. *The Journal of biological chemistry*, 275(50), p.39159-66.

Bizon, J.L., Lauterborn, J.C. & Gall, C.M., 1999. Subpopulations of striatal interneurons can be distinguished on the basis of neurotrophic factor expression. *The Journal of comparative neurology*, 408(2), p.283-98.

Björklund, A. & Dunnett, S.B., 2007. Dopamine neuron systems in the brain: an update. *Trends in neurosciences*, 30(5), p.194-202.

Blackinton, J.G. *et al.*, 2009. Post-transcriptional regulation of mRNA associated with DJ-1 in sporadic Parkinson disease. *Neuroscience letters*, 452(1), p.8-11.

Bonifati, V. *et al.*, 2003. Mutations in the DJ-1 gene associated with autosomal recessive early-onset parkinsonism. *Science (New York, N.Y.)*, 299(5604), p.256-9.

Bonifati, V. *et al.*, 2005. Early-onset parkinsonism associated with PINK1 mutations: frequency, genotypes, and phenotypes. *Neurology*, 65(1), p.87-95.

Bonyadi, M. *et al.*, 1997. Mapping of a major genetic modifier of embryonic lethality in TGF beta 1 knockout mice. *Nature genetics*, 15(2), p.207-11.

Borrello, M.G. *et al.*, 1996. The full oncogenic activity of Ret/ptc2 depends on tyrosine 539, a docking site for phospholipase Cgamma. *Molecular and cellular biology*, 16(5), p.2151-63.

Braak, H. *et al.*, Staging of brain pathology related to sporadic Parkinson's disease. *Neurobiology of aging*, 24(2), p.197-211.

Bretaud, S. *et al.*, 2007. p53-dependent neuronal cell death in a DJ-1-deficient zebrafish model of Parkinson's disease. *Journal of neurochemistry*, 100(6), p.1626-35.

Brown, T.P. *et al.*, 2006. Pesticides and Parkinson's disease--is there a link? *Environmental health perspectives*, 114(2), p.156-64.

Brug, M.P. van der *et al.*, 2008. RNA binding activity of the recessive parkinsonism protein DJ-1 supports involvement in multiple cellular pathways. *Proceedings of the National Academy of Sciences of the United States of America*, 105(29), p.10244-9.

Cacalano, G. *et al.*, 1998. GFRalpha1 is an essential receptor component for GDNF in the developing nervous system and kidney. *Neuron*, 21(1), p.53-62.

Canet-Avilés, R.M. *et al.*, 2004. The Parkinson's disease protein DJ-1 is neuroprotective due to cysteine-sulfinic acid-driven mitochondrial localization. *Proceedings of the National Academy of Sciences of the United States of America*, 101(24), p.9103-8.

Carlomagno, Francesca *et al.*, 1996. Molecular heterogeneity of RET loss of function in Hirschsprung's disease. *The EMBO journal*, 15(11), p.2717-25.

Carlsson, A., Lindqvist, M. & Magnusson, T., 1957. 3,4-Dihydroxyphenylalanine and 5-Hydroxytryptophan as Reserpine Antagonists. *Nature*, 180(4596), p.1200-1200.

Chan, C.S. *et al.*, 2007. "Rejuvenation" protects neurons in mouse models of Parkinson's disease. *Nature*, 447(7148), p.1081-6.

Chan, D.C., 2006. Mitochondria: dynamic organelles in disease, aging, and development. *Cell*, 125(7), p.1241-52.

Chandran, J.S. *et al.*, 2008. Progressive behavioral deficits in DJ-1-deficient mice are associated with normal nigrostriatal function. *Neurobiology of disease*, 29(3), p.505-14.

Chen, Linan *et al.*, 2005. Age-dependent motor deficits and dopaminergic dysfunction in DJ-1 null mice. *The Journal of biological chemistry*, 280(22), p.21418-26.

Christophersen, N.S. *et al.*, 2007. Midbrain expression of Delta-like 1 homologue is regulated by GDNF and is associated with dopaminergic differentiation. *Experimental neurology*, 204(2), p.791-801.

Chung, C.Y. *et al.*, 2005. Cell type-specific gene expression of midbrain dopaminergic neurons reveals molecules involved in their vulnerability and protection. *Human molecular genetics*, 14(13), p.1709-25.

Clark, I.E. *et al.*, 2006. Drosophila pink1 is required for mitochondrial function and interacts genetically with parkin. *Nature*, 441(7097), p.1162-6.

Cleland, M.M. *et al.*, 2011. Bcl-2 family interaction with the mitochondrial morphogenesis machinery. *Cell death and differentiation*, 18(2), p.235-47.

Clements, C.M. *et al.*, 2006. DJ-1, a cancer- and Parkinson's disease-associated protein, stabilizes the antioxidant transcriptional master regulator Nrf2. *Proceedings of the National Academy of Sciences of the United States of America*, 103(41), p.15091-6.

Corti, O. *et al.*, 2003. The p38 subunit of the aminoacyl-tRNA synthetase complex is a Parkin substrate: linking protein biosynthesis and neurodegeneration. *Human molecular genetics*, 12(12), p.1427-37.

Cribbs, J.T. & Strack, S., 2007. Reversible phosphorylation of Drp1 by cyclic AMP-dependent protein kinase and calcineurin regulates mitochondrial fission and cell death. *EMBO reports*, 8(10), p.939-44.

Dagda, R.K. *et al.*, 2009. Loss of PINK1 function promotes mitophagy through effects on oxidative stress and mitochondrial fission. *The Journal of biological chemistry*, 284(20), p.13843-55.

Dagda, R.K. *et al.*, 2008. Mitochondrially localized ERK2 regulates mitophagy and autophagic cell stress: implications for Parkinson's disease. *Autophagy*, 4(6), p.770-82.

Dauer, W. & Przedborski, S., 2003. Parkinson's disease: mechanisms and models. *Neuron*, 39(6), p.889-909.

Davies, A.M., 1996. The neurotrophic hypothesis: where does it stand? *Philosophical transactions of the Royal Society of London. Series B, Biological sciences*, 351(1338), p.389-94.

Deas, E. *et al.*, 2011. PINK1 cleavage at position A103 by the mitochondrial protease PARL. *Human molecular genetics*, 20(5), p.867-79.

Deeg, S. *et al.*, 2010. BAG1 restores formation of functional DJ-1 L166P dimers and DJ-1 chaperone activity. *The Journal of cell biology*, 188(4), p.505-13.

Den Eeden, S.K. Van *et al.*, 2003. Incidence of Parkinson's disease: variation by age, gender, and race/ethnicity. *American journal of epidemiology*, 157(11), p.1015-22.

Deng, H. *et al.*, 2008. The Parkinson's disease genes pink1 and parkin promote mitochondrial fission and/or inhibit fusion in Drosophila. *Proceedings of the National Academy of Sciences of the United States of America*, 105(38), p.14503-8.

Denison, S.R. *et al.*, 2003. Alterations in the common fragile site gene Parkin in ovarian and other cancers. *Oncogene*, 22(51), p.8370-8.

Doss-Pepe, E.W., Chen, Li & Madura, K., 2005. Alpha-synuclein and parkin contribute to the assembly of ubiquitin lysine 63-linked multiubiquitin chains. *The Journal of biological chemistry*, 280(17), p.16619-24.

Drosten, M. & Pützer, B.M., 2006. Mechanisms of Disease: cancer targeting and the impact of oncogenic RET for medullary thyroid carcinoma therapy. *Nature clinical practice. Oncology*, 3(10), p.564-74.

Dudanova, I., Gatto, G. & Klein, R., 2010. GDNF acts as a chemoattractant to support ephrinA-induced repulsion of limb motor axons. *Current biology : CB*, 20(23), p.2150-6.

Dudek, H. *et al.*, 1997. Regulation of neuronal survival by the serine-threonine protein kinase Akt. *Science (New York, N.Y.)*, 275(5300), p.661-5.

Durbec, P. *et al.*, 1996. GDNF signalling through the Ret receptor tyrosine kinase. *Nature*, 381(6585), p.789-93.

Ekstrand, M.I. *et al.*, 2007. Progressive parkinsonism in mice with respiratory-chain-deficient dopamine neurons. *Proceedings of the National Academy of Sciences of the United States of America*, 104(4), p.1325-30.

Encinas, M *et al.*, 2008. Analysis of Ret knockin mice reveals a critical role for IKKs, but not PI 3-K, in neurotrophic factor-induced survival of sympathetic neurons. *Cell death and differentiation*, 15(9), p.1510-21.

Encinas, Mario *et al.*, 2004. Tyrosine 981, a novel ret autophosphorylation site, binds c-Src to mediate neuronal survival. *The Journal of biological chemistry*, 279(18), p.18262-9.

Enomoto, H. *et al.*, 1998. GFR alpha1-deficient mice have deficits in the enteric nervous system and kidneys. *Neuron*, 21(2), p.317-24.

Exner, N. *et al.*, 2007. Loss-of-function of human PINK1 results in mitochondrial pathology and can be rescued by parkin. *The Journal of neuroscience : the official journal of the Society for Neuroscience*, 27(45), p.12413-8.

Fahn, Stanley, 2003. Description of Parkinson's disease as a clinical syndrome. *Annals of the New York Academy of Sciences*, 991, p.1-14.

Fallon, L. *et al.*, 2006. A regulated interaction with the UIM protein Eps15 implicates parkin in EGF receptor trafficking and PI(3)K-Akt signalling. *Nature cell biology*, 8(8), p.834-42.

Fan, J., Ren, H., Fei, E., *et al.*, 2008. Sumoylation is critical for DJ-1 to repress p53 transcriptional activity. *FEBS letters*, 582(7), p.1151-6.

Fan, J., Ren, H., Jia, N., *et al.*, 2008. DJ-1 decreases Bax expression through repressing p53 transcriptional activity. *The Journal of biological chemistry*, 283(7), p.4022-30.

Fernandes, C. & Rao, Y., 2011. Genome-wide screen for modifiers of Parkinson's disease genes in Drosophila. *Molecular brain*, 4, p.17.

Freed, C.R. *et al.*, 1992. Survival of implanted fetal dopamine cells and neurologic improvement 12 to 46 months after transplantation for Parkinson's disease. *The New England journal of medicine*, 327(22), p.1549-55.

Freed, C.R. *et al.*, 2001. Transplantation of embryonic dopamine neurons for severe Parkinson's disease. *The New England journal of medicine*, 344(10), p.710-9.

Fung, S. *et al.*, 2008. Expression profile of the cadherin family in the developing Drosophila brain. *The Journal of comparative neurology*, 506(3), p.469-88.

Gan, L., Johnson, D.A. & Johnson, J.A., 2010. Keap1-Nrf2 activation in the presence and absence of DJ-1. *The European journal of neuroscience*, 31(6), p.967-77.

Gandhi, S. *et al.*, 2009. PINK1-associated Parkinson's disease is caused by neuronal vulnerability to calcium-induced cell death. *Molecular cell*, 33(5), p.627-38.

Gash, D.M. *et al.*, 1996. Functional recovery in parkinsonian monkeys treated with GDNF. *Nature*, 380(6571), p.252-5.

Gautier, C.A., Kitada, T. & Shen, J., 2008. Loss of PINK1 causes mitochondrial functional defects and increased sensitivity to oxidative stress. *Proceedings of the National Academy of Sciences of the United States of America*, 105(32), p.11364-9.

Gegg, M.E. *et al.*, 2010. Mitofusin 1 and mitofusin 2 are ubiquitinated in a PINK1/parkin-dependent manner upon induction of mitophagy. *Human molecular genetics*, 19(24), p.4861-70.

Geisler, S. *et al.*, 2010. PINK1/Parkin-mediated mitophagy is dependent on VDAC1 and p62/SQSTM1. *Nature cell biology*, 12(2), p.119-31.

Gill, S.S. *et al.*, 2003. Direct brain infusion of glial cell line-derived neurotrophic factor in Parkinson disease. *Nature medicine*, 9(5), p.589-95.

Gispert, S. *et al.*, 2009. Parkinson phenotype in aged PINK1-deficient mice is accompanied by progressive mitochondrial dysfunction in absence of neurodegeneration. *PloS one*, 4(6), p.e5777.

Goldberg, M.S. *et al.*, 2003. Parkin-deficient mice exhibit nigrostriatal deficits but not loss of dopaminergic neurons. *The Journal of biological chemistry*, 278(44), p.43628-35.

Goldberg, M.S. *et al.*, 2005. Nigrostriatal dopaminergic deficits and hypokinesia caused by inactivation of the familial Parkinsonism-linked gene DJ-1. *Neuron*, 45(4), p.489-96.

Graaff, E. de *et al.*, 2001. Differential activities of the RET tyrosine kinase receptor isoforms during mammalian embryogenesis. *Genes & development*, 15(18), p.2433-44.

Greene, J.C. *et al.*, 2003. Mitochondrial pathology and apoptotic muscle degeneration in Drosophila parkin mutants. *Proceedings of the National Academy of Sciences of the United States of America*, 100(7), p.4078-83.

Gu, L. *et al.*, 2009. Involvement of ERK1/2 signaling pathway in DJ-1-induced neuroprotection against oxidative stress. *Biochemical and biophysical research communications*, 383(4), p.469-74.

Guzman, J.N. *et al.*, 2010. Oxidant stress evoked by pacemaking in dopaminergic neurons is attenuated by DJ-1. *Nature*, 468(7324), p.696-700.

Görner, K. *et al.*, 2007. Structural determinants of the C-terminal helix-kink-helix motif essential for protein stability and survival promoting activity of DJ-1. *The Journal of biological chemistry*, 282(18), p.13680-91.

Hahn, M. & Bishop, J., 2001. Expression pattern of Drosophila ret suggests a common ancestral origin between the metamorphosis precursors in insect endoderm and the vertebrate enteric neurons. *Proceedings of the National Academy of Sciences of the United States of America*, 98(3), p.1053-8.

Haque, M Emdadul *et al.*, 2008. Cytoplasmic Pink1 activity protects neurons from dopaminergic neurotoxin MPTP. *Proceedings of the National Academy of Sciences of the United States of America*, 105(5), p.1716-21.

Hayashi, H. *et al.*, 2000. Characterization of intracellular signals via tyrosine 1062 in RET activated by glial cell line-derived neurotrophic factor. *Oncogene*, 19(39), p.4469-75.

Hellmich, H.L. *et al.*, 1996. Embryonic expression of glial cell-line derived neurotrophic factor (GDNF) suggests multiple developmental roles in neural differentiation and epithelial-mesenchymal interactions. *Mechanisms of development*, 54(1), p.95-105.

Henn, I.H. *et al.*, 2007. Parkin mediates neuroprotection through activation of IkappaB kinase/nuclear factor-kappaB signaling. *The Journal of neuroscience : the official journal of the Society for Neuroscience*, 27(8), p.1868-78.

Hirata, Y. & Kiuchi, K., 2003. Mitogenic effect of glial cell line-derived neurotrophic factor is dependent on the activation of p70S6 kinase, but independent of the activation of ERK and up-regulation of Ret in SH-SY5Y cells. *Brain research*, 983(1-2), p.1-12.

Hofstra, R.M. *et al.*, 1994. A mutation in the RET proto-oncogene associated with multiple endocrine neoplasia type 2B and sporadic medullary thyroid carcinoma. *Nature*, 367(6461), p.375-6.

Holcik, M. & Sonenberg, N., 2005. Translational control in stress and apoptosis. *Nature reviews. Molecular cell biology*, 6(4), p.318-27.

Hoppins, S. *et al.*, 2011. The soluble form of Bax regulates mitochondrial fusion via MFN2 homotypic complexes. *Molecular cell*, 41(2), p.150-60.

Hulleman, J.D. *et al.*, 2007. Destabilization of DJ-1 by familial substitution and oxidative modifications: implications for Parkinson's disease. *Biochemistry*, 46(19), p.5776-89.

Imai, Y. *et al.*, 2010. The loss of PGAM5 suppresses the mitochondrial degeneration caused by inactivation of PINK1 in Drosophila. *PLoS genetics*, 6(12), p.e1001229.

Imai, Y. *et al.*, 2002. CHIP is associated with Parkin, a gene responsible for familial Parkinson's disease, and enhances its ubiquitin ligase activity. *Molecular cell*, 10(1), p.55-67.

Imai, Y. *et al.*, 2001. An unfolded putative transmembrane polypeptide, which can lead to endoplasmic reticulum stress, is a substrate of Parkin. *Cell*, 105(7), p.891-902.

Itier, J.-M. *et al.*, 2003. Parkin gene inactivation alters behaviour and dopamine neurotransmission in the mouse. *Human molecular genetics*, 12(18), p.2277-91.

Jain, S., Encinas, Mario, *et al.*, 2006. Critical and distinct roles for key RET tyrosine docking sites in renal development. *Genes & development*, 20(3), p.321-33.

Jain, S., Golden, J.P., *et al.*, 2006. RET is dispensable for maintenance of midbrain dopaminergic neurons in adult mice. *The Journal of neuroscience : the official journal of the Society for Neuroscience*, 26(43), p.11230-8.

Jin, S.M. *et al.*, 2010. Mitochondrial membrane potential regulates PINK1 import and proteolytic destabilization by PARL. *The Journal of cell biology*, 191(5), p.933-42.

Junn, E. *et al.*, 2009. Mitochondrial localization of DJ-1 leads to enhanced neuroprotection. *Journal of neuroscience research*, 87(1), p.123-9.

Junn, E. *et al.*, 2005. Interaction of DJ-1 with Daxx inhibits apoptosis signal-regulating kinase 1 activity and cell death. *Proceedings of the National Academy of Sciences of the United States of America*, 102(27), p.9691-6.

Kamp, F. *et al.*, 2010. Inhibition of mitochondrial fusion by α-synuclein is rescued by PINK1, Parkin and DJ-1. *The EMBO journal*, 29(20), p.3571-89.

Keane, T.M. *et al.*, 2011. Mouse genomic variation and its effect on phenotypes and gene regulation. *Nature*, 477(7364), p.289-294.

Kim, R.H., Peters, M., *et al.*, 2005. DJ-1, a novel regulator of the tumor suppressor PTEN. *Cancer cell*, 7(3), p.263-73.

Kim, R.H., Smith, P.D., *et al.*, 2005. Hypersensitivity of DJ-1-deficient mice to 1-methyl-4-phenyl-1,2,3,6-tetrahydropyrindine (MPTP) and oxidative stress. *Proceedings of the National Academy of Sciences of the United States of America*, 102(14), p.5215-20.

Kim, Y. *et al.*, 2008. PINK1 controls mitochondrial localization of Parkin through direct phosphorylation. *Biochemical and biophysical research communications*, 377(3), p.975-80.

Kinumi, T. *et al.*, 2004. Cysteine-106 of DJ-1 is the most sensitive cysteine residue to hydrogen peroxide-mediated oxidation in vivo in human umbilical vein endothelial cells. *Biochemical and biophysical research communications*, 317(3), p.722-8.

Kitada, T. *et al.*, 1998. Mutations in the parkin gene cause autosomal recessive juvenile parkinsonism. *Nature*, 392(6676), p.605-8.

Kitada, T. *et al.*, 2007. Impaired dopamine release and synaptic plasticity in the striatum of PINK1-deficient mice. *Proceedings of the National Academy of Sciences of the United States of America*, 104(27), p.11441-6.

Kitada, T. *et al.*, 2009. Absence of nigral degeneration in aged parkin/DJ-1/PINK1 triple knockout mice. *Journal of neurochemistry*, 111(3), p.696-702.

Klein, C. *et al.*, 2007. Deciphering the role of heterozygous mutations in genes associated with parkinsonism. *Lancet neurology*, 6(7), p.652-62.

Knowles, P.P. *et al.*, 2006. Structure and chemical inhibition of the RET tyrosine kinase domain. *The Journal of biological chemistry*, 281(44), p.33577-87.

Kodama, Y. *et al.*, 2005. The RET proto-oncogene: a molecular therapeutic target in thyroid cancer. *Cancer science*, 96(3), p.143-8.

Koide-Yoshida, S. *et al.*, 2007. DJ-1 degrades transthyretin and an inactive form of DJ-1 is secreted in familial amyloidotic polyneuropathy. *International journal of molecular medicine*, 19(6), p.885-93.

Kordower, J.H. *et al.*, 2000. Neurodegeneration prevented by lentiviral vector delivery of GDNF in primate models of Parkinson's disease. *Science (New York, N.Y.)*, 290(5492), p.767-73.

Kowsky, S. *et al.*, 2007. RET signaling does not modulate MPTP toxicity but is required for regeneration of dopaminergic axon terminals. *Proceedings of the National Academy of Sciences of the United States of America*, 104(50), p.20049-54.

Kramer, E.R. *et al.*, 2007. Absence of Ret signaling in mice causes progressive and late degeneration of the nigrostriatal system. R. G. M. Morris, ed. *PLoS biology*, 5(3), p.e39.

Kramer, E.R. *et al.*, 2006. Cooperation between GDNF/Ret and ephrinA/EphA4 signals for motor-axon pathway selection in the limb. *Neuron*, 50(1), p.35-47.

Kravitz, A.V. *et al.*, 2010. Regulation of parkinsonian motor behaviours by optogenetic control of basal ganglia circuitry. *Nature*, 466(7306), p.622-6.

Kurokawa, K. *et al.*, 2001. Identification of SNT/FRS2 docking site on RET receptor tyrosine kinase and its role for signal transduction. *Oncogene*, 20(16), p.1929-38.

Kurokawa, K. *et al.*, 2003. Cell signalling and gene expression mediated by RET tyrosine kinase. *Journal of internal medicine*, 253(6), p.627-33.

Laar, V.S. Van *et al.*, 2011. Bioenergetics of neurons inhibit the translocation response of Parkin following rapid mitochondrial depolarization. *Human molecular genetics*, 20(5), p.927-40.

Lang, A.E. *et al.*, 2006. Randomized controlled trial of intraputamenal glial cell line-derived neurotrophic factor infusion in Parkinson disease. *Annals of neurology*, 59(3), p.459-66.

Langston, J.W. *et al.*, 1983. Chronic Parkinsonism in humans due to a product of meperidine-analog synthesis. *Science (New York, N.Y.)*, 219(4587), p.979-80.

Lau, L.M.L. de & Breteler, M.M.B., 2006. Epidemiology of Parkinson's disease. *Lancet neurology*, 5(6), p.525-35.

Lewy, F., 1912. Paralysis agitans. Pathologische anatomie. *Hanbuch der Neurologie, ed. M Lewandowsky, Berlin: Springer*, p.920-33.

Liang, C.L. *et al.*, 1996. Midbrain dopaminergic neurons in the mouse that contain calbindin-D28k exhibit reduced vulnerability to MPTP-induced neurodegeneration. *Neurodegeneration : a journal for neurodegenerative disorders, neuroprotection, and neuroregeneration*, 5(4), p.313-8.

Lin, L.F. *et al.*, 1993. GDNF: a glial cell line-derived neurotrophic factor for midbrain dopaminergic neurons. *Science (New York, N.Y.)*, 260(5111), p.1130-2.

Lindvall, O. *et al.*, 1990. Grafts of fetal dopamine neurons survive and improve motor function in Parkinson's disease. *Science (New York, N.Y.)*, 247(4942), p.574-7.

Liu, S. & Lu, Bingwei, 2010. Reduction of protein translation and activation of autophagy protect against PINK1 pathogenesis in Drosophila melanogaster. *PLoS genetics*, 6(12), p.e1001237.

Lundgren, T.K. *et al.*, 2006. Engineering the recruitment of phosphotyrosine binding domain-containing adaptor proteins reveals distinct roles for RET receptor-mediated cell survival. *The Journal of biological chemistry*, 281(40), p.29886-96.

Lutz, A.K. *et al.*, 2009. Loss of parkin or PINK1 function increases Drp1-dependent mitochondrial fragmentation. *The Journal of biological chemistry*, 284(34), p.22938-51.

Lücking, C.B. *et al.*, 2000. Association between early-onset Parkinson's disease and mutations in the parkin gene. *The New England journal of medicine*, 342(21), p.1560-7.

Marongiu, R. *et al.*, 2009. Mutant Pink1 induces mitochondrial dysfunction in a neuronal cell model of Parkinson's disease by disturbing calcium flux. *Journal of neurochemistry*, 108(6), p.1561-74.

Martinat, C. *et al.*, 2004. Sensitivity to oxidative stress in DJ-1-deficient dopamine neurons: an ES- derived cell model of primary Parkinsonism. *PLoS biology*, 2(11), p.e327.

Martinou, J.-C. & Youle, R.J., 2011. Mitochondria in apoptosis: bcl-2 family members and mitochondrial dynamics. *Developmental cell*, 21(1), p.92-101.

Matsuda, N. *et al.*, 2010. PINK1 stabilized by mitochondrial depolarization recruits Parkin to damaged mitochondria and activates latent Parkin for mitophagy. *The Journal of cell biology*, 189(2), p.211-21.

Meissner, C. *et al.*, 2011. The mitochondrial intramembrane protease PARL cleaves human Pink1 to regulate Pink1 trafficking. *Journal of neurochemistry*, 117(5), p.856-67.

Melillo, R M *et al.*, 2001. The insulin receptor substrate (IRS)-1 recruits phosphatidylinositol 3-kinase to Ret: evidence for a competition between Shc and IRS-1 for the binding to Ret. *Oncogene*, 20(2), p.209-18.

Meng, X. *et al.*, 2000. Regulation of cell fate decision of undifferentiated spermatogonia by GDNF. *Science (New York, N.Y.)*, 287(5457), p.1489-93.

Merrill, R.A. *et al.*, 2011. Mechanism of neuroprotective mitochondrial remodeling by PKA/AKAP1. *PLoS biology*, 9(4), p.e1000612.

Meulener, M.C. *et al.*, 2006. Mutational analysis of DJ-1 in Drosophila implicates functional inactivation by oxidative damage and aging. *Proceedings of the National Academy of Sciences of the United States of America*, 103(33), p.12517-22.

Mijatovic, J. *et al.*, 2007. Constitutive Ret activity in knock-in multiple endocrine neoplasia type B mice induces profound elevation of brain dopamine concentration via enhanced synthesis and increases the number of TH-positive cells in the substantia nigra. *The Journal of neuroscience : the official journal of the Society for Neuroscience*, 27(18), p.4799-809.

Mo, J.-S. *et al.*, 2008. DJ-1 modulates UV-induced oxidative stress signaling through the suppression of MEKK1 and cell death. *Cell death and differentiation*, 15(6), p.1030-41.

Montessuit, S. *et al.*, 2010. Membrane remodeling induced by the dynamin-related protein Drp1 stimulates Bax oligomerization. *Cell*, 142(6), p.889-901.

Moore, D.J. *et al.*, 2005. Association of DJ-1 and parkin mediated by pathogenic DJ-1 mutations and oxidative stress. *Human molecular genetics*, 14(1), p.71-84.

Moore, M.W. *et al.*, 1996. Renal and neuronal abnormalities in mice lacking GDNF. *Nature*, 382(6586), p.76-9.

Nagakubo, D. *et al.*, 1997. DJ-1, a novel oncogene which transforms mouse NIH3T3 cells in cooperation with ras. *Biochemical and biophysical research communications*, 231(2), p.509-13.

Naour, F. Le *et al.*, 2001. Proteomics-based identification of RS/DJ-1 as a novel circulating tumor antigen in breast cancer. *Clinical cancer research : an official journal of the American Association for Cancer Research*, 7(11), p.3328-35.

Narendra, D.P. *et al.*, 2010. PINK1 is selectively stabilized on impaired mitochondria to activate Parkin. *PLoS biology*, 8(1), p.e1000298.

Neff, F. *et al.*, 2002. Signaling pathways mediate the neuroprotective effects of GDNF. *Annals of the New York Academy of Sciences*, 973, p.70-4.

Olanow, C.W. *et al.*, 2003. A double-blind controlled trial of bilateral fetal nigral transplantation in Parkinson's disease. *Annals of neurology*, 54(3), p.403-14.

Ooe, H., Iguchi-Ariga, S.M.M. & Ariga, H., 2006. Establishment of specific antibodies that recognize C106-oxidized DJ-1. *Neuroscience letters*, 404(1-2), p.166-9.

Palacino, J.J. *et al.*, 2004. Mitochondrial dysfunction and oxidative damage in parkin-deficient mice. *The Journal of biological chemistry*, 279(18), p.18614-22.

Pandey, A. *et al.*, 1996. Direct association between the Ret receptor tyrosine kinase and the Src homology 2-containing adapter protein Grb7. *The Journal of biological chemistry*, 271(18), p.10607-10.

Paratcha, G. & Ledda, F., 2008. GDNF and GFRalpha: a versatile molecular complex for developing neurons. *Trends in neurosciences*, 31(8), p.384-91.

Paratcha, G., Ledda, F. & Ibáñez, C.F., 2003. The neural cell adhesion molecule NCAM is an alternative signaling receptor for GDNF family ligands. *Cell*, 113(7), p.867-79.

Parcellier, A. *et al.*, 2008. PKB and the mitochondria: AKTing on apoptosis. *Cellular signalling*, 20(1), p.21-30.

Park, J., Lee, G. & Chung, J., 2009. The PINK1-Parkin pathway is involved in the regulation of mitochondrial remodeling process. *Biochemical and biophysical research communications*, 378(3), p.518-23.

Park, J. *et al.*, 2006. Mitochondrial dysfunction in Drosophila PINK1 mutants is complemented by parkin. *Nature*, 441(7097), p.1157-61.

Parkinson, J., 1817. An essay on the shaking palsy. *London: Whittingham & Rowland*.

Perez, F.A. & Palmiter, R.D., 2005. Parkin-deficient mice are not a robust model of parkinsonism. *Proceedings of the National Academy of Sciences of the United States of America*, 102(6), p.2174-9.

Periquet, M. *et al.*, 2003. Parkin mutations are frequent in patients with isolated early-onset parkinsonism. *Brain : a journal of neurology*, 126(Pt 6), p.1271-8.

Pesah, Y. *et al.*, 2004. Drosophila parkin mutants have decreased mass and cell size and increased sensitivity to oxygen radical stress. *Development (Cambridge, England)*, 131(9), p.2183-94.

Pham, T.-T. *et al.*, 2010. DJ-1-deficient mice show less TH-positive neurons in the ventral tegmental area and exhibit non-motoric behavioural impairments. *Genes, brain, and behavior*, 9(3), p.305-17.

Pichel, J.G. *et al.*, 1996. Defects in enteric innervation and kidney development in mice lacking GDNF. *Nature*, 382(6586), p.73-6.

Plaza-Menacho, I. *et al.*, 2010. Targeting the receptor tyrosine kinase RET sensitizes breast cancer cells to tamoxifen treatment and reveals a role for RET in endocrine resistance. *Oncogene*, 29(33), p.4648-57.

Plun-Favreau, H. *et al.*, 2007. The mitochondrial protease HtrA2 is regulated by Parkinson's disease-associated kinase PINK1. *Nature cell biology*, 9(11), p.1243-52.

Poole, A.C. *et al.*, 2008. The PINK1/Parkin pathway regulates mitochondrial morphology. *Proceedings of the National Academy of Sciences of the United States of America*, 105(5), p.1638-43.

Poole, A.C. *et al.*, 2010. The mitochondrial fusion-promoting factor mitofusin is a substrate of the PINK1/parkin pathway. *PLoS one*, 5(4), p.e10054.

Pridgeon, J.W. *et al.*, 2007. PINK1 protects against oxidative stress by phosphorylating mitochondrial chaperone TRAP1. *PLoS biology*, 5(7), p.e172.

Read, R.D. *et al.*, 2005. A Drosophila model of multiple endocrine neoplasia type 2. *Genetics*, 171(3), p.1057-81.

Ren, H. *et al.*, 2011. Oxidized DJ-1 interacts with the mitochondrial protein BCL-XL. *The Journal of biological chemistry*.

Ries, V. *et al.*, 2006. Oncoprotein Akt/PKB induces trophic effects in murine models of Parkinson's disease. *Proceedings of the National Academy of Sciences of the United States of America*, 103(49), p.18757-62.

Rodriguez-Oroz, M.C. *et al.*, 2009. Initial clinical manifestations of Parkinson's disease: features and pathophysiological mechanisms. *Lancet neurology*, 8(12), p.1128-39.

Sainio, K. *et al.*, 1997. Glial-cell-line-derived neurotrophic factor is required for bud initiation from ureteric epithelium. *Development (Cambridge, England)*, 124(20), p.4077-87.

Salvatore, D. *et al.*, 2001. Increased in vivo phosphorylation of ret tyrosine 1062 is a potential pathogenetic mechanism of multiple endocrine neoplasia type 2B. *Cancer research*, 61(4), p.1426-31.

Sanford, L.P. *et al.*, 2001. Influence of genetic background on knockout mouse phenotypes. *Methods in molecular biology (Clifton, N.J.)*, 158, p.217-25.

Santoro, Massimo *et al.*, 2002. Molecular mechanisms of RET activation in human cancer. *Annals of the New York Academy of Sciences*, 963, p.116-21.

Satake, W. *et al.*, 2009. Genome-wide association study identifies common variants at four loci as genetic risk factors for Parkinson's disease. *Nature genetics*, 41(12), p.1303-7.

Schlee, S., Carmillo, P. & Whitty, A., 2006. Quantitative analysis of the activation mechanism of the multicomponent growth-factor receptor Ret. *Nature chemical biology*, 2(11), p.636-44.

Schuchardt, A. *et al.*, 1994. Defects in the kidney and enteric nervous system of mice lacking the tyrosine kinase receptor Ret. *Nature*, 367(6461), p.380-3.

Schuringa, J.J. *et al.*, 2001. MEN2A-RET-induced cellular transformation by activation of STAT3. *Oncogene*, 20(38), p.5350-8.

Sekito, A. *et al.*, 2006. DJ-1 interacts with HIPK1 and affects H2O2-induced cell death. *Free radical research*, 40(2), p.155-65.

Sha, D., Chin, L.-S. & Li, L., 2010. Phosphorylation of parkin by Parkinson disease-linked kinase PINK1 activates parkin E3 ligase function and NF-kappaB signaling. *Human molecular genetics*, 19(2), p.352-63.

Shendelman, S. *et al.*, 2004. DJ-1 is a redox-dependent molecular chaperone that inhibits alpha-synuclein aggregate formation. *PLoS biology*, 2(11), p.e362.

Shi, G. *et al.*, 2011. Functional alteration of PARL contributes to mitochondrial dysregulation in Parkinson's disease. *Human molecular genetics*, 20(10), p.1966-74.

Shimura, H. *et al.*, 2001. Ubiquitination of a new form of alpha-synuclein by parkin from human brain: implications for Parkinson's disease. *Science (New York, N.Y.)*, 293(5528), p.263-9.

Shin, J.-H. *et al.*, 2011. PARIS (ZNF746) repression of PGC-1α contributes to neurodegeneration in Parkinson's disease. *Cell*, 144(5), p.689-702.

Shinbo, Y. *et al.*, 2005. DJ-1 restores p53 transcription activity inhibited by Topors/p53BP3. *International journal of oncology*, 26(3), p.641-8.

Sidransky, E. *et al.*, 2009. Multicenter analysis of glucocerebrosidase mutations in Parkinson's disease. *The New England journal of medicine*, 361(17), p.1651-61.

Silvestri, L. *et al.*, 2005. Mitochondrial import and enzymatic activity of PINK1 mutants associated to recessive parkinsonism. *Human molecular genetics*, 14(22), p.3477-92.

Simón-Sánchez, J. *et al.*, 2009. Genome-wide association study reveals genetic risk underlying Parkinson's disease. *Nature genetics*, 41(12), p.1308-12.

Slevin, J.T. *et al.*, 2005. Improvement of bilateral motor functions in patients with Parkinson disease through the unilateral intraputaminal infusion of glial cell line-derived neurotrophic factor. *Journal of neurosurgery*, 102(2), p.216-22.

Smith, M.P. & Cass, W.A., 2007. GDNF reduces oxidative stress in a 6-hydroxydopamine model of Parkinson's disease. *Neuroscience letters*, 412(3), p.259-63.

Smith, W.W. *et al.*, 2005. Leucine-rich repeat kinase 2 (LRRK2) interacts with parkin, and mutant LRRK2 induces neuronal degeneration. *Proceedings of the National Academy of Sciences of the United States of America*, 102(51), p.18676-81.

Stenqvist, A. *et al.*, 2008. Subcellular receptor redistribution and enhanced microspike formation by a Ret receptor preferentially recruiting Dok. *Neuroscience letters*, 435(1), p.11-6.

Suen, Der-Fen, Norris, K.L. & Youle, R.J., 2008. Mitochondrial dynamics and apoptosis. *Genes & development*, 22(12), p.1577-90.

Sugaya, R. *et al.*, 1994. A Drosophila homolog of human proto-oncogene ret transiently expressed in embryonic neuronal precursor cells including neuroblasts and CNS cells. *Mechanisms of development*, 45(2), p.139-45.

Sánchez, M.P. *et al.*, 1996. Renal agenesis and the absence of enteric neurons in mice lacking GDNF. *Nature*, 382(6586), p.70-3.

Taguchi, N. *et al.*, 2007. Mitotic phosphorylation of dynamin-related GTPase Drp1 participates in mitochondrial fission. *The Journal of biological chemistry*, 282(15), p.11521-9.

Tain, L.S., Chowdhury, R., *et al.*, 2009. Drosophila HtrA2 is dispensable for apoptosis but acts downstream of PINK1 independently from Parkin. *Cell death and differentiation*, 16(8), p.1118-25.

Tain, L.S., Mortiboys, H., *et al.*, 2009. Rapamycin activation of 4E-BP prevents parkinsonian dopaminergic neuron loss. *Nature neuroscience*, 12(9), p.1129-35.

Taira, T. *et al.*, 2004. DJ-1 has a role in antioxidative stress to prevent cell death. *EMBO reports*, 5(2), p.213-8.

Takahashi, K *et al.*, 2001. DJ-1 positively regulates the androgen receptor by impairing the binding of PIASx alpha to the receptor. *The Journal of biological chemistry*, 276(40), p.37556-63.

Takatori, S., Ito, G. & Iwatsubo, T., 2008. Cytoplasmic localization and proteasomal degradation of N-terminally cleaved form of PINK1. *Neuroscience letters*, 430(1), p.13-7.

Tanaka, A. *et al.*, 2010. Proteasome and p97 mediate mitophagy and degradation of mitofusins induced by Parkin. *The Journal of cell biology*, 191(7), p.1367-80.

Tang, B. *et al.*, 2006. Association of PINK1 and DJ-1 confers digenic inheritance of early-onset Parkinson's disease. *Human molecular genetics*, 15(11), p.1816-25.

Thomas, K.J. *et al.*, 2011. DJ-1 acts in parallel to the PINK1/parkin pathway to control mitochondrial function and autophagy. *Human molecular genetics*, 20(1), p.40-50.

Threadgill, D.W. *et al.*, 1995. Targeted disruption of mouse EGF receptor: effect of genetic background on mutant phenotype. *Science (New York, N.Y.)*, 269(5221), p.230-4.

Tillman, J.E. *et al.*, 2007. DJ-1 binds androgen receptor directly and mediates its activity in hormonally treated prostate cancer cells. *Cancer research*, 67(10), p.4630-7.

Tomac, A. *et al.*, 1995. Protection and repair of the nigrostriatal dopaminergic system by GDNF in vivo. *Nature*, 373(6512), p.335-9.

Trupp, M. *et al.*, 1996. Functional receptor for GDNF encoded by the c-ret proto-oncogene. *Nature*, 381(6585), p.785-9.

Uhl, G.R., Hedreen, J.C. & Price, D.L., 1985. Parkinson's disease: loss of neurons from the ventral tegmental area contralateral to therapeutic surgical lesions. *Neurology*, 35(8), p.1215-8.

Valente, E.M., Abou-Sleiman, P.M., *et al.*, 2004. Hereditary early-onset Parkinson's disease caused by mutations in PINK1. *Science (New York, N.Y.)*, 304(5674), p.1158-60.

Valente, E.M., Salvi, S., *et al.*, 2004. PINK1 mutations are associated with sporadic early-onset parkinsonism. *Annals of neurology*, 56(3), p.336-41.

Vasseur, S. *et al.*, 2009. DJ-1/PARK7 is an important mediator of hypoxia-induced cellular responses. *Proceedings of the National Academy of Sciences of the United States of America*, 106(4), p.1111-6.

Venda, L.L. *et al.*, 2010. α-Synuclein and dopamine at the crossroads of Parkinson's disease. *Trends in neurosciences*, 33(12), p.559-68.

Viglietto, G. *et al.*, 2000. Glial cell line-derived neutrotrophic factor and neurturin can act as paracrine growth factors stimulating DNA synthesis of Ret-expressing spermatogonia. *International journal of oncology*, 16(4), p.689-94.

Vives-Bauza, C. *et al.*, 2010. PINK1-dependent recruitment of Parkin to mitochondria in mitophagy. *Proceedings of the National Academy of Sciences of the United States of America*, 107(1), p.378-83.

Wakeman, D.R., Dodiya, H.B. & Kordower, J.H., Cell transplantation and gene therapy in Parkinson's disease. *The Mount Sinai journal of medicine, New York*, 78(1), p.126-58.

Wang, S. *et al.*, 2009. The tyrosine kinase Stitcher activates Grainy head and epidermal wound healing in Drosophila. *Nature cell biology*, 11(7), p.890-5.

Weihofen, A. *et al.*, 2009. Pink1 forms a multiprotein complex with Miro and Milton, linking Pink1 function to mitochondrial trafficking. Biochemistry, 48(9), p.2045-52.

Westermann, B., 2010. Mitochondrial fusion and fission in cell life and death. Nature reviews. Molecular cell biology, 11(12), p.872-84.

Whitworth, A.J. et al., Rhomboid-7 and HtrA2/Omi act in a common pathway with the Parkinson's disease factors Pink1 and Parkin. Disease models & mechanisms, 1(2-3), p.168-74; discussion 173.

Whitworth, A.J. *et al.*, 2005. Increased glutathione S-transferase activity rescues dopaminergic neuron loss in a Drosophila model of Parkinson's disease. *Proceedings of the National Academy of Sciences of the United States of America*, 102(22), p.8024-9.

Woodall, A.J. *et al.*, 2008. Growth factors differentially regulate neuronal Cav channels via ERK-dependent signalling. *Cell calcium*, 43(6), p.562-75.

Xu, J. *et al.*, 2005. The Parkinson's disease-associated DJ-1 protein is a transcriptional co-activator that protects against neuronal apoptosis. *Human molecular genetics*, 14(9), p.1231-41.

Yamaguchi, H. & Shen, J., 2007. Absence of dopaminergic neuronal degeneration and oxidative damage in aged DJ-1-deficient mice. *Molecular neurodegeneration*, 2, p.10.

Yang, F. *et al.*, 2001. GDNF acutely modulates excitability and A-type K(+) channels in midbrain dopaminergic neurons. *Nature neuroscience*, 4(11), p.1071-8.

Yang, Y. *et al.*, 2005. Inactivation of Drosophila DJ-1 leads to impairments of oxidative stress response and phosphatidylinositol 3-kinase/Akt signaling. *Proceedings of the National Academy of Sciences of the United States of America*, 102(38), p.13670-5.

Yang, Y. *et al.*, 2006. Mitochondrial pathology and muscle and dopaminergic neuron degeneration caused by inactivation of Drosophila Pink1 is rescued by Parkin. *Proceedings of the National Academy of Sciences of the United States of America*, 103(28), p.10793-8.

Youle, R.J. & Narendra, D.P., 2011. Mechanisms of mitophagy. *Nature reviews. Molecular cell biology*, 12(1), p.9-14.

Zabetian, C.P. *et al.*, 2007. Association analysis of MAPT H1 haplotype and subhaplotypes in Parkinson's disease. *Annals of neurology*, 62(2), p.137-44.

Zhang, L. *et al.*, 2005. Mitochondrial localization of the Parkinson's disease related protein DJ-1: implications for pathogenesis. *Human molecular genetics*, 14(14), p.2063-73.

Zhou, C. *et al.*, 2008. The kinase domain of mitochondrial PINK1 faces the cytoplasm. *Proceedings of the National Academy of Sciences of the United States of America*, 105(33), p.12022-7.

Zhu, J.-H. *et al.*, 2003. Localization of phosphorylated ERK/MAP kinases to mitochondria and autophagosomes in Lewy body diseases. *Brain pathology (Zurich, Switzerland)*, 13(4), p.473-81.

Ziviani, E., Tao, Ran N & Whitworth, A.J., 2010. Drosophila parkin requires PINK1 for mitochondrial translocation and ubiquitinates mitofusin. *Proceedings of the National Academy of Sciences of the United States of America*, 107(11), p.5018-23.

Acknowledgments

Curriculum Vitae

Full name	Pontus Fredrik Gunnar Klein
Date & place of birth	23 October 1982, Solna, Sweden

EDUCATION

since 05/2007	**Max Planck Institute of Neurobiology, Martinsried, Germany** International Max Planck Research School for Molecular and Cellular Life Sciences *Doctoral thesis*, supervisor: Prof. Dr. Rüdiger Klein
08/2006 – 04/2007	**Lund University, Lund, Sweden** *Master thesis,* supervisor: Dr. Jia-Yi Li
08/2005 – 05/2006	**University of Illinois, Urbana-Champaign, IL, USA** *Undergraduate exchange studies*
08/2001 – 08/2005	**Uppsala University, Uppsala, Sweden** *Biomedicine (M.Sc.)*
1998 – 2001	**Södra Latins gymnasium, Stockholm, Sweden**

PUBLICATIONS

Aron L, **Klein P**, Pham TT, Kramer ER, Wurst W, Klein R. *Pro-survival role for Parkinson's associated gene DJ-1 revealed in trophically impaired dopaminergic neurons.* PLoS Biology, 2010 Apr 6;8(4):e1000349.

Smith R, Bacos K, Fedele V, Soulet D, Walz HA, Obermüller S, Lindqvist A, Björkqvist M, **Klein P**, Onnerfjord P, Brundin P, Mulder H, Li JY. (2009): *Mutant huntingtin interacts with {beta}-tubulin and disrupts vesicular transport and insulin secretion.* Human Molecular Genetics, 2009 Oct 15;18(20):3942-54. Epub 2009 Jul 23.

Smith R, **Klein P**, Koc-Schmitz Y, Waldvogel H, Faull RM, Brundin P, Plomann M. and Li JY. *Loss of SNAP-25 and rabphilin-3a in sensory-motor cortex in Huntington's disease*, Journal of Neurochemistry, 2007 Oct ;103 (1):115-23